I. EXTENDED APPLICATIONS OF THE HOT-WIRE ANEMOMETER

II. INVESTIGATIONS OF THE FLOW IN ROUND, TURBULENT JETS

Thesis by

Stanley Corrsin

In Partial Fulfillment of the Requirements

for the

Degree of Doctor of Philosophy

California Institute of Technology

Pasadena, California

May, 1947

ACKNOWLEDGEMENT

Primarily, I wish to record my considerable debt to Dr. Hans-Wolfgang Liepmann; beyond acting as adviser for much of the experimental work, he is in great measure responsible for whatever I may exhibit of the scientific state of mind.

I would like to thank Mr. Carl Thiele for his excellent work in designing and constructing the hot-wire equipment used throughout the investigation, as well as for starting this free turbulent shear flow research program here at the Galcit.

Mr. Mahinder Uberoi has been of great assistance in the laboratory, and both he and Mr. Harry Ashkenas have contributed materially to the task of preparing this report. Discussions on many occasions with Dr. C. C. Lin (now at Brown University) and with Mr. John Laufer have been extremely helpful. My sincere appreciation is also due to Beverly Cottingham for preparing some of the figures in this report, and to my wife, Barbara Corrsin, who has so diligently typed both rough draft and final copy.

The experimental work reported here has been carried out with the financial support of the National Advisory Committee for Aeronautics, which is gratefully acknowledged.

PART I

EXTENDED APPLICATIONS OF THE HOT-WIRE ANEMOMETER

INDEX

A. SUMMARY

Two new fields of application of the hot-wire anemometer are proposed, and the appropriate response equations and measuring procedures are developed.

The first analysis leads to a method for the measurement of physically significant statistical quantities in a turbulent flow with heat transfer: for example, the turbulence levels, the temperature fluctuation level, the turbulent heat transfer coefficient, the velocity scale, the temperature scale and some spectra.

The second analysis involves the use of the hot-wire in the turbulent isothermal mixing of two appropriately different gases. If the thermal conductivity of the mixture is known and is a monotonic function of the relative concentration, it is possible to measure the mean velocity and mean concentration at any point. If no data are available on the thermal conductivity of the mixture, this additional unknown can be determined by an additional measurement. Furthermore, it is also possible to measure the various statistical functions of the fluctuating velocities and the local concentration fluctuation, provided, again, that the thermal conductivity is a known monotonic function of the concentration.

Although the details of the present analysis are dependent upon the accuracy of King's equation for the rate of heat loss from fine wires, the general approach is equally valid for any (possibly more accurate) equation that may be deduced.

B. INTRODUCTION

The hot-wire anemometer has been used for many years in the measurement of the mean velocities of flowing gases [1] and, more recently, in the measurement of various statistical quantities associated with the random velocity fluctuations occurring in turbulent flow [2, 3, 4, 5, 6, 7 and others]. It has also been used as a microphone [8]. This anemometer consists essentially of an electrically heated wire of extremely small mass, whose temperature varies in response to rapid changes in the instantaneous flow (cooling) velocity. If the heating current is maintained constant, the resulting voltage fluctuations, whose intensity is expressible as a function of the velocity fluctuations, may be amplified and measured. Attenuation and phase lag, due to the non-zero heat capacity of the wire and the finite rate of electrical heating, may be compensated by a suitable network between two of the amplifier stages. The essentials of the technique are admirably described in reference (2).

In a detailed consideration of turbulent fluid flow, there are several statistical functions of the randomly fluctuating velocities that are of importance. The simplest of these are the following:

(a) the three components of the turbulence level or intensity, $\frac{u'}{U}$, $\frac{v'}{U}$ and $\frac{w'}{U}$ which, squared and added, give the ratio of kinetic energy of random fluctuation to directed kinetic energy.

(b) the double correlation functions, i.e., the statistical correlation between two components at separate points, e.g., $R_2 = \frac{\overline{u_1 u_2}}{u_1' u_2'}$. Von Karman [9,10] and Howarth [10] have shown that only two of these functions are independent for isotropic turbulence.

(c) the energy spectrum of the turbulent fluctuations. Taylor [11] has demonstrated that this is the Fourier transform of one of the two principal components of the correlation tensor.

(d) the scale of turbulence, defined by Taylor [12] for isotropic turbulence as the integral of one of the double correlation functions, e.g., $L = \int_0^\infty R_2(y)\, dy$

(e) the micro-scale of turbulence, identified with the rate of dissipation of turbulent energy into heat, the size of the smallest eddies, was also defined by Taylor [12], who showed this to be the abcissa intercept of the vertex-tangent parabola of the $R_2(y)$ curve in isotropic turbulence.

(f) the turbulent shear stress, $\tau = -\rho \overline{uv}$ was first identified by Osborne Reynolds in his classic formulation of the equations of motion for turbulent flow [13]. This stress is, of course, a measure of the lateral rate of momentum transfer or diffusion.

All of the above functions have been measured for various turbulent flows (7, 14, 15, 16, 17, 18, 19, 20 and others), principally with the hot-wire technique, although the most detailed measurements have of necessity been confined to investigations of the "isotropic" turbulence far behind grids placed in an uniform airstream.

There are other kinematic quantities of considerable interest:

(g) Batchelor and Townsend (21) have recently measured three statistical functions of the time derivatives of the velocity fluctuation, $\overline{\left(\frac{\partial u}{\partial t}\right)^2}$, $\overline{\left(\frac{\partial^2 u}{\partial t^2}\right)^2}$ and $\overline{\left(\frac{\partial u}{\partial t}\right)^3}$. These enter into terms describing the time rate of change of vorticity in isotropic turbulence.

(h) the rate of lateral kinematic diffusion of turbulent energy in a turbulent shear flow ($\sim \rho \overline{u^2 v}$) has apparently not been measured yet, although suitable techniques are fairly well known.

(i) the pressure fluctuation diffusion term ($\sim \overline{pv}$) in the turbulent energy equation has not been measured, due principally to the difficulty of obtaining an instrument that responds to static pressure fluctuations independently of velocity fluctuations.

In a detailed consideration of turbulent motion, it is of interest to obtain information on the heat and material diffusion coefficients as well as the momentum and energy diffusion already mentioned. In fact, this information should be useful both as an end in itself, and as additional evidence to be applied in obtaining a better

understanding of the nature of turbulence.

Consequently, it seemed worthwhile to investigate the possibilities of exploiting the hot-wire beyond the simple anemometric applications.

The rate of cooling of a body immersed in a fluid stream clearly depends upon (a) the stream velocity, (b) the temperature difference, (c) the physical constants of the fluid and (d) the physical constants of the wire. For the simple hot-wire anemometer, (b), (c) and (d) are effectively fixed, and the instrument response measures (a). Changes in stream temperature certainly involve changes in (b) and possibly in (c). Thus the instrument responds to temperature changes or fluctuations.

Changes in the relative concentration of a flowing mixture of two fluids with different physical constants lead to variations in (c), and, in principal, the hot-wire instrument responds to concentration changes or fluctuations.

Considerations of algebraic and experimental complication have restricted the present treatment to cases in which fluctuations in velocity and only one of the above two quantities coexist, although this limitation is not dictated by principle.

With this experimental technique, the new quantities which may be of interest to measure are the temperature fluctuation level $\frac{\vartheta'}{\overline{\Theta}}$, the spectrum of temperature fluctuation, the heat diffusion ($\sim \overline{\vartheta v}$), the correlation coefficient $\frac{\overline{\vartheta_1 \vartheta_2}}{\overline{\Theta}^2}$, and the thermal scale and micro-scale, analogous to Taylor's kinematic scales, as well as

the corresponding statistical functions of the concentration fluctuation in the turbulent mixing of two gases.

That direct measurement of $\overline{\vartheta v}$ should be possible with a hot-wire instrument, has been known for many years (see, for example, remarks in reference 22), but no actual work appears to have been carried out.

Distributions of momentum, heat and material transport coefficients in a shear flow are directly calculable from measurements of the mean velocity, temperature and concentration profiles respectively. At least the first of these three has already been done for some specific cases [17, 23]. However, it has been found [17, 20] that the mean profile is relatively insensitive to phenomenological assumptions on the transfer coefficient, so that the inverse procedure can best be regarded as a check on direct measurements of the transfer or diffusion.

C. NOTATION

U	=	instantaneous total velocity
$\bar{U}$	=	mean velocity
u	=	instantaneous velocity fluctuation in direction of mean velocity $(= U - \bar{U})$
v, w	=	normal components of velocity fluctuation
u', v', w'	=	root mean square values
T_a	=	instantaneous absolute temperature of gas
$\bar{T}_a$	=	mean absolute temperature
ϑ	=	instantaneous temperature fluctuation $(= T_a - \bar{T}_a)$
ϑ'	=	root mean square value
T_r	=	absolute temperature of reference medium (e.g., the air at rest, for a free jet).
Θ	=	$T_a - T_r$
$\bar{\Theta}$	=	$\bar{T}_a - T_r$
Γ	=	instantaneous concentration of secondary gas. In the present applications.

$$\Gamma = \frac{\text{mols per unit volume of the secondary gas}}{\text{total mols, of air and gas, per unit volume}}$$

$\bar{\Gamma}$	=	mean Γ
γ	=	instantaneous concentration fluctuation
γ'	=	root mean square value
R	=	instantaneous resistance of electrically heated hot-wire
$\bar{R}$	=	mean R
r	=	$R - \bar{R}$
R_a	=	instantaneous resistance of unheated hot-wire

$\bar{R}_a$	=	mean R_a (resistance at $\bar{T}_a$)
r_a	=	$R_a - \bar{R}_a$
R_e	=	instantaneous "equilibrium" hot-wire resistance, i.e., the resistance the hot-wire would have at any moment if it had zero lag
$\bar{R}_e$	=	mean R_e
R_r	=	resistance of wire at at T_r
R_o	=	resistance of wire at 0° Centigrade
i	=	heating current
e	=	voltage fluctuation across hot-wire
l	=	hot-wire length
d	=	hot-wire diameter
σ_w	=	specific resistivity of wire material
α	=	thermal coefficient of change of resistance of wire material
ρ_w	=	density of wire material
m	=	mass of wire
s	=	specific heat of wire material
k	=	thermal conductivity of fluid at T_a
$\bar{k}$	=	thermal conductivity of fluid at $\bar{T}_a$
k_a	=	thermal conductivity of air
k_g	=	thermal conductivity of secondary gas
Δk	=	$k_g - k_a$
c_p	=	constant pressure specific heat of fluid at T_a
$\bar{c}_p$	=	constant pressure specific heat of fluid at $\bar{T}_a$
c_{p_a}	=	constant pressure specific heat of air
c_{p_g}	=	constant pressure specific heat of secondary gas
Δc_p	=	$c_{p_g} - c_{p_a}$

ρ	=	density of fluid at T_a
$\bar{\rho}$	=	density of fluid at $\bar{T}_a$
ρ_a	=	density of air
ρ_g	=	density of secondary gas
k', c_p', ρ'	=	fluctuations
$\Delta\rho$	=	$\rho_g - \rho_a$
H	=	heat energy in hot-wire
T	=	wire temperature
t	=	time

D. THE CONVENTIONAL HOT-WIRE ANEMOMETER

RESPONSE EQUATIONS

Following the approach of Dryden and Kuethe [2], we assume King's semi-empirical form for the rate of heat loss from a wire immersed in a flowing fluid. For the time rate of increase of heat energy in the wire this gives

$$\frac{dH}{dt} = i^2 R - \left(A' + B' \sqrt{U} \right) (T - T_a) \qquad (1)$$

where the physical make-up of A' and B' as deduced by King is

$$A' = a \ell k \; ; \qquad B' = b \ell \sqrt{d c_p \rho k}$$

a and b will be regarded here as numerical constants, although they are dimensional, and should show some variation if a wide enough temperature range is considered.

The term $A'(T - T_a)$ presumably represents heat loss due to free convection and radiation. Therefore, it is clear that the constant a must include such physical quantities as the acceleration of gravity, the thermal expansion coefficient of the fluid, the specific heat of the fluid, a temperature function, a radiation constant, etc. The term $B' \sqrt{U} \; (T - T_a)$ represents forced convection, and after k has been factored out, the term can be written as proportion to the product of a Reynolds Number and a Prandtl Number.

Eq. (1) can be written as

$$\frac{4.2 \, ms}{R_o \alpha} \frac{dR}{dt} = i^2 R - (A + B \sqrt{U})(R - R_a) \qquad (1a)$$

and if we consider equilibrium conditions such that $\frac{dR}{dt} = 0$, writing the equilibrium value of R as R_e,

$$\frac{i^2 R_e}{R_e - R_a} = A + B\sqrt{U} \qquad (2)$$

where

$$A = \frac{a\ell}{R_o \alpha} k \; ; \qquad B = \frac{b\ell}{R_o \alpha} \sqrt{d c_p \rho k}$$

In considerations of averaged or steady state operation, R_e in Eq. (2) may be replaced by $\bar{R}$, and this equation is the usual mean velocity calibration of the hot-wire.

King deduced his equation for steady state operation, and a primary assumption of the hot-wire anemometer theory is that this rate of heat loss is independent of acceleration.

A convenient alternative form of Eq. (2) is

$$\frac{i^2 R_a}{R - R_a} = A - i^2 + B\sqrt{U} \qquad (2a)$$

For the measurement of turbulence, we are interested in the voltage fluctuation set up across the hot-wire due to a small fluctuation in velocity. The analysis for large fluctuations has proved intractable, but, as illustrated in Appendix I of Part II, the error committed in applying the small perturbation results in the measurement of rather large fluctuation levels is not necessarily excessive.

Letting $U = \bar{U} + u$

$R = \bar{R} + r$

$e = ir$

where $\frac{u}{\bar{U}} << 1$ & $\frac{r}{\bar{R} - R_a} << 1$

and substituting these into Eq. (2),

$$\frac{i^2 (\bar{R} + r)}{(\bar{R} - R_a)\left(1 + \frac{r}{\bar{R} - R_a}\right)} = A + B\sqrt{\bar{U}}\left(1 + \frac{u}{\bar{U}}\right)^{1/2}$$

Keeping only the linear terms of the appropriate binomial expansions, otherwise neglecting the squares of small quantities, and substituting from Eq. (2) for $(A + B\sqrt{\bar{U}})$, we finally obtain

$$e = -\frac{\bar{R}-R_a}{2iR_a}\left[i^2\bar{R} - A(\bar{R}-R_a)\right]\cdot\frac{u}{\bar{U}} \qquad (3)$$

Thus, the coefficient of $\frac{u}{\bar{U}}$ is the sensitivity of a single hot-wire to velocity fluctuations along the main stream direction.

Since the wire has a non-zero heat capacity and only a finite rate of electrical heating, there is a time lag in the response which normally leads to an appreciable drop in the hot-wire response-vs.-frequency curve above some particular frequency. The characteristic "time constant", M , can be computed approximately by substituting from Eq. (2) into Eq. (1a) to obtain

$$\frac{4.2\ ms}{R_o\alpha}\ \frac{dR}{dt} = \frac{i^2R_a(R_e-R)}{R_e-R_a} \qquad (4)$$

Dryden and Kuethe [2] transform this further, but find no useful general solution. Therefore, they use the assumption of small perturbations to justify the replacement of $(R_e - R_a)$ by $(\bar{R} - R_a)$ in the denominator of the right side, which leads to the simple form

$$\frac{dR}{dt} + \frac{1}{M}R = \frac{1}{M}R_e \qquad (5)$$

or

$$\frac{d}{dt}(R-\bar{R}) + \frac{1}{M}(R-R_e) = 0$$

where the time constant, $M = \frac{4.2\ ms\,(\bar{R}-R_a)}{i^2R_aR_o\alpha}$,

is the time required for $(R - \bar{R})$ to become equal to $\frac{1}{e}$ times an original step-function difference, say $(R_i - \bar{R})$. The definition of M is, of course, not dependent upon the assumption of small perturbation. Further details are discussed in reference (2).

Physically, the time constant can be considered as proportional to the product of three factors, functions of the wire material, size and operating conditions respectively:

$$M \sim \left(\frac{\rho_w S}{\gamma_w \alpha}\right)\left(d^4\right)\left(\frac{\bar{R} - R_a}{i^2 R_a}\right) \qquad (6)$$

The attenuation and phase lag in the hot-wire response are compensated up to appropriate frequencies by a suitable network between two of the amplifier stages.

The technique for the measurement of specific statistical kinematic quantities in a turbulent flow need not be discussed in detail here. Adequate descriptions are given in other papers (2, 7, 19 and others). It will be sufficient to point out that $\frac{u'}{\bar{U}}$ is computed directly from a measurement of $\sqrt{\overline{e^2}}$ as given in Eq. (3). $\frac{v'}{\bar{U}}$, $\frac{w'}{\bar{U}}$ and $\overline{uv}$ are measured with directionally sensitive hot-wire instruments, customarily in the form of an X with polar axis perpendicular to the mean velocity direction. Each of the two wires in such an instrument, being inclined to the mean flow, responds to both longitudinal and lateral fluctuations, so that, instead of Eq. (3), we have something like

$$e_{1,2} = \delta \frac{u}{\bar{U}} \pm \varepsilon \frac{v}{\bar{U}}$$

for the two wires. Thus, for example,

$$\frac{u'}{\bar{U}} \sim \sqrt{\overline{(e_1 + e_2)^2}}$$

$$\frac{v'}{U} \sim \sqrt{\overline{(e_1 - e_2)^2}}$$

$$\frac{\overline{uv}}{U} \sim \overline{e_1^2} - \overline{e_2^2}$$

The correlation between u-fluctuations at two different points is obtained in the same way as the shear. Integration of the correlation curve gives the scale of turbulence.

The energy spectrum of turbulence is obtained conventionally with a narrow band-pass filter.

Some corrections for the effect of wire length have been worked out by Skramstad [7], but further detailed analysis along this line is necessary, particularly for the measurement of correlation functions, shear and turbulence spectra. K. Zebb [33] has made some approximate computations for the length correction of X-meters in v' measurements.

E. MEASUREMENT OF MEAN VELOCITY AND TEMPERATURE

In applications of King's equation for thermal equilibrium,

$$\frac{i^2 R}{\bar{R} - \bar{R}_a} = \bar{A} + \bar{B}\sqrt{\bar{v}} \tag{2a}$$

where

$$\bar{A} = \frac{a\,l}{R_o\,\kappa}\,\bar{k} \quad \& \quad \bar{B} = \frac{b\,l}{R_o\,\alpha}\sqrt{d\,\bar{c}_p\,\bar{\rho}\,\bar{k}}$$

to the measurement of mean velocity and temperature in flow with a temperature gradient, the only change from the first part of Section D is that $\bar{A}$ and $\bar{B}$ now vary from point to point in the flow. These variations are determined from the changes in the physical constants of the fluid. The present investigation is restricted to atmospheric air.

Since air is very nearly a perfect gas,

$$\frac{\rho}{\rho_r} = \frac{T_r}{T_a} \tag{7}$$

where the subscript r corresponds to an appropriate reference temperature.

From the International Critical Tables [24], the thermal conductivity of air can be approximated for temperatures up to a few hundred degrees Centigrade by the empirical equation

$$\frac{k}{k_r} = \frac{T_r + 125}{T_a + 125}\left(\frac{T_a}{T_r}\right)^{3/2} \tag{8}$$

This can be approximated by a straight line over a fairly wide temperature range, and, in fact, the linear approximation will be used in the next section.

The variation in C_p with temperature can be neglected in the present discussion, from 0° C to about 300° C.

Thus

$$\frac{\bar{A}}{A_r} = \frac{\bar{k}}{k_r}, \qquad \& \qquad \frac{\bar{B}}{B_r} = \sqrt{\frac{\bar{k}\bar{\rho}}{k_r \rho_r}}$$

or

$$\left.\begin{aligned} \frac{\bar{A}}{A_r} &= \frac{\bar{T}_r + 125}{T_a + 125}\left(\frac{\bar{T}_a}{\bar{T}_r}\right)^{3/2} \\ \text{and} \qquad \frac{\bar{B}}{B_r} &= \sqrt{\frac{\bar{T}_r + 125}{T_a + 125}\left(\frac{\bar{T}_a}{\bar{T}_r}\right)^{1/2}} \end{aligned}\right\} \tag{9}$$

In practice, it is convenient to have these expressions in terms of wire resistances. With

$$\left.\begin{aligned} R_a &= R_o\left[1 + \alpha\,(T_a - 273)\right] \\ R_r &= R_o\left[1 + \alpha\,(T_r - 273)\right] \end{aligned}\right\} \tag{10}$$

Eq. (9) can be written in the form

$$\left.\begin{aligned} \frac{\bar{A}}{A_r} &= \frac{\bar{T}_r + 125}{\bar{T}_r + 125 + \left[\frac{1}{\alpha} + (\bar{T}_r - 273)\right]\left(\frac{\bar{R}_a}{R_n} - 1\right)} \left\{\frac{\bar{T}_r + \left[\frac{1}{\alpha} + (\bar{T}_r - 273)\right]\left(\frac{\bar{R}_a}{\bar{R}_r} - 1\right)}{\bar{T}_r}\right\}^{3/2} \\ \frac{\bar{B}}{B_r} &= \left\{\frac{\bar{T}_r + 125}{\bar{T}_r + 125 + \left[\frac{1}{\alpha} + (\bar{T}_r - 273)\right]\left(\frac{\bar{R}_a}{\bar{R}_r} - 1\right)}\right\}^{1/2} \left\{\frac{\bar{T}_r + \left[\frac{1}{\alpha} + (\bar{T}_r - 273)\right]\left(\frac{\bar{R}_a}{\bar{R}_r} - 1\right)}{\bar{T}_r}\right\}^{1/4} \end{aligned}\right\} \tag{11}$$

For a platinum wire, $\alpha = 0.0037$, $\frac{1}{\alpha} = 270$,

and these can be approximated by

$$\left.\begin{aligned} \frac{\bar{A}}{A_r} &= \left[\frac{\bar{T}_r + 125}{\frac{\bar{R}_a}{\bar{R}_r}\bar{T}_r + 125}\right]\left(\frac{\bar{R}_a}{\bar{R}_r}\right)^{3/2} \\ \frac{\bar{B}}{B_r} &= \left[\frac{\bar{T}_r + 125}{\frac{\bar{R}_a}{\bar{R}_r}\bar{T}_r + 125}\right]^{1/2}\left(\frac{\bar{R}_a}{\bar{R}_r}\right)^{1/4} \end{aligned}\right\} \tag{12}$$

and these are presented in Fig. (1), for $T_r = 293^\circ K$.

With these values of $\bar{A}$ and $\bar{B}$, the mean velocity is determined just as in the case of the simple anemometer. The mean temperature $\bar{T}_a$ is, of course, obtained directly from Eq. (10) which can be combined to give

$$\bar{T}_a = T_r + \left[\frac{1}{\alpha} + (T_r - 273)\right]\left(\frac{\bar{R}_a}{R_r} - 1\right) \qquad (13)$$

which, for a platinum wire becomes approximately

$$\bar{T}_a = T_r\left(\frac{\bar{R}_a}{R_r}\right)$$

It should be emphasized that the accuracy of these results, as well as all those in the following sections, depends upon the accuracy of the physical form of the cooling terms in King's equations. The linear variation of $\frac{i^2\bar{R}}{\bar{R} - \bar{R}_a}$ with $\bar{U}^{1/2}$ has been checked with considerable accuracy by many experimenters; Fig. (2) is a typical isothermal mean velocity calibration of a hot-wire anemometer.

However, there has apparently been no attempt to check the exponents of the other physical quantities as derived by King. Appendix I contains a discussion of this problem, as well as some preliminary experimental results.

F. RESPONSE OF A HOT-WIRE IN AN AIR STREAM WITH BOTH VELOCITY AND TEMPERATURE FLUCTUATIONS

1. The Voltage Fluctuation.

In order to deduce an equation analogous to Eq. (3), we start with King's equation for thermal equilibrium,

$$\frac{i^2 R}{R - R_a} = \frac{a l}{R_o \alpha} k + \frac{b l}{R_o \alpha} \left(d c_p \rho k U \right)^{1/2} \qquad (2)$$

with small fluctuations in velocity and air temperature, we introduce

$$R = \bar{R} + r \qquad U = \bar{U} + u$$

$$R_a = \bar{R}_a + r_a \qquad \rho = \bar{\rho} + \rho'$$

$$k = \bar{k} + k' \qquad c_p = \bar{c}_p$$

so that Eq. (2) becomes, writing $\frac{a l}{R_o \alpha} = P$ and $\frac{b l \sqrt{d c_p}}{R_o \alpha} = Q$,

$$\frac{i^2 (\bar{R} + r)}{(\bar{R} - \bar{R}_a) + (r - r_a)} = P(\bar{k} + k') + Q\left[(\bar{\rho} + \rho')(\bar{k} + k')(\bar{U} + u) \right]^{1/2}$$

Using a binomial expansion for the denominator of the left side, and neglecting products of small quantities on both sides,

$$\frac{i^2 R}{\bar{R} - \bar{R}_a} + \frac{i^2}{(\bar{R} - \bar{R}_a)^2} (\bar{R} r_a - \bar{R}_a r) = P(\bar{k} + k')$$

$$+ Q\left[\bar{\rho} \bar{k} \bar{U} + \rho' \bar{k} \bar{U} + \bar{\rho} k' \bar{U} + \bar{\rho} \bar{k} u \right]^{1/2}$$

Keeping the linear terms of the binomial expansion of the last part,

$$\frac{i^2\bar{R}}{\bar{R}-\bar{R}_a} + \frac{i^2}{(\bar{R}-\bar{R}_a)^2}\left(\bar{R}r_a - \bar{R}_a r\right) = P(\bar{k}+k') + Q(\bar{\rho}\bar{k}\bar{U})^{1/2}\left[1+\frac{1}{2}\left(\frac{\rho'}{\bar{\rho}}+\frac{k'}{\bar{k}}+\frac{u}{\bar{U}}\right)\right]$$

In order to get the fluctuation equation, we subtract the averaged King's equation

$$\frac{i^2\bar{R}}{\bar{R}-\bar{R}_a} = P\bar{k} + Q(\bar{\rho}\bar{k}\bar{U})^{1/2}$$

which leaves

$$\frac{i^2}{(\bar{R}-\bar{R}_a)^2}\left(\bar{R}r_a - \bar{R}_a r\right) = Pk' + \frac{Q}{2}(\bar{\rho}\bar{k}\bar{U})^{1/2}\left(\frac{\rho'}{\bar{\rho}}+\frac{k'}{\bar{k}}+\frac{u}{\bar{U}}\right) \qquad (14)$$

and the next step is to express r_a, k' and ρ' in terms of the small temperature fluctuation, ϑ.

Obviously,

$$r_a = R_o \alpha \vartheta \qquad (15)$$

As mentioned in the previous section, the rather complicated empirical expression for the temperature dependence of the thermal conductivity of air, Eq. (8), can be well approximated over a large temperature range by a single straight line. Hence, with considerable accuracy, we can write

$$k' = n\vartheta \qquad (16)$$

where n is sensibly constant over a range of a few hundred degrees centigrade.

For the density fluctuation, we again consider air as a perfect gas, and approximate to the $\rho(T)$ hyperbola in the vicinity of $\bar{T}_a$ by its tangent. Thus

$$\rho = \bar{\rho}\frac{\bar{T}_a}{T_a} = \bar{\rho} + \rho'$$

$$\therefore \bar{\rho} + \rho' = \bar{\rho}\,\frac{\bar{T}_a}{\bar{T}_a+\vartheta} = \bar{\rho}\,\frac{1}{1+\frac{\vartheta}{\bar{T}_a}}$$

and for $\frac{\vartheta}{\bar{T}_a} << 1$, we find

$$\rho' = -\bar{\rho}\,\frac{\vartheta}{\bar{T}_a} \tag{17}$$

Substituting Eqs. (15), (16) and (17), and introducing the hot-wire voltage fluctuation, $e = ir$, as well as the expressions for P and Q ,

$$\frac{i^2\bar{R}R_0\alpha}{(\bar{R}-\bar{R}_a)^2}\vartheta - \frac{i\bar{R}_a}{(\bar{R}-\bar{R}_a)^2}e = \frac{a\ell n}{R_0\alpha}\vartheta$$

$$+\frac{b\ell}{R_0\alpha}(dc_p\bar{\rho}k\bar{U})^{1/2}\left(-\frac{\vartheta}{\bar{T}_a}+\frac{n\vartheta}{k}+\frac{u}{\bar{U}}\right) \tag{18}$$

Calculation with typical numerical values (see Appendix II) shows that, for most practical purposes, the sum of the two ϑ-terms in the final bracket can be neglected in comparison with the first term in the equation, so they will be omitted in the rest of the discussion.

Collecting the remaining terms

$$\frac{i\bar{R}_a}{(\bar{R}-\bar{R}_a)^2}e = \left[\frac{i^2\bar{R}R_0\alpha}{(\bar{R}-\bar{R}_a)^2}-\frac{a\ell n}{R_0\alpha}\right]\vartheta + \frac{b\ell}{2R_0\alpha}(dc_p\bar{\rho}k\bar{U})^{1/2}\frac{u}{\bar{U}}$$

The functional form desired is $e = e\left(\frac{\vartheta}{\bar{\Theta}}, \frac{u}{\bar{U}}\right)$

Since,

$$\bar{\Theta} = \bar{T}_a - T_r = \frac{\bar{R}_a - R_r}{R_0\alpha} ,$$

we multiply the ϑ-term by $\left(\frac{\bar{R}_a-R_r}{R_0\alpha}\cdot\frac{1}{\bar{\Theta}}\right)$. It is also convenient to replace $\frac{b\ell}{R_0\alpha}(dc_p\bar{\rho}k\bar{U})^{1/2}$ by its equivalent as given in King's

equation. Then, finally,

$$e = \frac{\bar{R}_a - R_r}{i\bar{R}_a}\left[i^2 R - a\ell n\frac{(\bar{R}-\bar{R}_a)^2}{(R_o\alpha)^2}\right]\frac{\theta}{\bar{\Theta}} - \frac{\bar{R}-\bar{R}_a}{2i\bar{R}_a}\left[i^2\bar{R} - \bar{A}(\bar{R}-\bar{R}_a)\right]\frac{u}{\bar{U}} \qquad (19)$$

which obviously reduces to Eq. (3) when the temperature fluctuation level becomes much smaller than the velocity fluctuation level. $\bar{A}$ is determined from the mean speed calibration of the hot-wire, and, of course $\frac{a\ell}{R_o\alpha} = \frac{\bar{A}}{\bar{k}}$.

2. Time Constant.

The general equation is given in Section D:

$$\frac{4.2\,ms}{R_o\alpha}\frac{dR}{dt} = i^2R - (A + B\sqrt{U})(R-R_a) \qquad (1c)$$

Eq. (2) describes an hypothetical equilibrium reached at the instantaneous flow conditions. Substituting for $(A+B\sqrt{U})$ from Eq. (2), we obtain

$$\frac{4.2\,ms}{R_o\alpha}\frac{dR}{dt} = \frac{i^2R_a(R_e-R)}{R_e-R_a} \qquad (20)$$

which is identical with Eq. (4) of reference (2), with the essential difference that here R_a is a fluctuating function of time.

Since, as for the simple anemometer, the general solution of Eq. (20) is apparently not expressible in any applicable form, we now consider possible simplifications for the restriction of small fluctuations, i.e.,

$$\left|\frac{R-\bar{R}}{\bar{R}}\right| << 1 \qquad \& \qquad \left|\frac{R_a-\bar{R}_a}{\bar{R}_a}\right| << 1$$

Hence we may replace R_a by $\bar{R}_a$ in the numerator of the right side of Eq. (20). We may examine the denominator in somewhat the same way as Dryden and Kuethe obtain their Eq. (15), i.e., write

$$R_e - R_a = (\bar{R} - \bar{R}_a) + (R_e - \bar{R}) + (\bar{R}_a - R_a)$$

Then we see that the last two brackets are small compared with the first if we use appreciable heating current. In some cases, when only the temperature fluctuation level is being measured, relatively little heating current is used. With negligible sensitivity to velocity, it is apparent that $(R_e - R_a) \doteq$ const., and, therefore, may be replaced by the average, $(\bar{R}_e - \bar{R}_a)$. However, for small fluctuations, $\bar{R}_e \doteq \bar{R}$, so that we may replace $(R_e - R_a)$ by $(\bar{R} - \bar{R}_a)$ Eq. (20) becomes approximately,

$$\frac{4.2\, ms}{R_o \alpha} \frac{dR}{dt} = \frac{i^2 \bar{R}_a (R_e - R)}{(\bar{R} - \bar{R}_a)} \tag{21}$$

or

$$M' \frac{dR}{dt} = R_e - R \tag{21a}$$

where

$$M' = \frac{4.2\, ms\, (\bar{R} - \bar{R}_a)}{i^2 \bar{R}_a R_o \alpha} \tag{22}$$

so that Eq. (21a) is identical with Dryden and Kuethe's Eq. (15), and $M' = M$, the simple anemometric time constant.

Clearly, from the above analysis, this will not be true for large fluctuations.

With negligible heating current, Eq. (1c) becomes

$$\frac{4.2\, ms}{R_o \alpha} \frac{dR}{dt} = -(A + B\sqrt{U})(R - R_a)$$

From equilibrium, $R_e = R_a$

$$\therefore \frac{4.2\ ms}{R_o \alpha} \frac{dR}{dt} = (A + B\sqrt{U})(R_e - R)$$

or
$$M' \frac{dR}{dt} = R_e - R \tag{21a}$$

where
$$M' = \frac{4.2\ ms}{R_o \alpha (\bar{A} + \bar{B}\sqrt{\bar{U}})} \tag{23}$$

But $(\bar{A} + \bar{B}\sqrt{\bar{U}}) = \frac{i^2 \bar{R}}{\bar{R} - \bar{R}_a} \doteq \frac{i^2 \bar{R}_a}{\bar{R} - \bar{R}_a}$

for the case of extremely small current, so that Eq. (23) is effectively the same as Eq. (22).

A more direct connection appears if we write Eq. (22) as

$$M' = \frac{4.2\ ms}{R_o \alpha} \cdot \frac{1}{(\bar{A} - i^2) + \bar{B}\sqrt{\bar{U}}} \tag{22a}$$

G. MEASUREMENT PROCEDURES

Single Normal Wire

We have seen that the response of a hot-wire to simultaneous velocity and temperature fluctuations is given approximately by

$$e = \frac{\bar{R}_a - \bar{R}_r}{i\,\bar{R}_a}\left[i^2\bar{R} - a\ln\frac{(\bar{R}-\bar{R}_a)^2}{(R_a\alpha)^2}\right]\frac{\vartheta}{\bar{\Theta}} - \frac{\bar{R}-\bar{R}_a}{2i\bar{R}_a}\left[i^2\bar{R} - \bar{A}(\bar{R}-\bar{R}_a)\right]\frac{u}{\bar{U}} \qquad (19)$$

This can be written simply as

$$e = \beta\frac{\vartheta}{\bar{\Theta}} + \delta\frac{u}{\bar{U}} \qquad (19a)$$

where β and δ are functions of the mean-velocity calibration constants, and of the hot-wire operating conditions.

First consider the quantities that can be obtained from the root-mean-square output of single wires set perpendicular to mean flow:

$$\overline{e^2} = \beta^2\overline{\left(\frac{\vartheta}{\bar{\Theta}}\right)^2} + 2\beta\delta\left(\frac{\overline{\vartheta u}}{\bar{\Theta}\bar{U}}\right) + \delta^2\overline{\left(\frac{u}{\bar{U}}\right)^2} \qquad (24)$$

Since β and δ do not increase in the same proportion for a given increase in hot-wire temperature, readings of $\overline{e^2}$ at three different currents at the same point in the flow will give simultaneous linear algebraic equations from which the three unknown quantities can be obtained:

$$\left.\begin{aligned}
\overline{e_1^2} &= \beta_1^2\overline{\left(\frac{\vartheta}{\bar{\Theta}}\right)^2} + 2\beta_1\delta_1\left(\frac{\overline{\vartheta u}}{\bar{\Theta}\bar{U}}\right) + \delta_1^2\overline{\left(\frac{u}{\bar{U}}\right)^2} \\
\overline{e_2^2} &= \beta_2^2\overline{\left(\frac{\vartheta}{\bar{\Theta}}\right)^2} + 2\beta_2\delta_2\left(\frac{\overline{\vartheta u}}{\bar{\Theta}\bar{U}}\right) + \delta_2^2\overline{\left(\frac{u}{\bar{U}}\right)^2} \\
\overline{e_3^2} &= \beta_3^2\overline{\left(\frac{\vartheta}{\bar{\Theta}}\right)^2} + 2\beta_3\delta_3\left(\frac{\overline{\vartheta u}}{\bar{\Theta}\bar{U}}\right) + \delta_3^2\overline{\left(\frac{u}{\bar{U}}\right)^2}
\end{aligned}\right\} \qquad (25)$$

It immediately follows that

$$\overline{\left(\frac{\vartheta}{\bar{\Theta}}\right)^2} = \frac{1}{\Delta} \begin{vmatrix} \overline{e_1^2} & 2\beta_1\delta_1 & \delta_1^2 \\ \overline{e_2^2} & 2\beta_2\delta_2 & \delta_2^2 \\ \overline{e_3^2} & 2\beta_3\delta_3 & \delta_3^2 \end{vmatrix}$$

$$\overline{\left(\frac{\vartheta u}{\bar{\Theta}\bar{U}}\right)} = \frac{1}{\Delta} \begin{vmatrix} \beta_1^2 & \overline{e_1^2} & \delta_1^2 \\ \beta_2^2 & \overline{e_2^2} & \delta_2^2 \\ \beta_3^2 & \overline{e_3^2} & \delta_3^2 \end{vmatrix}$$

$$\overline{\left(\frac{u}{\bar{U}}\right)^2} = \frac{1}{\Delta} \begin{vmatrix} \beta_1^2 & 2\beta_1\delta_1 & \overline{e_1^2} \\ \beta_2^2 & 2\beta_2\delta_1 & \overline{e_2^2} \\ \beta_3^2 & 2\beta_3\delta_3 & \overline{e_3^2} \end{vmatrix}$$

where $$\Delta = \begin{vmatrix} \beta_1^2 & 2\beta_1\delta_1 & \delta_1^2 \\ \beta_2^2 & 2\beta_2\delta_2 & \delta_2^2 \\ \beta_3^2 & 2\beta_3\delta_3 & \delta_3^2 \end{vmatrix}$$

In general, due to the rather complicated forms of β and δ, these determinants will be tedious to evaluate. However, the procedure may be made a bit more convenient by fixing the ratio $\bar{R}_1 : \bar{R}_2 : \bar{R}_3$, and setting up appropriate calculation charts.

Possible Shortcuts

I. In order to measure either $\overline{\left(\frac{\vartheta}{\bar{\Theta}}\right)^2}$ or $\overline{\left(\frac{u}{\bar{U}}\right)^2}$ directly, it is necessary to make either δ or β negligible, i.e.,

$$(\bar{R}_a - R_r)\left[i^2\bar{R} - a\ln\frac{(\bar{R}-\bar{R}_a)^2}{(R_0\alpha)^2}\right] \begin{matrix} >> \\ \text{or} \\ << \end{matrix} \frac{1}{2}(\bar{R}-\bar{R}_a)\left[i^2\bar{R} - \bar{A}(\bar{R}-\bar{R}_a)\right]$$

We can find what this means in terms of operating conditions at a given point in the flow by replacing the electrical quantities with fluid mechanical quantities as far as possible. Then the inequality can be written, after some algebra, as

$$\left[\left(\bar{A} + \bar{B}\sqrt{\bar{U}}\right)\frac{R_o a}{(\bar{R}-\bar{R}_a)} - \frac{\bar{A}}{\bar{R}}\right]\bar{\Theta} \overset{>> \text{ or } <<}{} \frac{\bar{B}}{2}\sqrt{\bar{U}} \qquad (26)$$

For the entire range of practicable operation, the first term in the bracket is larger than the second. Therefore, it is evident that for a given flow, β is maximized relative to δ by minimizing $(\bar{R} - \bar{R}_a)$, and vice-versa. Whether either of these extremes can, in practice, make $\beta >> \delta$ or $\beta << \delta$ can be checked numerically from a typical hot-wire calibration.

It will be noted that the first term in the bracket is the only one of the three that can be varied by changing the hot-wire current. It turns out that, when both $\bar{\Theta}$ and $\bar{U}$ are large, the only feasible inequality is that obtained by reducing the heating current so that $\beta >> \delta$; this ordinarily leads to the additional simplification,

$$\beta \doteq i\,(\bar{R}_a - R_r)$$

for the sensitivity of the simple resistance thermometer.

Eq. (26) also gives the obvious result that reducing $\bar{\Theta}$ toward zero will eventually make $\beta << \delta$, and then the wire is a simple anemometer.

II. Another possibility for direct measurement is the use of two close parallel wires of different diameters, whose voltage is subtracted before entering the amplifier. Then, if $\beta_1 = \beta_2$, the

difference will measure $\overline{\left(\frac{u}{\bar{U}}\right)^2}$, while if $\delta_1 = \delta_2$, the difference will measure $\overline{\left(\frac{\vartheta}{\bar{\Theta}}\right)^2}$. Of course, they must be far enough apart to be insensitive to lateral velocity fluctuations.

The general requirements for $\beta_1 = \beta_2$ are extremely complicated if the general expression for β is used. However, for fairly small currents, the second term in β is negligible compared with the first. In cases where this is true, $\beta_1 = \beta_2$ means

$$i \frac{\bar{R}_1}{\bar{R}_{a_1}} (\bar{R}_{a_1} - R_{r_1}) = i_2 \frac{\bar{R}_2}{\bar{R}_{a_2}} (\bar{R}_{a_2} - R_{r_2})$$

But $\frac{\bar{R}_{a_1} - R_{r_1}}{\bar{R}_{a_1}} = \frac{\bar{R}_{a_2} - R_{r_2}}{\bar{R}_{a_2}}$ so that

$$i_1 \bar{R}_1 = i_2 \bar{R}_2 \tag{27}$$

This relation can be satisfied physically, but the problem of correct compensation for the two wires of different diameters would probably require that the fluctuating voltages be subtracted after leaving matched amplifiers, before entering the output circuit.

The requirement for $\delta_1 = \delta_2$ is rather complicated, and this case will not ordinarily be necessary, since it is usually possible to make $\delta \ll \beta$

Directionally Sensitive Meters (e.g., X and II)

In an ideal meter, the two wires are identical, so that the voltage fluctuations will be

$$\left.\begin{aligned} e_1 &= \beta \frac{\vartheta}{\bar{\Theta}} + \delta \frac{u}{\bar{U}} + \varepsilon \frac{v}{\bar{U}} \\ e_2 &= \beta \frac{\vartheta}{\bar{\Theta}} + \delta \frac{u}{\bar{U}} - \varepsilon \frac{v}{\bar{U}} \end{aligned}\right\} \tag{28}$$

Subtracting the voltages before amplification and measuring the mean square leads to

$$\overline{\left(\frac{v}{\bar{U}}\right)^2} = \frac{\overline{(e_1 - e_2)^2}}{4\varepsilon^2} \tag{29}$$

thus giving the lateral turbulence level.

Taking the mean square output of each wire separately, we get

$$\overline{e_1^2} = \beta^2\overline{\left(\frac{\vartheta}{\bar{\Theta}}\right)^2} + \delta^2\overline{\left(\frac{u}{\bar{U}}\right)^2} + \varepsilon^2\overline{\left(\frac{v}{\bar{U}}\right)^2} + 2\beta\delta\frac{\overline{\vartheta u}}{\bar{\Theta}\bar{U}} + 2\beta\varepsilon\frac{\overline{\vartheta v}}{\bar{\Theta}\bar{U}} + 2\delta\varepsilon\frac{\overline{uv}}{\bar{U}^2}$$

$$\overline{e_2^2} = \beta^2\overline{\left(\frac{\vartheta}{\bar{\Theta}}\right)^2} + \delta^2\overline{\left(\frac{u}{\bar{U}}\right)^2} + \varepsilon^2\overline{\left(\frac{v}{\bar{U}}\right)^2} + 2\beta\delta\frac{\overline{\vartheta u}}{\bar{\Theta}\bar{U}} - 2\beta\varepsilon\frac{\overline{\vartheta v}}{\bar{\Theta}\bar{U}} - 2\delta\varepsilon\frac{\overline{uv}}{\bar{U}^2}$$

After subtraction,

$$\overline{e_1^2} - \overline{e_2^2} = 4\beta\varepsilon\frac{\overline{\vartheta v}}{\bar{\Theta}\bar{U}} + 4\delta\varepsilon\frac{\overline{uv}}{\bar{U}^2} \tag{30}$$

The turbulent momentum and heat transfer are determined by repeating Eq. (30) at a different current and solving the resulting pair of simultaneous linear equations. Of cours, the two terms in Eq. (30) are proportional to the turbulent shear and heat transfer only if the density fluctuations can be neglected (Appendix V).

If the hot-wire instrument is unsymmetrical, the analysis is more complicated, but essentially the same. For purely kinematic measurements, the generalization is given in reference (20).

Just as in the case of the single wire, direct measurement of $\frac{\overline{\vartheta v}}{\bar{\Theta}\bar{U}}$ or $\frac{\overline{uv}}{\bar{U}^2}$ is possible if $\delta \ll \beta$ or $\delta \gg \beta$, respectively. Again it is to be expected that in a fairly hot jet only the former condition is obtainable.

In the general case, corresponding to Eq. (30), and in all other correlation measurements involving thermal and kinematic variables simultaneously, the direct measurement of correlation coefficients (e.g., $\frac{\overline{\vartheta v}}{\vartheta' v'}$, $\frac{\overline{uv}}{u'v'}$, etc.) is apparently not usually possible. Such direct determination is common practice in purely kinematic measurements.

Correlations Between Different Points

For two single wires, set parallel to each other and perpendicular to the flow, assuming the ideal case of identical wires at the same sensitivity,

$$\left.\begin{aligned} e_1 &= \beta \frac{\vartheta_1}{\overline{\Theta}} + \delta \frac{u_1}{\overline{U}} \\ e_2 &= \beta \frac{\vartheta_2}{\overline{\Theta}} + \delta \frac{u_2}{\overline{U}} \end{aligned}\right\} \qquad (31)$$

Adding and subtracting the fluctuating voltages gives

$$\overline{(e_1 + e_2)^2} = \beta^2 \overline{\left(\frac{\vartheta_1 + \vartheta_2}{\overline{\Theta}}\right)^2} + 2\beta\delta \overline{\left(\frac{\vartheta_1 + \vartheta_2}{\overline{\Theta}}\right)\left(\frac{u_1 + u_2}{\overline{U}}\right)} + \delta^2 \overline{\left(\frac{u_1 + u_2}{\overline{U}}\right)^2}$$

$$\overline{(e_1 - e_2)^2} = \beta^2 \overline{\left(\frac{\vartheta_1 - \vartheta_2}{\overline{\Theta}}\right)^2} + 2\beta\delta \overline{\left(\frac{\vartheta_1 - \vartheta_2}{\overline{\Theta}}\right)\left(\frac{u_1 - u_2}{\overline{U}}\right)} + \delta^2 \overline{\left(\frac{u_1 - u_2}{\overline{U}}\right)^2}$$

Expanding the above expressions, and subtracting,

$$\begin{aligned} \overline{(e_1 + e_2)^2} - \overline{(e_1 - e_2)^2} &= 4\beta^2 \left(\frac{\overline{\vartheta_1 \vartheta_2}}{\overline{\Theta}^2}\right) \\ &+ 4\beta\delta \left[\left(\frac{\overline{\vartheta_1 u_2}}{\overline{\Theta}\,\overline{U}}\right) + \left(\frac{\overline{\vartheta_2 u_1}}{\overline{\Theta}\,\overline{U}}\right)\right] + 4\delta^2 \left(\frac{\overline{u_1 u_2}}{\overline{U}^2}\right) \end{aligned} \qquad (32)$$

and the three bracketed quantities on the right side can be obtained by making readings at three different hot-wire currents. The physical significance of the cross-product term is not immediately evident.

Of course, with $\beta \gg \delta$, the thermal correlation function, and hence the thermal scale, is measurable directly.

The correlation between v-fluctuations at different points can be determined by using two double wire meters, measuring the mean square of the sum of the differences of the individual meter differences. It can also be measured with symmetrically inclined single wires.

Spectrum

If $\frac{\vartheta'}{\Theta}$ and $\frac{u'}{U}$ are the same order of magnitude in a flow with appreciable velocity and temperature differences, it may be possible to measure only the ϑ'-spectrum directly. This is true for cases in which it is not feasible to make $\delta \gg \beta$ because of wire temperature limitations. Then it may be necessary to obtain the u'-spectrum with a meter made up of two wires of differing diameters as described previously.

However, for temperature differences up to perhaps 100° C, it does not seem likely that the nature of the turbulence will be changed essentially in a flow of moderate velocity. Therefore, to a good approximation, it would seem satisfactory to determine the u'-spectrum at reduced $\bar{\Theta}$.

It should be noted that the v'-spectrum is directly measurable in all cases.

H. MEASUREMENT OF MEAN VELOCITY AND CONCENTRATION IN AN ISOTHERMAL FLOWING MIXTURE OF TWO GASES

As in Section E, we start with King's equation for thermal equilibrium,

$$\frac{i^2\bar{R}}{\bar{R}-R_a} = \bar{A} + \bar{B}\sqrt{\bar{U}} \qquad (2)$$

where $\bar{A} = \frac{a\ell}{R_o\alpha}\bar{k}$ and $\bar{B} = \frac{b\ell}{R_o\alpha}(d\,\bar{c}_p\,\bar{\rho}\,\bar{k}\,\bar{U})^{1/2}$

Again, $\bar{A}$ and $\bar{B}$ are not constants, but depend upon the local physical constants of the flow, and, therefore, are a function of the relative concentration.

As indicated in the table of notation, the concentration used in this analysis is the molal concentration. Further remarks on this are included in Appendix IV.

We write the expressions for the mean physical constants of the mixture as

$$\left.\begin{aligned} \bar{\rho} &= \rho_a + \bar{\Gamma}\Delta\rho \\ \bar{c}_p &= c_{p_a} + \bar{\Gamma}\Delta c_p \\ \bar{k} &= k_a + f(\bar{\Gamma})\,\Delta k \end{aligned}\right\} \qquad (33)$$

The thermal conductivity of gas mixtures is generally not a simple weighted average [25], and varies considerably for different pairs of gases. If $k(\Gamma)$ is a known function, the procedure is relatively simple, and for most pairs of gases for which data are available [26], $f(\Gamma)$ can be well approximated by a quadratic or cubic polynomial. If $k(\Gamma)$ is unknown, which is

still the case for many pairs of common gases, it can be determined as one of the unknowns by an extra measurement at each point in the flow. We shall treat both cases.

I. $k(T)$ a Known Function

For this discussion, assume that $f(\bar{T})$ can be approximated by a parabola:

$$\bar{k} = k_a + (\xi \bar{T} + \varsigma \bar{T}^2)\,\Delta k \qquad (33a)$$

Eq. (2) can be written as

$$\frac{i^2 R}{\bar{R} - R_a} = \frac{a l}{R_o \alpha}\left[k_a + (\xi \bar{T} + \varsigma \bar{T}^2)\,\Delta k\right] + \frac{b l \sqrt{d}}{R_o \alpha}\left(C_{p_a} + \bar{T}\Delta C_p\right)^{1/2}\left(\rho_a + \bar{T}\Delta\rho\right)^{1/2}\left[k_a + (\xi \bar{T} + \varsigma \bar{T}^2)\,\Delta k\right]^{1/2} \bar{U}^{1/2} \qquad (34)$$

This equation is to be used to transform appropriate readings of $\frac{i^2 \bar{R}}{\bar{R} - R_a}$ at a point into values of the two unknowns, $\bar{U}$ and $\bar{T}$. Perhaps the most convenient method is to record $\frac{i^2 \bar{R}}{\bar{R} - R_o}$ at the same point with two hot-wires differing in diameter, so that $\left(\frac{b l \sqrt{d}}{R_o \alpha}\right)_1 \neq \left(\frac{b l \sqrt{d}}{R_o \alpha}\right)_2$. According to King's equation, the coefficients of the first term will be the same if the wires are of the same material, but, experimentally, they usually turn out to be different also.

Then the readings of the two hot-wires yield simultaneous equations for $\bar{U}$ and $\bar{T}$:

$$\phi_1 = M_1\left[k_a + (\xi \bar{T} + \varsigma \bar{T}^2)\,\Delta k\right] + N_1\left(C_{p_a} + \bar{T}\Delta C_p\right)^{1/2}\left(\rho_a + \bar{T}\Delta\rho\right)^{1/2}\left[k_a + (\xi \bar{T} + \varsigma \bar{T}^2)\,\Delta k\right]^{1/2} \bar{U}^{1/2}$$

$$\phi_2 = M_2\left[k_a + (\xi \bar{T} + \varsigma \bar{T}^2)\,\Delta k\right] + N_2\left(C_{p_a} + \bar{T}\Delta C_p\right)^{1/2}\left(\rho_a + \bar{T}\Delta\rho\right)^{1/2}\left[k_a + (\xi \bar{T} + \varsigma \bar{T}^2)\,\Delta k\right]^{1/2} \bar{U}^{1/2}$$

where

$$\phi = \frac{i^2 R}{\bar{R} - R_a} \quad ; \quad M = \frac{a\,l}{R_a \alpha} \quad ; \quad N = \frac{b\,l\sqrt{d}}{R_a \alpha}$$

Multiplying the first equation by N_2 and the second by N_1 and subtracting, we can solve for $[k_a + (\xi \bar{\Gamma} + \varphi \bar{\Gamma}^2)\Delta k]$ and the resulting quadratic equation can be solved for $\bar{\Gamma}$ Provided that $k(\Gamma)$ is a monotonic function, only one of the two solutions of this quadratic will have any physical meaning.

This value of $\bar{\Gamma}$ can then be substituted into either equation to obtain $\bar{U}$. This latter step can be done graphically if we draw up a mean velocity calibration of either hot-wire, giving $\frac{i^2 \bar{R}}{\bar{R} - R_a}$ versus $\sqrt{\bar{U}}$ with straight lines of constant $\bar{\Gamma}$. The two limiting lines, $\bar{\Gamma} = 0$ and $\bar{\Gamma} = 1.0$, can be determined experimentally.

For research in turbulent material diffusion it will be of particular interest to use a gas such that $\rho_g \doteq \rho_a$ (e.g., ethylene). In that case, a somewhat shorter technique can be used: a pitot tube will give $\bar{U}$ directly, and then $\bar{\Gamma}$ can be determined from a single hot-wire reading and the family of calibration curves described above.

II. $k(\Gamma)$ Unknown

In this case it is convenient to work with the readings of two different hot-wires and a pitot tube at each point.

The two hot-wires give

$$\phi_1 = M_1\left[k_a + f(\bar{\Gamma})\Delta k\right] + N_1 (c_{\rho_a} + \bar{\Gamma}\Delta c_\rho)^{1/2} (\rho_a + \bar{\Gamma}\Delta\rho)^{1/2} \left[k_a + f(\bar{\Gamma})\Delta k\right]^{1/2} \bar{U}^{1/2}$$

$$\phi_2 = M_2\left[k_a + f(\bar{\Gamma})\Delta k\right] + N_2 (c_{\rho_a} + \bar{\Gamma}\Delta c_\rho)^{1/2} (\rho_a + \bar{\Gamma}\Delta\rho)^{1/2} \left[k_a + f(\bar{\Gamma})\Delta k\right]^{1/2} \bar{U}^{1/2} \qquad (35)$$

where $$\phi = \frac{i^2 \bar{R}}{\bar{R} - R_a} \; ; \quad M = \frac{a\ell}{R_o \alpha} \quad ; \quad N = \frac{b\ell \sqrt{\sigma}}{R_o \alpha}$$

Multiplying the first equation by N_2, the second by N_1, and subtracting, we get

$$k_a + f(\bar{\Gamma}) \Delta k = \frac{\phi_1 N_2 - \phi_2 N_1}{M_1 N_2 - M_2 N_1} = K_a \quad (say) \tag{36}$$

Substituting Eq. (36) into the expression for ϕ_1,

$$\phi_1 = M_1 K_a + N_1 (c_p + \bar{\Gamma} \Delta c_p)^{1/2} (\rho_a + \bar{\Gamma} \Delta \rho)^{1/2} K_a^{1/2} \bar{U}^{1/2}$$

or, $$(c_{p_a} + \bar{\Gamma} \Delta c_p)^{1/2} (\rho_a + \bar{\Gamma} \Delta \rho)^{1/2} \bar{U}^{1/2} = \frac{\phi_1 - M_1 K_a}{N_1 K_a^{1/2}} = K_b \quad (say) \tag{37}$$

A reading at the same point with a pitot tube gives

$$q = \tfrac{1}{2} (\rho_a + \bar{\Gamma} \Delta \rho) \bar{U}^2 \tag{38}$$

Thus

$$(\rho_a + \bar{\Gamma} \Delta \rho)^{1/2} = \frac{(2q)^{1/2}}{\bar{U}}$$

which is substituted into Eq. (37) to give $\bar{\Gamma}(\bar{U})$:

$$\bar{\Gamma} = \frac{1}{\Delta c_p} \left(\frac{K_b^2}{2q} \bar{U} - c_{p_a} \right) \tag{39}$$

However, Eq. (38) also gives $\bar{\Gamma}(\bar{U})$ directly:

$$\bar{\Gamma} = \frac{1}{\Delta \rho} \left(\frac{2q}{\bar{U}^2} - \rho_a \right) \tag{38a}$$

and these two expressions are equated to give a cubic for $\bar{U}$:

$$\bar{U}^3 + \frac{2q \Delta c_p}{K_b^2} \left(\frac{\rho_a}{\Delta \rho} - \frac{c_{p_a}}{\Delta c_p} \right) \bar{U}^2 - \frac{4q^2}{K_b^2} \frac{\Delta c_p}{\Delta \rho} = 0 \tag{40}$$

Having the value of $\bar{U}$ at a point, we obtain $\bar{\Gamma}$ from Eq. (38a) or Eq. (39). The last unknown is the function $k(\bar{\Gamma})$

The values of K_a at several points immediately permit solution for $f(\bar{\Gamma})$. For example, suppose it is assumed that f

can be approximated by a cubic, $f = a_1 \bar{\Gamma} + a_2 \bar{\Gamma}^2 + a_3 \bar{\Gamma}^3$

From readings at three different points in the flow, Eq. (36) yields three simultaneous equations for the unknown coefficients,

$$\left.\begin{aligned} \bar{\Gamma}_1 a_1 + \bar{\Gamma}_1^2 a_2 + \bar{\Gamma}_1^3 a_3 &= \frac{K a_1 - k_a}{\Delta k} \\ \bar{\Gamma}_2 a_1 + \bar{\Gamma}_2^2 a_2 + \bar{\Gamma}_2^3 a_3 &= \frac{K a_2 - k_a}{\Delta k} \\ \bar{\Gamma}_3 a_1 + \bar{\Gamma}_3^2 a_2 + \bar{\Gamma}_3^3 a_3 &= \frac{K a_3 - k_a}{\Delta k} \end{aligned}\right\} \qquad (41)$$

Of course, the three points should be rather widely spaced, and errors can be reduced by choosing several sets of three points at random.

I. RESPONSE OF A HOT-WIRE IN AN ISOTHERMAL FLOWING MIXTURE WITH BOTH VELOCITY AND CONCENTRATION FLUCTUATIONS

I. Voltage Fluctuations

We start again with King's equation

$$\frac{i^2 R}{R - R_a} = \frac{a l}{R_a \alpha} k + \frac{b l}{R_a \alpha} (d c_p \rho k U)^{1/2} \tag{2}$$

and introduce small fluctuations in velocity and concentration:

$$\left.\begin{aligned} R &= \bar{R} + r & \rho &= \bar{\rho} + \rho' \\ k &= \bar{k} + k' & U &= \bar{U} + u \\ c_p &= \bar{c}_p + c_p' & \Gamma &= \bar{\Gamma} + \gamma \end{aligned}\right\} \tag{42}$$

From Eq. (33),

$$\left.\begin{aligned} \rho' &= \gamma \Delta \rho \\ c_p' &= \gamma \Delta c_p \\ k' &= \frac{d f(\bar{\Gamma})}{d \bar{\Gamma}} \gamma \Delta k \end{aligned}\right\} \tag{43}$$

Substituting Eq. (38) into Eq. (2), using appropriate binomial expansions, neglecting products of small quantities, and subtracting the averaged form of Eq. (2), we obtain

$$-\frac{i^2 R_a r}{(\bar{R} - R_a)^2} = \bar{A} \frac{k'}{\bar{k}} + \frac{\bar{B}}{2} \bar{U}^{1/2} \left[\frac{c_p'}{\bar{c}_p} + \frac{\rho'}{\bar{\rho}} + \frac{k'}{\bar{k}} + \frac{u}{\bar{U}} \right] \tag{44}$$

But e.ir , the $\bar{B}$ can be replaced according to the averaged equation, and c_p', ρ' and k' are given in Eq. (43). Thus

$$e = -\frac{(\bar{R} - R_a)^2}{i R_a} \left\{ \bar{A} \bar{\Gamma} \frac{d f}{d \bar{\Gamma}} \frac{\Delta k}{\bar{k}} + \frac{1}{2} \left(\frac{i^2 \bar{R}}{\bar{R} - R_a} - \bar{A} \right) \left[\frac{\Delta c_p}{\bar{c}_p} + \frac{\Delta \rho}{\bar{\rho}} + \frac{d f}{d \bar{\Gamma}} \frac{\Delta k}{\bar{k}} \right] \bar{\Gamma} \right\} \frac{\gamma}{\bar{\Gamma}}$$

$$- \frac{(\bar{R} - R_a)^2}{2 i R_a} \left(\frac{i^2 \bar{R}}{\bar{R} - R_a} - \bar{A} \right) \frac{u}{\bar{U}} \tag{45}$$

A more convenient form is obtained by substituting

$$\frac{\Delta c_p}{\bar{c}_p}\bar{\Gamma} = \frac{\Delta c_p \bar{\Gamma}}{c_{p_a} + \bar{\Gamma}\Delta c_p} = \frac{1}{1 + \frac{c_{p_a}}{\bar{\Gamma}\Delta c_p}}$$

$$\frac{\Delta \rho}{\bar{\rho}}\bar{\Gamma} = \frac{1}{1 + \frac{\rho_a}{\bar{\Gamma}\Delta\rho}}$$

$$\frac{\Delta k}{\bar{k}}\bar{\Gamma} = \frac{1}{\frac{f}{\bar{\Gamma}} + \frac{k_a}{\bar{\Gamma}\Delta k}}$$

Also, the $\frac{\Delta k}{\bar{k}}$ -terms can be combined. Then the final form of the equation giving the instantaneous voltage fluctuation due to concentration and velocity fluctuations is

$$e = -\frac{(\bar{R}-R_a)^2}{2iR_a}\left\{\left(\frac{i^2\bar{R}}{\bar{R}-R_a} + \bar{A}\right)\frac{\frac{df}{d\bar{\Gamma}}}{\frac{f}{\bar{\Gamma}} + \frac{k_a}{\bar{\Gamma}\Delta k}} + \left(\frac{i^2\bar{R}}{\bar{R}-R_a} - \bar{A}\right)\left[\frac{1}{1+\frac{c_{p_a}}{\bar{\Gamma}\Delta c_p}} + \frac{1}{1+\frac{\rho_a}{\bar{\Gamma}\Delta\rho_a}}\right]\right\}\frac{\gamma}{\bar{\Gamma}}$$

$$-\frac{(\bar{R}-R_a)^2}{2iR_a}\left(\frac{i^2\bar{R}}{\bar{R}-R_a} - \bar{A}\right)\frac{u}{\bar{U}} \qquad (46)$$

For $\bar{\Gamma} = 0$ or $\frac{\gamma}{\bar{\Gamma}} = 0$, Eq. (46) reduces to Eq. (30), the response equation for the simple anemometer. In general, for concentration and velocity fluctuations of the same order of magnitude, none of the terms in Eq. (46) is negligible. Typical values are given in Appendix II.

As mentioned in the previous section, investigations on material diffusion in turbulent flow will first be concerned with the mixing of two gases of equal densities, in which case $\Delta\rho = 0$.

II. Time Constant

From Section D,

$$\frac{4.2 m s}{R_o \alpha} \frac{dR}{dt} = i^2 R - (A + B\sqrt{\bar{U}})(R - R_a) \qquad (1c)$$

With Eq. (2), this again gives

$$\frac{4.2 m s}{R_o \alpha} \frac{dR}{dt} = \frac{i^2 R_a (R_e - R)}{R_e - R_a} \qquad (4)$$

which is identical with Eq. (4) of reference (2). Hence, with the usual restriction of small fluctuations, we use the same approximation in the denominator of the right side:

$$R_e - R_a = (\bar{R} - R_a) + (R_e - \bar{R}) \doteq \bar{R} - R_a$$

so that Eq. (4) becomes approximately

$$\frac{4.2 m s}{R_o \alpha} \frac{dR}{dt} = \frac{i^2 R_a (R_e - R)}{\bar{R} - R_a} \qquad (5)$$

or

$$\frac{d}{dt}(R - \bar{R}) + \frac{1}{M''}(R - R_e) = 0$$

where

$$M'' = \frac{4.2 m s (\bar{R} - R_a)}{i^2 R_a R_o \alpha}$$

just as for the simple anemometer.

Of course, the numerical value of the time constant in this case is a function of both local mean velocity and mean concentration.

J. MEASUREMENT PROCEDURES

Single Normal Wire

The voltage fluctuation for a simple hot-wire set normal to the mean flow direction, Eq. (46), may be written as

$$e = \mu \frac{r}{\bar{r}} + \delta \frac{u}{\bar{U}} \qquad (46a)$$

The general procedure to be followed in using Eq. (46) to determine $\overline{\left(\frac{r}{\bar{r}}\right)^2}$, $\overline{\left(\frac{u}{\bar{U}}\right)^2}$ and $\left(\frac{\overline{ru}}{\bar{r}\bar{U}}\right)$ is similar to that for the temperature fluctuation problem, with an essential difference: in this case the three readings of $\overline{e^2}$ taken at a given point in the flow cannot ordinarily be made simply with the same hot-wire operating at different temperatures. This is due, of course, to the fact that μ and δ vary proportionally with changes in wire current (or temperature) at a given point in the flow. Instead, three wires with non-proportional mean calibration constants must be used. According to King's equation, this is possible only with three wires of differing diameters. However, in actual practice, the ordinary differences in A and B between two wires of the same nominal diameter may provide sufficient variation for this method.

It should also be pointed out that, since A is a function of the radiation loss, it may be possible to make at least two of the three necessary readings by using one hot-wire at widely differing temperatures.

Thus, the equations to be solved are completely analogous to Eq. (25), and need not be written out.

Possible Shortcuts

In general, it is not possible to make $\mu \ll \delta$ or $\mu \gg \delta$ for ordinary ranges of concentration and velocity. However, it may be possible to use two close parallel wires whose voltage is subtracted before entering the amplifier. Then, if $\mu_1 = \mu_2$, the difference will measure $\left(\overline{\frac{u}{U}}\right)^2$, while if $\delta_1 = \delta_2$, the difference will measure $\left(\overline{\frac{r}{R}}\right)^2$. As pointed out in Section G, the wires must, of course, be far enough apart to have negligible sensitivity to v'.

The conditions necessary for making $\mu_1 = \mu_2$ without simultaneously making $\delta_1 = \delta_2$ are so complex as to seem impracticable. The inverse condition is a bit simpler:

$$\frac{(\bar{R}_1 - R_{a_1})^2}{i_1 R_{a_1}} B_1 = \frac{(\bar{R}_2 - R_{a_2})^2}{i_2 R_{a_2}} B_2 \qquad (47)$$

But even this is extremely difficult to employ. In fact, let us consider perhaps the simplest conceivable assumptions which may still be satisfied by a pair of wires: let $B_1 = B_2$ and $R_{a_1} = R_{a_2}$ with the specific condition that $A_1 \neq A_2$, since equal A's together with the other conditions would also make $\mu_1 = \mu_2$. Now Eq. (47) becomes

$$\frac{i_1}{i_2} = \frac{(\bar{R}_1 - R_a)^2}{(\bar{R}_2 - R_a)^2} \qquad (48)$$

In order to predict the necessary currents, the R_1 and R_2 must be eliminated. This leads to

$$\frac{i_2^3}{i_1^3} = \frac{(\bar{A}_2 - i_2^2 + \bar{B}\sqrt{\bar{U}})^2}{(\bar{A}_1 - i_1^2 + \bar{B}\sqrt{\bar{U}})^2}$$

which should be solved explicitly for $i_2(i_1)$. This is not

generally possible. Therefore, if this approach is to be used for direct measurement of $\overline{\left(\frac{r}{\bar{r}}\right)^2}$, perhaps a feasible technique would be to satisfy Eq. (48) by trial and error.

Also, it should be noted that, since this assumes nearly identical wires operating at different temperatures, the time constants will be different, and separate matched amplifiers will be necessary.

Directionally Sensitive Meters

The general approach and procedure is completely analogous to that described for simultaneous temperature and velocity fluctuations.

Assuming a symmetrical meter,

$$\left.\begin{aligned} e_1 &= \mu \frac{r}{\bar{r}} + \delta \frac{u}{\bar{U}} + \varepsilon \frac{v}{\bar{U}} \\ e_2 &= \mu \frac{r}{\bar{r}} + \delta \frac{u}{\bar{U}} - \varepsilon \frac{v}{\bar{U}} \end{aligned}\right\} \tag{49}$$

These give

$$\overline{\left(\frac{v}{\bar{U}}\right)^2} = \frac{\overline{(e_1 - e_2)^2}}{4\varepsilon^2} \tag{50}$$

and

$$\overline{e_1^2} - \overline{e_2^2} = 4\mu\varepsilon\left(\frac{\overline{rv}}{\bar{r}\bar{U}}\right) + 4\delta\varepsilon\left(\frac{\overline{uv}}{\bar{U}^2}\right) \tag{51}$$

Thus the turbulent shear and lateral diffusion of material are obtained by repeating Eq (51) with an appropriately different instrument, and solving the resulting pair of simultaneous equations. Of course, the terms in Eq. (51) are proportional to the turbulent shear and material transfer only if the density fluctuations can be neglected (Appendix V).

Correlations Between Different Points

An approach identical with that for the temperature and velocity fluctuations gives, instead of Eq. (32),

$$\overline{(e_1 + e_2)^2} - \overline{(e_1 - e_2)^2} = 4\mu^2\left(\frac{\overline{r_1 r_2}}{\bar{r}^2}\right) + 4\mu\delta\left(\frac{\overline{r_1 u_2}}{\bar{r}\bar{v}} + \frac{\overline{r_2 u_1}}{\bar{r}\bar{v}}\right) + 4\delta^2\left(\frac{\overline{u_1 u_2}}{\bar{v}^2}\right) \qquad (52)$$

and the three bracketed quantities on the right side can be obtained by repeating the readings with two other appropriately different pairs of hot-wires.

Again, unlike the case of Section G, we cannot measure either $\frac{\overline{r_1 r_2}}{\bar{r}^2}$ or $\frac{\overline{u_1 u_2}}{\bar{v}^2}$ directly.

The correlation between v-fluctuations at two different points is determinable as outlined in Section G.

Spectrum

Since, in general, we cannot make $\mu \gg \delta$ or $\mu \ll \delta$ no direct measurement of either the r'-spectrum or the u'-spectrum can be made.

In the case of gases whose densities and viscosities are not too widely different, the u'-spectrum in the mixing gases is probably quite close to that in a similar flow of either component alone, for which case it is easily measurable. A comparison of this pure gas u'-spectrum with an e'-spectrum measured in the mixture may, at least, give a rough idea of the direction in which the r'-spectrum varies as compared with u'.

Again it should be noted that the v'-spectrum is measurable directly in a flowing gas mixture with concentration fluctuations.

K. DISCUSSION

In general, the errors inherent in these new applications of the hot-wire anemometer are the same as for the simple anemometer (2, 27, 28 and others), and hence need not be discussed here.

Perhaps the only additional source of error arises simply from the added complication of many of these measurements. This influences the result in two ways: (a) the final numerical result is obtained from more separate readings of fluctuating quantities than is the case in ordinary anemometric applications; (b) the appreciably greater time required for measurement at each point in the flow results in greater difficulty in maintaining the "steady state" condition of the apparatus, both aerodynamic and electrical.

It should also be noted that the hot-wire length corrections will be different for the different quantities, since each case must be computed form the correlation function of the physical quantity in question.

The details of the present analysis assume the validity of King's equation in its conventional form. The accuracy with which this equation predicts the influence of velocity changes has been verified countless times; preliminary attempts to verify or disprove the rest of this equation

(Appendix I) have been indecisive. Considerably more careful measurements must be made, both in different pure gases and in a pure gas at various temperatures.

However, the general method presented here is equally applicable to a possibly more accurate heat transfer equation that may be found in the future.

The possible usefulness of a method for such detailed investigation of non-kinematic quantities in a turbulent flow is clear. For basic research, most of the measurable statistical quantities should be of interest; for some practical problems, perhaps the direct measurement of mean distributions and of turbulent transfer will be paramount.

In principle, there appears to be no necessity for restriction of the method to measurement in a flow with only two simultaneous fluctuating quantities. However, the complication that arises upon consideration of simultaneous fluctuations in velocity, temperature and concentration would appear to render this generalization impracticable. One is naturally intrigued by the idea of being able to make such measurements in a turbulent combustion zone. However, this extremely important problem presents at least two certain major difficulties: (a) in reasonable density ranges, the flame temperatures are excessive, (b) the intermediate stages of most chemical reactions would involve dealing with a mixture of several components instead of just two. In addition to these difficulties, we might also make note of the possible catalytic action of the instrument in the reaction zone, as well as the probability that the hot-wire would act as an igniter.

In casting about for possible methods of making direct measurement of the various kinematic quantities in a flowing gas mixture, we should not ignore the possibility of finding a pair of gases whose densities, specific heats and thermal conductivities are so related that the net response to a concentration fluctuation is negligible. It can be seen from the numerical values in Appendix II that such a situation is not beyond the realm of possibility.

APPENDIX I. REMARKS ON KING'S EQUATION

1. General

As pointed out by McAdams [29], the forced convection term in King's equation can be written in terms of the product of a Reynolds number and a Prandtl number, so that the rate of heat loss from the wire is

$$i^2R = k(T-T_a)\left[a' + b'\sqrt{R\cdot\sigma}\right] \qquad (1)$$

Inserting an extra d, and introducing a heat transfer coefficient, h, and the Nusselt number, $\eta = \frac{hd}{k}$, McAdams writes this in the form

$$\eta = K_1 + K_2\sqrt{R\cdot\sigma} \qquad (1a)$$

Conventionally, the first term in King's equation is described as including radiation and free convection, while the second term is due to forced convection. The latter appears to be quite reasonable, but it is apparent that free convection effects, if appreciable, cannot enter the heat transfer equation simply additively; the free convection phenomenon is complex, and in most current applications, the direction of bouyancy-induced velocity is perpendicular to the main flow. The form of A, as given by King, gives no clue as to its physical origin, although it is physically obvious that radiation must be included. The question is perhaps further clouded by the fact that measurements of the ero-velocity point in constant-resistance hot-wire calibrations seem to agree rather well with the A obtained by

the extrapolation of the points measured at relatively large flow velocities.

It would seem that, in view of the extended possibilities of the hot-wire anemometer as described in the present report, a complete reexamination of the fundamental heat transfer equation for the flow past a heated cylinder at small Reynolds numbers is in order, with particular emphasis on explicit inclusion of all the significant physical quantities. For example, if A actually does represent a free convection term, it should include a Grashof number, which generally has a rather complicated variation with temperature.

For the purposes of the present work, preliminary attempts have been made to check the validity of King's equation. These are described briefly below.

2. Mean Calibration of Hot-Wire in Air at Various Temperatures

Due to the difficulty of obtaining a series of velocities at each of several temperatures with the present equipment, single measurements were made at various velocities and temperatures, keeping $(\bar{R} - \bar{R}_a) = \text{constant}$. Since King's $\bar{B}$ is relatively insensitive to temperature changes, and since this forced convection term seems physically sound, the measured points were used to compute the intercept, $\bar{A}$, on the assumption that the theoretical variation of $\bar{B}(\bar{T}_a)$ is correct. Thus, an $\bar{A}$ was computed from each measured point instead of from a complete faired calibration curve at each temperature.

In this computation, the data of Taylor and Johnston (30) for the thermal conductivity of dry air were used. The air was, in fact, fairly humid, but here only the relative values are important, and an error in absolute magnitude of k would have no effect. The specific heat was assumed constant ($c_p = 0.24$) over the temperature range, in accordance with the International Critical Tables. For the density variation, the air was assumed to be a perfect gas.

The results, Fig. (3), show considerable scatter because this form of presentation involves small differences between two relatively large quantities, one of which has appreciable scatter itself. From the figure it appears that $\bar{A}(\bar{T}_a)$ probably varies more slowly than $k(\bar{T}_a)$; however, the large amount of scatter precludes the deduction of an alternative, empirical expression. The agreement appears to be sufficiently good to justify the use of King's equation in the present, fairly rough measurements of velocity and temperature fluctuations in a free jet.

3. Comparison of Mean Calibrations in Air and Carbon Dioxide

In a further attempt to check King's equation, a hot-wire was calibrated in both air and carbon dioxide. Then, with the assumption that the forms of King's A and B are correct, the carbon dioxide calibration was computed from the air calibration. The curves are given in Fig. (4).

For the computation of A_{co_2} and B_{co_2} from A_{air} and B_{air}, the thermal conductivities were taken from references (30) and (31), which correspond to pure gases. The specific heats and densities were taken from the International Critical Tables, and both gases were assumed to be perfect gases.

From the figure it can be seen that, although the agreement between measured and "computed" B_{CO_2} is good, the two values of A_{CO_2} are relatively far apart.

The principal possible source of error in the determination of A_{CO_2} and B_{CO_2} from the air calibration is the use of thermal conductivities measured in relatively pure gases. The laboratory air undoubtedly contained appreciable amounts of CO_2 and water vapor (the measurements were made on a cloudy day); the jet CO_2 was commercial type, stated at 99½% pure, probably containing air, H_2O and other impurities. Small amounts of impurities may have an appreciable effect upon thermal conductivity, much larger, for example, than the effect upon density and specific heat. Unfortunately, insufficient experimental data exist on the thermal conductivity of gas mixtures, and the theoretical approach has proved to be tremendously complicated, even the first approximation for monatomic gases (25). Thus, it would be extremely difficult to estimate the error due to impurities, even if a quantitative analysis were available. It is recommended that the measurements be repeated with pure gases, or that the actual thermal conductivities be measured.

APPENDIX II. TYPICAL NUMERICAL VALUES OR TERMS IN THE RESPONSE EQUATIONS

1. Temperature and Velocity Fluctuations

The complete Eq. (18) can be written in the form

$$\frac{i\bar{R}_a}{(\bar{R}-\bar{R}_a)^2}\,e = \underbrace{(\bar{A}+\bar{B}\sqrt{\bar{U}})\frac{R_o\alpha}{(\bar{R}-\bar{R}_a)}\vartheta}_{(a)} - \underbrace{n\frac{\bar{A}}{\bar{k}}\vartheta}_{(b)} \qquad (18b)$$

$$\underbrace{-\frac{\bar{B}}{2}\sqrt{\bar{U}}\left(\frac{n}{\bar{k}}-\frac{1}{\bar{T}_a}\right)\vartheta}_{(c)} - \underbrace{\frac{\bar{B}}{2}\frac{u}{\sqrt{\bar{U}}}}_{(d)}$$

and we are interested in comparing the relative magnitudes of the four terms as indicated.

Assume the following typical numerical values:

$\bar{U} = 1000$ cm/sec.	$d = 0.000611$ cm.	$\bar{A} = 0.0035$
$\bar{\Theta} = 100$ °C	$R_o = 11.0\ \Omega$	$\bar{B} = 0.00010$
$T_r = 290$ °K	$\ell = 0.30$ cm.	$\bar{k} = 7.55 \times 10^{-5}$ (ref. 30)
$\frac{u}{\bar{U}} = 0.20$	$i = 0.040$ amp.	$\bar{\rho} = 7.00 \times 10^{-4}$
$\frac{\vartheta}{\bar{\Theta}} = 0.20$	$\alpha = 0.0037$ (platinum)	$\bar{c}_p = 0.24$
		$n = 1.62 \times 10^{-7}$ (ref. 30)

These values give

$$R_r = R_o\left[1 + \alpha(T_r - 273)\right] = 11.69\ \Omega$$

$$\bar{R}_a = R_o\left[1 + \alpha(\bar{T}_a - 273)\right] = 15.76\ \Omega$$

and, from the equation for thermal equilibrium,

$$\bar{R} = \bar{R}_a + \frac{i^2\bar{R}_a}{\bar{A} - i^2 + \bar{B}\sqrt{\bar{U}}} = 20.74\ \Omega$$

We now get the following numerical values for the terms in Eq. (18a):

$$\textcircled{a} = 10.90 \cdot 10^{-4}$$
$$\textcircled{b} = 1.22 \times 10^{-4}$$
$$\textcircled{c} = -0.13 \times 10^{-4}$$
$$\textcircled{d} = 3.16 \times 10^{-4}$$

Term © is only a little more than 1% of @ , and is apparently negligible for all anticipated operating conditions.

2. Concentration and Velocity Fluctuations (Air-CO_2 Mixture)

Since there is no information available on precise measurements of the thermal conductivity of air-CO_2 mixtures, we shall assume for the purposes of this calculation that the variation is linear, i.e., $f(\bar{\Gamma}) = \bar{\Gamma}$. Then Eq. (46) can be written in the form

$$-\frac{2iR_a}{(\bar{R}-R_a)^2}e = \underbrace{\frac{(2\bar{A}+\bar{B}\sqrt{\bar{U}})}{1+\frac{k_a}{\bar{\Gamma}\Delta k}}\left(\frac{\gamma}{\bar{\Gamma}}\right)}_{\textcircled{a}} + \underbrace{\frac{\bar{B}\sqrt{\bar{U}}}{1+\frac{c_{pa}}{\bar{\Gamma}\Delta c_p}}\left(\frac{\gamma}{\bar{\Gamma}}\right)}_{\textcircled{b}} + \underbrace{\frac{\bar{B}\sqrt{\bar{U}}}{1+\frac{\rho_a}{\bar{\Gamma}\Delta\rho}}\left(\frac{\gamma}{\bar{\Gamma}}\right)}_{\textcircled{c}} + \underbrace{B\frac{u}{\sqrt{\bar{U}}}}_{\textcircled{d}} \qquad (46b)$$

Assume the following typical numerical values,

$\bar{U} = 1000$ cm/sec. $\quad \ell = 0.30$ cm. $\quad \rho_a = 1.165 \times 10^{-3}$

$\bar{\Gamma} = 0.50 \quad i = 0.040$ amp. $\quad \rho_g = 1.785 \times 10^{-3}$

$T_r = T_a = 290\ ^\circ K \quad \alpha = 0.0037 \quad c_{p_a} = 0.25$

$\frac{u}{\bar{U}} = 0.20 \quad \bar{A} = 0.0020 \quad c_{p_g} = 0.199$

$\frac{\gamma}{\bar{\Gamma}} = 0.20 \quad \bar{B} = 0.00010 \quad \Delta k = -2.13 \times 10^{-5}$

$d = 0.000611 \quad k_a = 5.93 \times 10^{-5} \quad \Delta\rho = 0.620 \times 10^{-3}$

$R_o = 11.0\ \Omega \quad k_g = 3.80 \times 10^{-5} \quad \Delta c_p = -0.051$

These give

$$\textcircled{a} = -3.14 \times 10^{-4}$$

$$\textcircled{b} = -0.72 \times 10^{-4}$$

$$\textcircled{c} = 1.33 \times 10^{-4}$$

$$\textcircled{d} = 3.16 \times 10^{-4}$$

and none of the terms is negligible.

APPENDIX III: COMPENSATION RESISTANCE FOR SIMPLE RESISTANCE THERMOMETER

With appreciable heating current, we can use the ordinary anemometric expression for the time constant:

$$M = \frac{4.2\, m s}{R_o \alpha} \frac{(\bar{R} - \bar{R}_a)}{i^2 \bar{R}_a} \tag{1}$$

which is more convenient than the equivalent form

$$M = \frac{4.2\, m s}{R_o \alpha} \frac{1}{[\bar{A} - i^2 + \bar{B}\sqrt{\bar{U}}]} \tag{1a}$$

The compensation resistance is then given by

$$R_c = \frac{L}{M} \tag{2}$$

where L is the inductance of the coil in the compensation network.

However, in order to measure temperature fluctuation level directly, it is convenient to operate with negligible heating current. Then $(\bar{R} - \bar{R}_a)$ becomes too difficult to measure in a turbulent flow, and we must go to the limit with Eq. (1a) rather than with Eq. (1). Then

$$M' = \frac{4.2\, m s}{R_o \alpha} \cdot \frac{1}{[\bar{A} + \bar{B}\sqrt{\bar{U}}]} \tag{3}$$

where, as in Eq. (1a), the values of $\bar{A}$ and $\bar{B}$ to be used are the average values corresponding to temperature $\overline{T_a}$.

In the actual process of measurement, perhaps the shortest method is to determine $[\bar{A} + \bar{B}\sqrt{\bar{U}}]$ by a measurement of $\frac{i^2 \bar{R}}{\bar{R} - \bar{R}_a}$ with the wire appreciably heated, since this reading is also necessary for the determination of mean velocity.

APPENDIX IV. MIXTURE OF PERFECT GASES

In vies of the sections discussing measurements in gas mixtures, it seems appropriate to include a brief review of pertinent relations occurring in the theory of mixtures of perfect gases. Extensive treatment is to be found, for example, in reference (32).

Notation

V = total volume (for most problems in fluid mechanics, unit volume is considered)

M_i = molecular weight of i^{th} component

N_i = number of mols of i^{th} component

p_i = partial pressure of i^{th} component

ρ_i = density of i^{th} component at pressure p_i

ρ_i^* = density of i^{th} component at pressure p

R = universal gas constant

T = absolute temperature

p, ρ, M = characteristics of the muxture (M = apparent molecular weight)

We have immediately,

$$p = \sum_i p_i \tag{1}$$

$$\rho_i = \frac{N_i M_i}{V} \tag{2}$$

$$\rho_i^* = \rho_i \frac{p}{p_i} \tag{3}$$

Also, the equation of state is satisfied for each component and for the mixture:

$$p_i V = N_i RT \tag{4}$$

$$pV = \sum_i N_i \cdot RT \tag{5}$$

or $$p_i = \frac{\rho_i}{M_i} RT \tag{4a}$$

and $$p = \sum_i \frac{\rho_i}{M_i} \cdot RT = \frac{\rho}{M} RT \tag{5a}$$

Since $\rho = \sum_i \rho_i$, we have $\sum_i \frac{\rho_i}{M_i} = \frac{1}{M} \sum_i \rho_i$

so that $$M = \frac{\sum_i \rho_i}{\sum_i \frac{\rho_i}{M_i}} \tag{6}$$

We are particularly interested in relative concentrations. Define the molal concentration of the i^{th} component by

$$\gamma_i = \frac{N_i}{\sum_k N_k} \tag{7}$$

But, from Eqs. (4) and (5),

$$\frac{p_i}{p} = \frac{N_i}{\sum_k N_k}$$

so that $$\gamma_i = \frac{p_i}{p} \tag{8}$$

We are interested in $\rho(\rho_i^*, \gamma_i)$; from Eq. (3),

$$\rho = \sum_i \rho_i = \sum_i \left(\rho_i^* \frac{p_i}{p}\right)$$

or $$\rho = \sum_i (\rho_i^* \gamma_i) \tag{9}$$

For a mixture of two gases, $\gamma_2 = 1 - \gamma_1$, and

$$\rho = \rho_2^* + (\rho_1^* - \rho_2^*)\gamma_1 \tag{10}$$

We can also define a mass concentration,

$$\lambda_i = \frac{\rho_i}{\sum_k \rho_k} = \frac{\rho_i}{\rho} \tag{11}$$

A general expression for $\rho(\rho_i^*, \lambda_i)$ is rather complex. But we can transform Eq. (11) to

$$\lambda_i = \frac{\rho_i^*}{\sum_k \rho_k} \gamma_i \tag{12}$$

Specializing at once to a two component mixture,

$$\rho = \frac{\rho_1^*}{\lambda_1} \gamma_1 \tag{12a}$$

but from Eq. (10),

$$\gamma_1 = \frac{\rho - \rho_2^*}{\rho_1^* - \rho_2^*}$$

We substitute this into Eq. (12a) and solve for ρ :

$$\rho = \frac{\rho_1^* \rho_2^*}{\rho_1^* + (\rho_2^* - \rho_1^*)\lambda_1} \tag{13}$$

which may be compared with Eq. (10).

A relation between these two definitions of concentration is obtained by equating Eqs. (10) and (13):

$$\lambda_1 = \frac{\rho_1^* \gamma_1}{\rho_2^* + (\rho_1^* - \rho_2^*)\gamma_1} \tag{14}$$

or

$$\gamma_1 = \frac{\rho_2^* \lambda_1}{\rho_1^* + (\rho_2^* - \rho_1^*)\lambda_1} \tag{14a}$$

The relative significance of these two concentrations in the field of fluid mechanics merits consideration. In investigations of mass transfer in gas flow, the mass concentration would appear to be the more significant parameter. For example, in a comparison of lateral rates of diffusion of momentum, heat

and material in a particular turbulent shear flow, the λ -distribution is to be compared with the veolcity and temperature distributions.

On the other hand, a treatment of material diffusion prior to chemical reaction would obviously be more concerned with the molal concentration.

For hot-wire measurements, the simplicity of Eq. (10) relative to Eq. (13) recommends the determination of molal concentration and fluctuations first, and, if necessary, the use of Eq. (14) to obtain mass concentration.

Of course, if $\rho_1^* = \rho_2^*$, a case of particular interest in the investigation of material diffusion in turbulent flow, the distinction vanishes.

APPENDIX V: TRANSFER IN TURBULENT SHEAR FLOW WITH DENSITY FLUCTUATIONS

In the sections on measurement procedures, methods are given for the determination of shear, heat transfer and material transfer by measurement with a directionally sensitive hot-wire meter. The procedures given actually lead to the quantities $\overline{uv}$, $\overline{\vartheta v}$ and $\overline{\gamma v}$. These, of course, are proportional to the respective transfer rates only in cases for which the density and specific heat fluctuations are sufficiently small, in which case the local mean density can be used to give

$$\begin{aligned} &\text{Shear:} && \tau = -\bar{\rho}\,\overline{uv} \\ &\text{Heat Transfer:} && Q = -\bar{\rho}\,\bar{c}_p\,\overline{\vartheta v} \\ &\text{Material Transfer:} && D = -\bar{\rho}\,\overline{\gamma v} \end{aligned} \qquad (1)$$

Since the density fluctuations have been taken into account for the computation of the hot-wire response, it may be well to investigate the limitations introduced by the use of Eq. (1).

A. Temperature and Velocity Fluctuations

The general expression for turbulent shear is

$$\tau = -\overline{\rho U V} \qquad (2)$$

but

$$\begin{aligned} \rho &= \bar{\rho} + \rho' \\ U &= \bar{U} + u \\ V &= v \\ \Theta &= \bar{\Theta} + \vartheta \end{aligned} \qquad (3)$$

For turbulent shear flow with temperature gradient, it may reasonably be assumed that $\frac{u}{\bar{U}}$, $\frac{v}{\bar{U}}$ and $\frac{\vartheta}{\bar{\Theta}}$ are all the same order of magnitude; in fact, in the previous discussion they are assumed small. We are interested in finding the restriction on Θ such that Eq. (1) may be applied with at least the same accuracy as may be expected from the measuring technique.

With Eq. (3), Eq. (2) becomes

$$\tau = -\bar{\rho}\,\overline{uv} - \bar{U}\,\overline{\rho' v} - \overline{\rho' u v}$$

and the third term is clearly negligible.

Since the density fluctuation is due to temperature fluctuation, from Eq. (17) of the text,

$$\rho' = -\bar{\rho}\,\frac{\vartheta}{\bar{T}_a}$$

$$\therefore \quad \tau = -\bar{\rho}\,\overline{uv} + \frac{\bar{\rho}\,\bar{U}}{\bar{T}_a}\,\overline{\vartheta v} \tag{4}$$

Hence, for Eq. (1) to be valid,

$$\overline{uv} \gg \frac{\bar{U}}{\bar{T}_a}\,\overline{\vartheta v}$$

$$\text{or,} \quad \frac{\overline{uv}}{\bar{U}^2} \gg \frac{\overline{\vartheta v}}{\bar{\Theta}\,\bar{U}} \cdot \frac{\bar{\Theta}}{\bar{T}_a} \tag{5}$$

If $\frac{\overline{uv}}{\bar{U}^2}$ and $\frac{\overline{\vartheta v}}{\bar{\Theta}\,\bar{U}}$ are the same order of magnitude, this requires that

$$\frac{\bar{\Theta}}{\bar{T}_a} \ll 1 \tag{6}$$

If this condition is not satisfied with sufficient accuracy, the turbulent shear is calculable from Eq. (4) after $\overline{uv}$ and $\overline{\vartheta v}$

have been obtained in accordance with Eq. (30).

The turbulent heat transfer is

$$Q = - \overline{c_p \rho \Theta V} \tag{7}$$

but with Eq. (3) and with $c_p \doteq$ constant,

$$Q = - c_p \bar{\rho} \overline{\vartheta v} - c_p \bar{\Theta} \overline{\rho' v} - c_p \overline{\rho' \vartheta v}$$

where the third term can be neglected. Substituting for ρ' , we get

$$Q = - c_p \bar{\rho} \overline{\vartheta v} + c_p \bar{\rho} \frac{\bar{\Theta}}{\bar{T}_a} \overline{\vartheta v} \tag{8}$$

so that, for Eq. (1) to be valid, we require

$$\frac{\bar{\Theta}}{\bar{T}_a} \ll 1 \tag{6}$$

as before. If Eq. (6) is not satisfied, the turbulent heat transfer is easily calculable from

$$Q = - c_p \bar{\rho} \left(1 - \frac{\bar{\Theta}}{\bar{T}_a} \right) \overline{\vartheta v} \tag{8a}$$

after $\overline{\vartheta v}$ has been obtained from Eq. (30).

B. Concentration and Velocity Fluctuations

With Eq. (2), Eq. (3) and the expression for the density fluctuation,

$$\rho' = \gamma \Delta \rho$$

where $\Gamma = \bar{\Gamma} + \gamma$, we obtain for the turbulent shear stress,

approximately $$\tau = - \bar{\rho} \overline{uv} - \bar{U} \Delta \rho \overline{\gamma v} \tag{9}$$

If Eq. (1) is to be reasonably accurate, and if $\frac{\overline{uv}}{\bar{U}^2}$

is roughly equal to $\frac{\overline{\gamma v}}{\bar{\Gamma}\bar{U}}$, the following inequality must be satisfied:

$$\frac{\Delta\rho}{\bar{\rho}} \ll \frac{1}{\bar{\Gamma}} \tag{10}$$

If Eq. (10) is not satisfied, $\overline{uv}$ and $\overline{\gamma v}$ can be obtained from Eq. (51) in Section J, and Eq. (9), above, gives the shearing stress.

The turbulent material transfer is

$$\mathcal{D} = -\overline{\rho\,\Gamma v} \tag{11}$$

Introducing the mean values and fluctuations, and neglecting the triple product of the small fluctuating quantities as before, Eq. (11) becomes

$$\mathcal{D} = -\bar{\rho}\,\overline{\gamma v} - \bar{\Gamma}\,\overline{\rho' v} \tag{12}$$

But $\rho' = \gamma\Delta\rho$, so that

$$\mathcal{D} = -\left(\bar{\rho} + \bar{\Gamma}\Delta\rho\right)\overline{\gamma v} \tag{13}$$

and the condition for the $\mathcal{D}$ in Eq. (1) to be valid is again

$$\frac{\Delta\rho}{\bar{\rho}} \ll \frac{1}{\bar{\Gamma}} \tag{10}$$

As before, Eq. (13) may be used after $\overline{\gamma v}$ has been obtained from Eq. (51).

REFERENCES

1. L. V. King, Phil. Trans. Roy. Soc., A 214, 373 (1914);

2. H. L. Dryden and A. M. Kuethe, T. R. No. 320, N.A.C.A. (1929);

3. E. Huguenard, A. Magnan and A. Planiol, La Tech. Aero., Nov.-Dec. (1923), Jan.-Feb. (1924). Also N.A.C.A. T.M. No. 264);

4. J. M. Burgers, Versl. der Kon. Acad. v. Wetensch, Amsterdam 29, 547 (1926;

5. L. F. G. Simmons and C. Salter, Proc. Roy. Soc., A 145 (1934)

6. F. L. Wattendorf, Jour. Aero. Sci., 3, No. 8 (1936);

7. H. L. Dryden, G. B. Schubauer, W. C. Mock, Jr., and H. K. Skramstad, T.R. No. 581, N.A.C.A. (1937);

8. W. S. Tucker and E. T. Paris, Phil. Trans. Roy. Soc., A 221, (1920-21);

9. Th. v. Kármán, Jour. Aero. Sci., 4, No. 4 (1937);

10. Th. v. Kármán and L. Howarth, Proc. Roy. Soc., A 164, (1938);

11. G. I. Taylor, Proc. Roy. Soc., A 164 (1938);

12. G. I. Taylor, Proc. Roy. Soc., A 151 (1935);

13. O. Reynolds, Phil. Trans. Roy. Soc., A 186 (1895);

14. A. M. Kuethe, Jour. Appl. Mech., Sept. (1935);

15. H. Reichardt, Naturwissenschaften, 26, (1938);

16. F. L. Wattendorf, Proc. Roy. Soc., A 148 (1935);

17. S. Corrsin, A. C.R. No. 3L23, N.A.C.A. (1943);

18. L. F. G. Simmons and C. Salter, Proc. Roy. Soc., A 165 (1938;

19. G. B. Schubauer and P. Klebanoff, A.C.R. No. 5K27, N.A.C.A. (1946);

20. H. W. Liepmann and J. Laufer, T.N. (in press) N.A.C.A. (1947;

21. G. K. Batchelor and A. A. Townsend, F.M. 991, Aero. Res. Council (1946);

22. H. Reichardt, Z.A.M.M., 18 (1938);

23. H. B. Squire, Rept. No. Aero. 2023, R.A.E. (1945);

24. International Critical Tables, McGraw-Hill (1927);

25. S. Chapman and T. G. Cowling, The Mathematical Theory of Non-Uniform Gases, Cambridge University Press (1939);

26. Landolt, Börnstein, Roth, Scheel, Physikalisch-Chemische Tabellen, 5 Auflage, Julius Springer (1927-36);

27. H. L. Dryden, v. Karman Anniversary Volume (1941);

28. L. F. G. Simmons, R. & M. 1919 (1939);

29. W. H. McAdams, Heat Transfer, McGraw-Hill (1942);

30. W. J. Taylor and H. L. Johnston, Jour. Chem. Phys., 14 No. 4 (1946);

31. H. L. Johnston and E. R. Grilly, Jour. Chem. Phys. 14 No. 4 (1946);

32. P. S. Epstein, Textbook of Thermodynamics, John Wiley and Sons (1937);

33. K. Z ebb, A.E. Thesis, C.I.T. (1943).

FIGURE 1

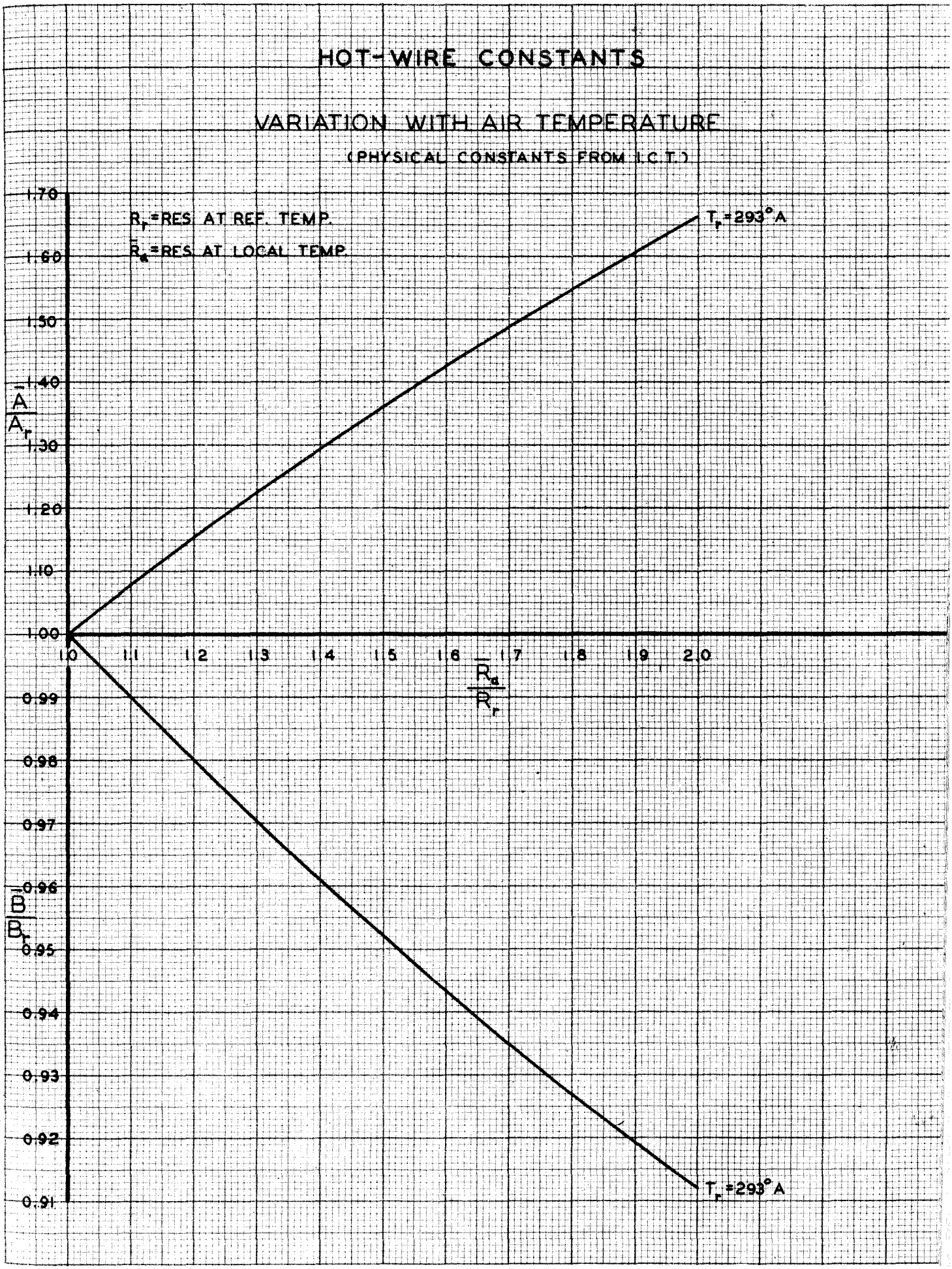
HOT-WIRE CONSTANTS
VARIATION WITH AIR TEMPERATURE
(PHYSICAL CONSTANTS FROM I.C.T.)
R_r = RES. AT REF. TEMP.
R_a = RES. AT LOCAL TEMP.
T_r = 293° A
$\frac{A}{A_r}$
$\frac{B}{B_r}$
$\frac{R_a}{R_r}$
1.70
1.60
1.50
1.40
1.30
1.20
1.10
1.00
1.0
1.1
1.2
1.3
1.4
1.5
1.6
1.7
1.8
1.9
2.0
0.99
0.98
0.97
0.96
0.95
0.94
0.93
0.92
0.91
T_r = 293° A

FIGURE 2

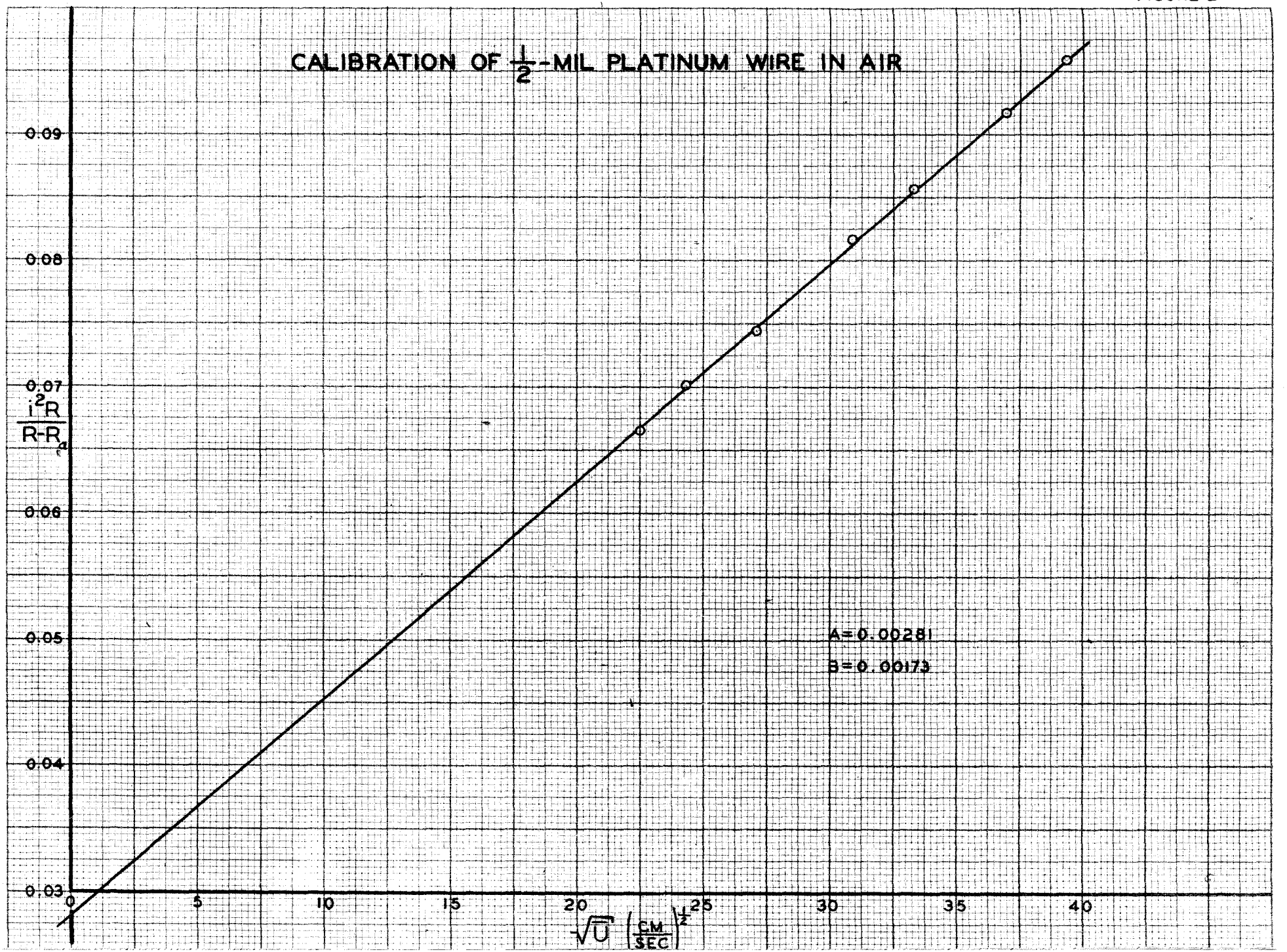
CALIBRATION OF 1/2-MIL PLATINUM WIRE IN AIR
0.09
0.08
0.07
0.06
0.05
0.04
0.03
i²R / R-Ra
A=0.00281
B=0.00173
0
5
10
15
20
25
30
35
40
√U (CM/SEC)^1/2

FIGURE 3

HOT-WIRE CALIBRATION IN HEATED AIR

$20^{\circ}C \leq T_a \leq 87^{\circ}C$

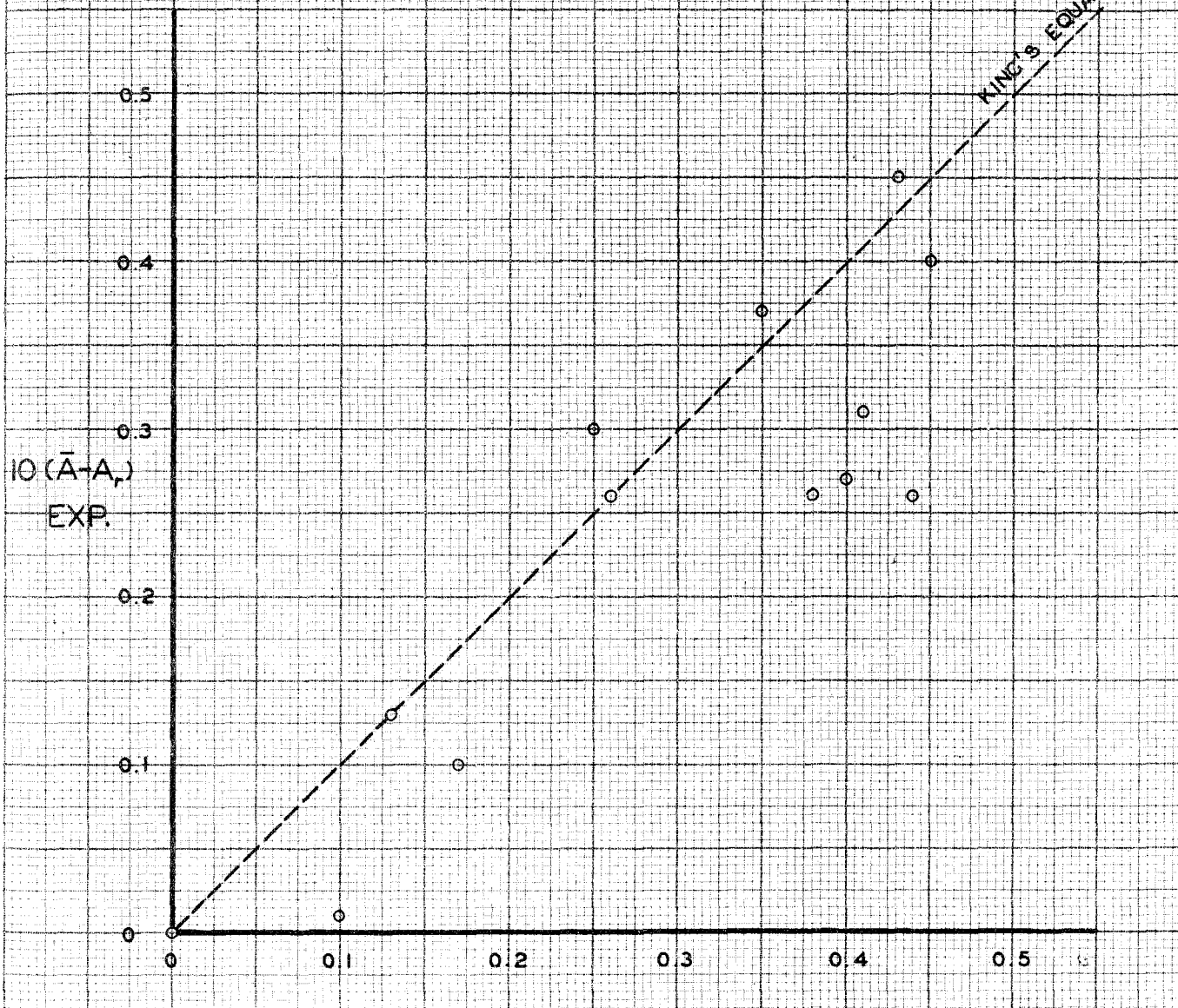

[PHYSICAL CONSTANTS FROM I.C.T. AND REFS. ( ) AND. ( )]

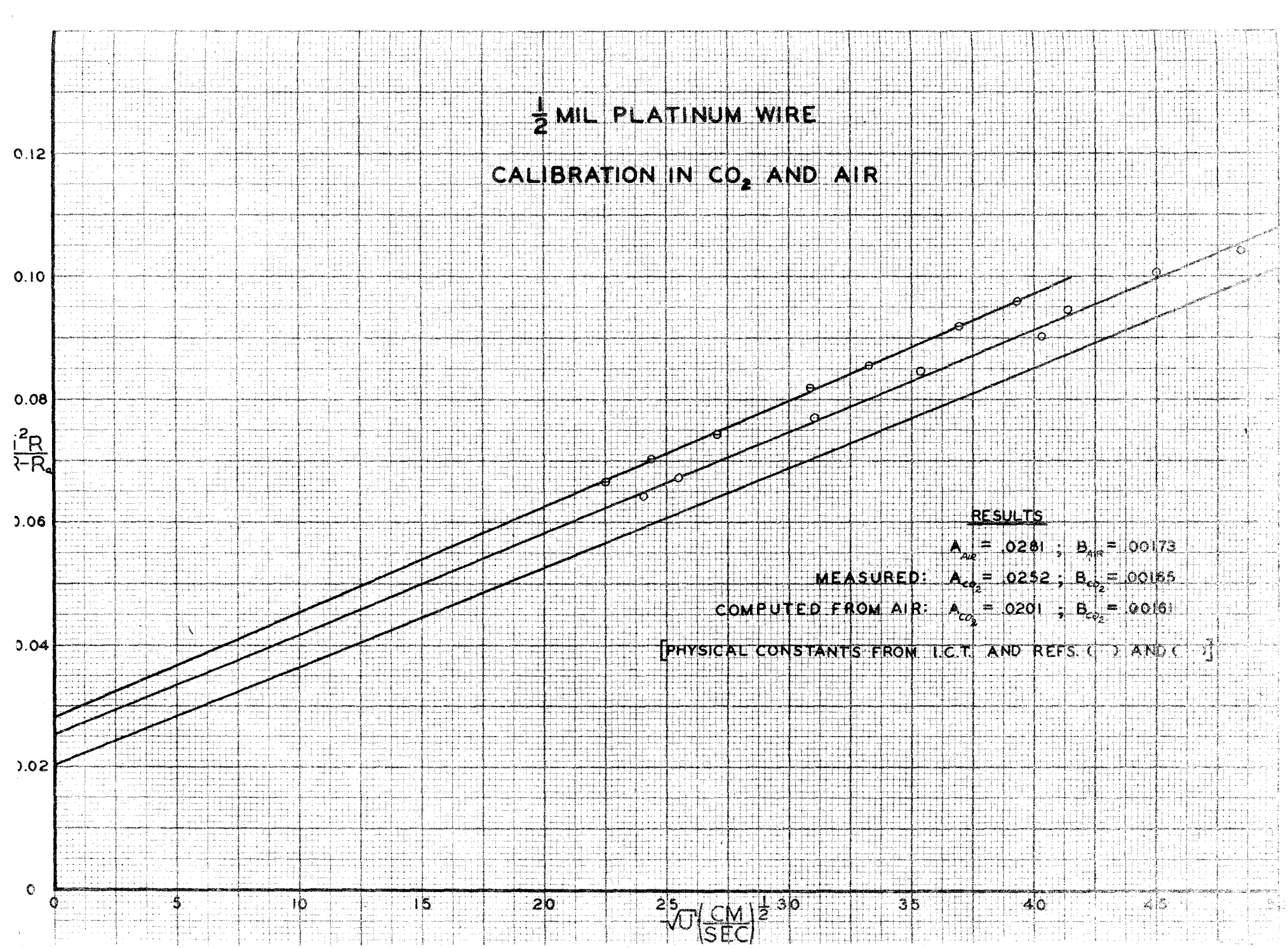
½ MIL PLATINUM WIRE
CALIBRATION IN CO_2 AND AIR
0.12
0.10
0.08
$\frac{i^2R}{R-R_o}$
0.06
0.04
0.02
0
0
5
10
15
20
25
30
35
40
45
$\sqrt{U}\left(\frac{CM}{SEC}\right)^{\frac{1}{2}}$
RESULTS
A_{AIR} = .0281 ; B_{AIR} = .00173
MEASURED: A_{CO_2} = .0252 ; B_{CO_2} = .00165
COMPUTED FROM AIR: A_{CO_2} = .0201 ; B_{CO_2} = .00161
[PHYSICAL CONSTANTS FROM I.C.T. AND REFS. ( ) AND ( )]

PART II

INVESTIGATIONS OF THE FLOW IN ROUND TURBULENT JETS

CONTENTS

A. SUMMARY

A detailed investigation has been made of the flow in a round turbulent air jet, heated slightly to permit measurement of mean temperature.

Oscillograms of the velocity fluctuation plus direct measurement of the turbulent shear both show that the flow in a fully developed "turbulent" jet is completely turbulent only out to approximately the radius at which the velocity is half the maximum at a section. The flow at the extreme outer edge is in the nature of a "laminar collar", with predominantly radial (inward) mean velocity, and in between the turbulent core and the laminar collar is a rather wide annular transition region.

A study of the downstream history of the radial distribution of turbulent velocity shows that the fully developed state of this round jet is reached between 15 and 20 diameters. This conclusion is corroborated by examination of the partition between turbulent motion and mean motion, of total kinetic energy crossing planes perpendicular to the axis in unit time.

The directly measured shear distribution is checked roughly by a computation of the same quantity from the mean velocity distribution.

A measurement of the double correlation function between points symmetrical about the jet axis shows considerable similarity to the corresponding function in isotropic turbulence, and permits calculation of scale and microscale.

With the assumption of constant microscale across a section, a rough estimate is made of the energy balance distribution of production, dissipation and diffusion of turbulent energy across a section is made.

A comparison with momentum transfer, modified vorticity transfer and constant exchange coefficient theories shows that none of them is satisfactory.

A comparison of mean velocity and temperature distributions verifies Ruden's result that the lateral rate of heat transfer in turbulent shear flow is appreciably greater than the lateral rate of momentum transfer.

The use of considerably increased heating, in a second jet unit, has permitted direct measurement of the temperature fluctuation level. Velocity fluctuations were also measured in this case for comparison, and they were found to be the same order of magnitude.

The final result is the direct measurement of temperature-velocity correlation and of velocity correlation in the hot jet. This gives a direct measure of the turbulent heat transfer and momentum transfer in the jet, and directly verifies the fact that the former is appreciably greater than the latter.

B. INTRODUCTION

Turbulent flows may be divided into two general classes according to the absence or presence of a continuous generation of turbulent kinetic energy from the mean flow kinetic energy. The first classification includes the simplest physically conceivable turbulent flow, isotropic turbulence, which has been treated theoretically with most success by G. I. Taylor (1,2,etc.), Th. von Kármán (4,5), L. Howarth (5), A. N. Kolmogoroff (6,7), A. Obukhoff (8), L. Onsager (9), C. F. v. Weizsäcker (10) and W. Heisenberg (11). It also includes a generalization to axially symmetric turbulence treated by G. K. Batchelor (12). The chief characteristic of these two flows is the lack of mean velocity gradient, with the result that the production term in the turbulent energy equation (see, for example, reference 13) is zero.

Isotropic turbulence, in which there is no distinguished direction, can be generated to a reasonable degree of accuracy by a regular grid mounted in a uniform, low turbulence airstream. A considerable amount of experimental work has been done on this type of flow (14, 15, 16, 17, 18, 19, 20 and 21), primarily because it has been the first type to be treated by a reasonable statistical method of theoretical analysis and because of the relative simplicity of some of the more significant measurements. Axially symmetrical turbulence is obtainable by an axially symmetrical contraction of an isotropic flow, and is met with in the working sections of most

wind tunnels. Although a little experimental work has been done on the effect of channel changes upon an initially isotropic turbulent flow [22, 23], no detailed study has yet been made of this type of turbulence.

The second general classification of turbulent flows is that of all turbulent shear flows. These are conventionally subdivided into wall turbulence and free turbulence, the former including boundary layer and channel flows, the latter including jets, wakes and single mixing regions. It seems likely that in the central regions, far from either axis of symmetry and/or outer boundaries, the turbulent shear flows are more or less alike. Therefore, it would appear that a subdivision according to the types of boundary conditions might well be applicable. For symmetrical configurations, the boundary conditions are applied on the axis and at the outer edges, while for unsymmetrical configurations, they are applied at the two boundaries.

The first possible boundary condition on a turbulent shear flow is a region of fully developed turbulence with no production of turbulent energy. This condition occurs on the axis of channel and pipe flow and of free jets and wakes. The turbulence on these axes may perhaps be expected to approximate the isotropic or axially symmetric in character. Here a chief distinction between "wall" and "free" enters, i.e., the turbulent motion in a fully developed channel flow has an "absolute"steady state, since the mean motion is constant, while in the fully developed jet or wake, the state is also steady relative to the mean motion, but the latter varies with downstream distance.

The second possible boundary condition on a turbulent shear flow is a laminar region. This condition occurs at the wall for a channel or boundary layer, and at the zero-velocity edge of a free jet or single mixing zone entering a medium at rest. Of course, there is a transition region between the fully turbulent flow and the laminar flow. The existence of this transition region in a turbulent boundary layer has been known for a long time. The present measurements establish its existence in the outer part of a turbulent jet. The detailed nature of this laminar boundary condition is also somewhat different for wall flows and free flows. In the former case the fluid in the laminar layer moves essentially parallel to the main flow direction, while in the latter case the fluid in the laminar region is principally induced flow from the receiving medium, and moves primarily perpendicular to the main turbulent stream. Although the contrast can be expected to lead to quantitative differences in the wall and free transition regions, it seems likely that qualitatively they are the same. Also, it might be remarked parenthetically that an investigation of the laminar edge and transition region of a free jet should give some insight, particularly into the corresponding and far less accessible regions in a turbulent boundary layer or channel flow with continuous fluid addition through porous walls.

The third possible boundary condition on a turbulent shear flow is a "free stream" condition such as occurs at the outer edge of a turbulent boundary layer, the outer edges of a wake, or the high velocity side of a single mixing region between semi-infinite moving and stationary flow. This boundary condition is apparently characterized

by a continuous and steady transition region (as contrasted with the unsteady transition to low-velocity laminar regions) from fully developed turbulent shear flow to a steady flow of effectively zero turbulence. It has been found that, at such a boundary, the turbulence is felt further out into the free stream than is the velocity defect [13, 24, 25, 26]. This is perhaps in contrast to the second type of boundary condition mentioned above, in which the mean flow effect of the shear region extends further than do the turbulent fluctuations. Although no measurements have been reported, it seems likely that the low-velocity boundary of a free jet entering a moving medium may also have a condition similar to this third one.

In addition to classification by boundary conditions and by the "relative" or "absolute" nature of the steady state, it is quite appropriate to classify shear flows according to the relative lateral locations of the regions of maximum production of turbulent energy and maximum dissipation of turbulent energy. In wall flows, the maximum production, proportional to the product of shear and slope of mean velocity profile, is at the wall, while in free flows it is found that the maximum production is in the vicinity of the inflection point of the mean velocity profile. The rate of dissipation was shown by Taylor [1] to be proportional to the product of kinematic viscosity by the mean square of the turbulent velocity, divided by the square of the microscale of the turbulence, for isotropic turbulence. For symmetrical flows, such as channel and free jet, this is a maximum on or near the axis, while for unsymmetrical flows, such as boundary layer and single mixing region, this is a maximum in the central region, well away from either boundary. It should be noted that the single mixing region bears the unique distinction of having maximum production and dissipation in the same vicinity. This has

been established by measurements in reference (13).

As pointed out by H. W. Liepman and J. Laufer [13], there exists no satisfactory theory of turbulent shear flow. The principal phenomenological theories based upon L. Prandtl's conception of "mixing length" [27] are Prandtl's momentum transport [27], Taylor's vorticity transport [28] and Kármán's similarity [29]. These are discussed in references (30), (31) and (16). Furthermore, as illustrated in reference (13), results just as useful can be obtained from dimensional considerations and the integral forms of the equations of motion.

More recently, a somewhat different approach to the problem of turbulent shear flow has been made by P. Y. Chou [32,33] by neglecting the higher order correlations in the system of correlation equations. However, this procedure has not as yet been experimentally justified.

Kármán [4] has given a solution for plane turbulent Couette flow based on a statistical approach.

A great deal of experimental effort has been put into measurements in turbulent shear flow, but most of these have been only on the mean velocity and temperature distributions. Investigations of some of the details of the turbulent motion have been made by H. Reichardt [35] and F. Wattendorf [36,37] for channel flow, Liepmann and Laufer for single mixing regions [13] and G. B. Schubauer and P. Klebanoff [24] for boundary layers.*

The round free jet, in addition to representing a typical turbulent shear flow, is a particularly convenient configuration

---

*Measurements in turbulent channel and boundary layer flow have also been made by R. P. Harington, J. W. Margosian and J. Heller: (unpublished) report for N.A.C.A. (1945). However, some peculiarities in the measured $\overline{uv}$ in the boundary layer need clarification.

from the experimental point of view. For these reasons, and because of the possibility of some immediate applicability, the present investigation was undertaken.

P. Ruden [37] and A. M. Kuethe [25] have both made measurements in jets with axial symmetry. Ruden measured mean velocity and temperature distributions in a slightly heated (constant density) jet out to an axial distance ofabout 15 diameters; Kuethe measured mean velocity profiles and some turbulence level distributions out to 9 diameters in an unheated jet. Both investigators found that effective similarity of velocity profiles was reached before 10 diameters, which led to the general belief that complete mechanical similarity in a jet was reached there. It seemed, however, that the turbulence distribution in a radial direction might serve as a more sensitive indicator of the attainment of the fully developed state. Kuethe's turbulence distributions indicated an effectively fully-developed flow at 9 diameters, but he went out no further for verification. Therefore, the present investigation was set up to include measurements out as far as 40 diameters from the orifice.

All turbulent-jet analyses published up to the present time are based upon the assumption that the flow is completely turbulent across the entire width of the jet. The momentum transfer assumptions were applied to a solution of the fully developed round jet by W. Tollmien [38]; S. Tomotika [39] computed the round jet according to the modified vorticity transfer theory, and the results of these two were summarized by Howarth [40]. The application of Chou's theory to this problem was made by C. C. Lin [41], and this

approach turns out, in this case, to be equivalent to the assumption for turbulent shear suggested by Kármán (4). Certain specific assumptions in Lin's treatment lead to a constant shear coefficient. The assumption of a constant shear coefficient for the calculation of free jet flow was independently suggested later by Prandtl (42) and H. Görtler (43).

In addition to the measurement of kinematical quantities, it seems highly desirable to investigate turbulence also by a determination of the rates of diffusion of various quantities. The mean velocity profile and temperature profiles give a measure of the rates of diffusion of momentum and heat respectively. However, the mean distributions in fluid flows appear to be relatively insensitive to local variations in the transfer. Hence, a direct measurement of turbulent shear and of turbulent heat transfer seemed highly desirable. The first direct measurement of turbulent shear appears to have been made by H. K. Skramstad (17), by means of a hot-wire inclined to the mean flow direction so that it is sensitive to both u and v fluctuations. This is essentially the method used here to determine $\overline{uv}$ in an isothermal jet. A method of using a similar hot-wire instrument for the determination of $\overline{uv}$ and $\overline{\vartheta v}$ in a hot jet has been described in Part I of this thesis. There is also presented in Part I a method of using a hot-wire for the measurement of the turbulence level and the temperature fluctuation level in such a flow, and this has been applied here.

Summarizing, the general purposes of the present investigation were the following:

(a) to examine the general nature of the flow in the free turbulent jet issuing from a round orifice into an infinite receiving medium of identical fluid at rest;

(b) to make a rather detailed investigation of the turbulence in the isothermal jet;

(c) to measure and compare velocity and temperature fluctuation levels in an appreciably heated jet;

(d) to make direct measurement of the turbulent shear and turbulent heat transfer and to compare these with the values computed from the measured distributions of the mean quantities.

The results of (a) and (b) have been published by the National Advisory Committee for Aeronautics [26].

C. NOTATION

d diameter of orifice

x axial distance from orifice

r radial distance from jet axis

$\bar{U}$ axial component of mean velocity

$\bar{V}$ radial component of mean velocity

$\bar{U}_m$ maximum $\bar{U}$ at a section (i.e., on the axis)

$\bar{U}_o$ maximum $\bar{U}$ in the jet (i.e., in the potential cone)

$\bar{T}_a$ mean absolute temperature at a point in the flow

T_r absolute temperature of the air at rest

$\bar{\theta} = \bar{T}_a - T_r$

$\bar{\theta}_m$ maximum $\bar{\theta}$ at a section

$\bar{\theta}_o$ maximum $\bar{\theta}$ in the jet (i.e, at the orifice)

u axial component of instantaneous velocity fluctuation

v radial component of instantaneous velocity fluctuation

w tangential component of instantaneous velocity fluctuation

ϑ instantaneous temperature fluctuation

$u' = \sqrt{\overline{u^2}}$

$v' = \sqrt{\overline{v^2}}$

$w' = \sqrt{\overline{w^2}}$

$\vartheta' = \sqrt{\overline{\vartheta^2}}$

r_o at any section, the value of r for which $\bar{U} = \frac{1}{2}\bar{U}_m$

r_i at any section, the value of r for which $\bar{\theta} = \frac{1}{2}\bar{\theta}_m$

p — static pressure

ρ — air density

$\bar{\rho}$ — mean density

ρ' — density fluctuation

μ — viscosity coefficient of air

$\nu = \frac{\mu}{\rho}$, kinematic viscosity

τ — shear stress

Q — heat transfer

l — "mixing length"

$$R_{uv} = \frac{\overline{uv}}{u'v'}$$
$$R_{\vartheta v} = \frac{\overline{\vartheta v}}{\vartheta' v'}$$
$$R_{\vartheta u} = \frac{\overline{\vartheta u}}{\vartheta' u'}$$

} double correlation coefficients at a point

$$R_u = \frac{\overline{u_1 u_2}}{u'^2}$$

correlation coefficient between two different points

$$L = \int_0^\infty R_u(r)\, dr$$

scale of turbulence

λ — microscale of turbulence

E_T — total kinetic energy crossing a section perpendicular to the jet axis in unit time

E_{T_o} — initial total kinetic energy

E_M — mean flow kinetic energy crossing a section in unit time

E' — turbulent kinetic energy crossing a section in unit time

D. EQUIPMENT

1. Aerodynamic Equipment

Two different aerodynamic units have been used in this investigation. The first is shown schematically in Fig. 1. The blower is a four-blade steel propeller, driven by a three-phase induction motor rated at 15 horsepower and run from a variable frequency generator. In all this work the blowers were operated at only a small fraction of rated power.

The 6½ foot square pressure box was adapted from the former GALCIT calibration tunnel. Sixteen Calrod heating elements were mounted in the primary contraction to provide slight but uniform heating of the jet air. There were two screens mounted between the heaters and the final contraction, a spun aluminum convergent nozzle, ending in an one-inch orifice. In an effort to obtain a uniform temperature distribution across the mouth of the nozzle, part of the heated air was ducted along the outside of the large circular pipe leading to the contraction. The initial velocity distribution was effectively rectangular, and the initial temperature distribution was down only about 4% at the edge.

A wall was set up in the plane of the jet mouth, perpendicular to the axis (Fig. 2), in order to reproduce more precisely the boundary conditions assumed in the theoretical analyses. However, a check run made without the wall in position showed no appreciable difference in the fully-developed region of the jet.

All runs in Jet #1 were made at a nozzle velocity of 10 meters per second and an initial temperature difference of 10° C. It was confirmed experimentally that this temperature difference had no measurable effect upon the aerodynamic jet characteristics. Inclination of the jet axis due to free convection was negligible.

Jet #2 has been built for the attainment of considerably higher initial temperatures, in order to permit measurement of temperature fluctuations in the fully-developed region of the jet. The unit is shown schematically in Fig. 3. The three-stage axial blower (reference 44) is driven by a two horsepower variable frequency motor operated at a fraction of rating. Heat is added through two double banks of coils of no. 16 nichrome wire. As in Jet #1, a good part of the heated air is ducted around the outside of the jet-air pipe in order to maintain a flat initial temperature distribution in the jet.

A Black and Decker vacuum cleaner blower is used to help the air through this secondary heating annulus. Since heat is discharged from this part of the system at an appreciable rate, it is exhausted outside of the building in order to minimize the rate of increase of the room temperature. Plans were made to make the system partially cyclic by exhausting this secondary air at the blower intake, but sufficiently high temperatures were reached without such an arrangement.

Jet Unit #2 is photographed in Fig. 4a, and Fig. 4b is a close-up of the asbestos orifice plate and the traversing mechanism.

The relatively high velocity section between heaters and final pressure box is to promote adequate turbulent mixing to insure a uniform initial temperature distribution in the jet. An earlier, simpler unit had the heating coils in the final pressure box; as a result, the Reynolds number of the coil wire, and even that of a ceramic grid, were too low to produce adequate mixing.

Runs with Jet Unit #2 have been made at orifice velocities between 20 and 35 meters persecond, and at orifice temperature differences between 0° C and 300° C. The initial velocity distribution is effectively rectangular, and the initial temperature distribution drops off only about 3% at the edge.

2. Measuring Equipment

The principal measuring instruments used were a hot-wire anemometer, thermocouple and hypodermic needle total-head tube.

The wires were nominally 0.00025" platinum etched from Wollaston. The etched platinum was soft-soldered to the tips of small steel needle supports.

The hot-wire anemometer heating circuits and amplifier were designed and built by Carl Thiele in 1941, and are given in Figs. 5 and 6 respectively. Fig. 7 is a photograph of the complete unit with four heating circuits and two amplifiers. The bridge circuit is so arranged that hot-wire time constants can be determined by superimposing equal A.C. voltages at two frequencies upon the balanced D.C. bridge circuit.

The amplifier gain is constant to within ± 2% over a frequency range from at least 7 cycles to 7000 cycles (Fig. 8). No check was made below 7 cycles since that was the lower limit of the available oscillators. Compensation is achieved by a resistance-inductance network between two stages of the amplifier. As illustrated by Fig. 9, for a typical wire time constant, the compensation circuit is satisfactory over the entire flat range of the uncompensated amplifier.

The amplifier output was read on a damped wall galvanometer of 10-second period, by means of a thermocouple.

In Jet #1, mean velocity was measured point by point with a hot-wire and mean temperature with a copper-constantan thermocouple. In Jet #2, mean total head and mean temperature were photographically recorded by means of an automatic traversing arrangement, used in combination with a hypodermic needle total-head tube and a chromel-alumel thermocouple. The total-head pressure line is run into a small copper bellows which tilts a mirror, thereby deflecting a narrow light beam upon a uniformly moving sheet of sensitized paper. The simultaneous recording of temperature on the paper utilizes directly the light beam reflected from the mirror of a sensitive galvanometer. The thermocouple-galvanometer circuit is arranged so that the galvanometer is critically damped for all sensitivity settings. The possible error arising from changes in "steady state" conditions during a continuous uni-directional traverse was investigated by means of a few continuous check runs in the opposite direction; these showed no appreciable difference.

The automatic traversing is accomplished by means of a screw-driven carriage running horizontally along a steel track (see Figs 2b and 4b). The screw is rotated through a gear and worm, by a reversible electric motor with an extremely wide speed range, operating on a continuously adjustable transformer. The sensitized paper holder is mechanically connected to the moving carriage, so that the abcissas of the recorded curves are equal to the true radial distance. Fig. 10 is a typical simultaneous photographic record of total-head and temperature distributions. The symmetry axes are offset laterally because of the necessary distance between total-head tube and thermocouple.

E. PROCEDURES

1. Mean Velocity, $\bar{U}$:

Measured in Jet #1 with a single hot-wire, by either constant current or constant resistance method. Measured in Jet #2 by hypodermic-needle total-head tube. No correction has been made for the effect of turbulence upon the readings, unless specifically mentioned. A brief discussion of this correction is given in Appendix I. Of course, the mean velocity measured by hot-wire is acutally $\sqrt{\bar{U}^2 + \bar{V}^2}$ rather than simply $\bar{U}$. However, a comparison with total-head tube measurements showed that the difference between the two was within the experimental error.

2. Mean Temperature, $\bar{\theta}$:

Measured with small copper-constantan and chromel-alumel thermocouples across a sensitive galvanometer. Since the galvanometer deflection varies linearly with temperature, there is no reading error specifically attributable to the fluctuations.

3. Axial Component of Turbulence $\frac{u'}{\bar{U}}$:

In Jet #1, always run effectively as an isothermal jet, this was measured with a single hot-wire in the conventional manner.

In Jet #2, run well above room temperature, the u' turbulence was measured simultaneously with temperature fluctuation level and $\overline{\vartheta u}$ correlation, as described in Sections F and G of Part I.

4. Temperature Fluctuation Level, $\frac{\vartheta'}{\theta}$:

This was measured directly in Jet #2 by use of the wire as a pure resistance thermometer.

5. Radial Component of Turbulence, $\frac{v'}{U}$:

This was measured in both isothermal and hot jets with an X-type meter made up of two wires whose voltage fluctuations were subtracted before entering the amplifier. Due to slight, almost unavoidable, unsymmetry, the meter was slightly sensitive to $\frac{u'}{U}$; appropriate correction has been made in the results.

6. Double Correlation at a Point

(a) $\overline{uv}$ in isothermal jet:

This was measured with the same type of instrument as $\frac{v'}{U}$ In this case the mean square outputs of the two wires were subtracted. Unsymmetry was corrected by repeating readings with the meter rotated through 180°.

(b) $\overline{uv}$ in hot jet:

This was measured simultaneously with $\overline{\vartheta v}$ by the method described in Part I. The extreme slowness of the measurements precluded the use of a simple inversion procedure for unsymmetry correction. Instead, the results were computed directly with the sensitivity calibrations of the individual wires, as described in Appendix II.

(c) $\overline{\vartheta v}$ in hot jet:

This was measured simultaneously with $\overline{uv}$.

7. Double Correlation Between Two Points, $\overline{u_1 u_2}$:

A correlation curve was measured between the axial components of turbulence at equal-velocity points on

opposite sides of the isothermal jet. This was obtained in the conventional way, by measuring the mean square of the sum and the difference of the fluctuating voltages of two u'-meters.

F. EXPERIMENTAL RESULTS

1. Isothermal Jet (Jet #1)

(a) Mean Velocity and Temperature:

Fig. 11 includes axial traverses of mean velocity and temperature, and shows, in agreement with Ruden [37], that the latter drops off more rapidly. Fig. 12 gives the velocity and temperature "half-widths" as a function of x. It is clear from Fig. 11 and 12 that the heat transfer is more rapid than the momentum transfer in a turbulent jet.

It is perhaps an interesting coincidence that the effective origin of the fully developed jet, indicated by the horizontal intercept of the $r_0(x)$ curve in Fig. 12, falls very close to the orifice location.

Fig. 13a shows typical traverses in the fully-developed region of the jet. The relative dimensions of the velocity and temperature profiles are in satisfactory agreement with Ruden's measurements. Since the initial velocity is 10 meters per second and the initial temperature difference is 10°C, the maxima at this cross section are about 2.5 m/s and 2.3° C.

Effective similarity of mean velocity and temperature profiles is reached before 10 diameters.

(b) Turbulence Level:

Figs. 11 and 13 also show axial and sectional distributions of u'. The hot-wire measures $\frac{u'}{U}$, but, because of the large differences in local mean velocities, this quantity does not give

a picture of the turbulent kinetic energy distribution. Therefore, the $\frac{u'}{U_m}$ distribution has also been plotted in Fig. 13, and the $\frac{u'}{\bar{U}_o}$ distribution in Fig. 11.

The lateral $\frac{u'}{U_o}$ distributions for several sections are presented in Fig. 14. This gives a clear picture of the radial spread of the turbulent kinetic energy as the flow travels in the axial direction.

A typical v'-distribution is compared with u' at the same section in Fig. 13b.

Oscillograms of the u-fluctuations at various distances from the axis of the fully developed jet (Fig. 15) indicate a definite deviation from the fully turbulent regime toward the outer edge. A completely turbulent core exists out to approximately r_o, the radius at which the mean velocity is one-half the maximum at the section.

(c) Correlation Between Velocity Fluctuations at a Point:

The correlation coefficient and the dimensionless correlation across the fully developed jet $\left(\frac{x}{d} = 20\right)$ are shown in Fig. 16. The extremely large scatter of R_{uv} in the outer annulus, as well as the sharp decrease in both R_{uv} and $\overline{uv}$ toward this region also indicate a deviation from the fully turbulent state.

The turbulent shear stress is, of course, $\tau = -\rho\overline{uv}$

(d) Correlation Between Fluctuations at Different Points:

Fig. 17 is the distribution of $R_u = \frac{\overline{u_1 u_2}}{u'^2}$ between points symmetrical about the axis. In addition to giving a fairly accurate value of the scale of turbulence and an extremely

rough value of the microscale, the curve shows that there was no whipping of the jet as a whole. If such a condition existed, the correlation would not go to zero at large Δr, but would have a negative value.

2. Hot Jet (Jet #2)

The measurements to be included here were all made at a section 15 diameters from the orifice of a hot air jet with initial temperature difference of 175°C and initial velocity of 35 m/sec. Since the jet was appreciably less dense than the receiving medium, the fully developed region as indicated by a more or less flat $\frac{u'}{\bar{U}_m}$ distribution near the axis, is reached somewhat earlier than in the isothermal case.

(a) Mean Velocity and Temperature:

Although a detailed study of the mean velocity and temperature fields, as a function of initial temperature difference, is being made as a separate problem, it is not of explicit interest here, and the results are not included.

The typical mean velocity and temperature profiles included in Fig. 18 indicate, by comparison with Fig. 13, that the relative magnitudes of momentum and heat transfer are about the same as in the isothermal case. These distributions were obtained by averaging three photographically recorded traverses at each section.

(b) Fluctuation Levels:

The u' and v' turbulence levels are plotted in Figs. 18a and 18b, relative to local velocity and maximum velocity respectively. It will be noted that these are somewhat lower than the values obtained for the isothermal case in Jet. #1.

A check of the isothermal case in Jet #2 showed that the lower values are not due to the heating (i.e., the density variation), but are characteristic of this flow field. Apparently the density variation ($\bar{\theta}_m = 45\,°C$ at $\frac{x}{d} = 15$) is not sufficient to cause any appreciable change in the turbulence.

The temperature fluctuation level is also included in three figures. It appears to be everywhere a bit lower than the $\frac{u'}{\bar{U}}$ level, with which it can most logically be compared.

(c) Correlations at a Point:

As described in Section I, the $\frac{\overline{\vartheta u}}{\vartheta' u'}$ correlation comes out as a by-product of the measurement of $\frac{u'}{\bar{U}}$ and $\frac{\vartheta'}{\bar{\theta}}$. This correlation is related to the turbulent heat transfer in the mean flow direction, which may generally be neglected relative to the mean heat transport. However, the dimensionless correlation and the correlation coefficient are presented in Fig. 19. No points are plotted for radii greater than 2.2 inches, since the excessive scatter in this transition region puts points far outside of both limits of the ordinate scale.

The quantities $\overline{uv}$ and $\overline{\vartheta v}$ are of greater interest, and the corresponding dimensionless correlations and correlation coefficients are given in Fig. 20. In spite of the large experimental scatter, it is evident that, as anticipated from mean velocity and temperature profiles, the radial heat transport is greater than the radial momentum transport.

C. THEORIES

1. Velocity

For a free jet of this type the usual turbulent boundary layer assumptions are applied to the general Navier-Stokes equation. The simplified equation must be solved with the boundary conditions, $\bar{V} = 0$ and $\frac{\partial \bar{U}}{\partial r} = 0$ at $r=0$ (on the axis). Also the velocities and their derivatives must vanish as becomes infinite. Since the axial pressure gradient is neglected, the rate of flow of axial momentum across all sections is the same:

$$2\pi\rho\int_0^\infty \bar{U}^2 r\,dr = \text{const.}$$

Since viscosity is neglected, $\tau = -\rho\overline{uv}$,

(a) Momentum Transfer Theory

The assumption that momentum is the transportable quantity with a mechanism analogous to the kinetic theory of gases leads to $\tau = -\rho\overline{lv}\ \frac{\partial \bar{U}}{\partial r}$, which gives the equation of motion:

$$\bar{U}\frac{\partial \bar{U}}{\partial x} + \bar{V}\frac{\partial \bar{U}}{\partial r} = -\frac{1}{r}\frac{\partial}{\partial r}\left(\overline{lv}\, r\frac{\partial \bar{U}}{\partial r}\right)$$

Prandtl further suggested the assumption of $v = l\left|\frac{\partial \bar{U}}{\partial r}\right|$, or $\tau = \rho l^2\left|\frac{\partial \bar{U}}{\partial r}\right|\left(\frac{\partial \bar{U}}{\partial r}\right)$.

Thus, $$\bar{U}\frac{\partial \bar{U}}{\partial x} + \bar{V}\frac{\partial \bar{U}}{\partial r} = \frac{1}{r}\frac{\partial}{\partial r}\left[l^2 r\left|\frac{\partial \bar{U}}{\partial r}\right|\left(\frac{\partial \bar{U}}{\partial r}\right)\right]$$

or $$\bar{U}\frac{\partial \bar{U}}{\partial x} + \bar{V}\frac{\partial \bar{U}}{\partial r} = -\frac{1}{r}\frac{\partial}{\partial r}\left[l^2 r\left(\frac{\partial \bar{U}}{\partial r}\right)^2\right]$$

Tollmien assumes similarity at different sections of the jet and assumes that ℓ is constant across any section and proportional to the radii r_o of the sections. Having found experimentally that $r_o \sim x$, he assumes $\ell = cx$.

(b) Modified Vorticity Transfer Theory

Taylor assumes that vorticity is the transportable quantity and is carried unchanged from one layer of fluid to another. This, with the assumption of isotropy of turbulence, yields the equation of motion

$$\bar{U}\frac{\partial \bar{U}}{\partial x} + \bar{V}\frac{\partial \bar{U}}{\partial r} = \overline{\ell v}\left(\frac{\partial^2 \bar{U}}{\partial r^2} + \frac{1}{r}\frac{\partial \bar{U}}{\partial r}\right)$$

Assuming with Prandtl, that $\overline{\ell v} = \ell^2\left|\frac{\partial \bar{U}}{\partial r}\right|$, Howarth and Tomotika have

$$\bar{U}\frac{\partial \bar{U}}{\partial x} + \bar{V}\frac{\partial \bar{U}}{\partial r} = -\ell^2\frac{\partial \bar{U}}{\partial r}\left(\frac{\partial^2 \bar{U}}{\partial r^2} + \frac{1}{r}\frac{\partial \bar{U}}{\partial r}\right)$$

and they also assume $\ell = cx$.

(c) A third approach to the calculation of the velocities in turbulent flow was presented by P. Y. Chou. The equations are obtained by constructing correlation functions from the equations of turbulent fluctuations.

In the application of this theory to the jet, Lin has employed, in addition to the boundary layer approximations,

(1) the assumption of mechanical similarity of mean quantities extended to include all the double (and triple) correlations;

(2) certain considerations based upon similarity of fluctuations, and the microscale of turbulence;

(3) the assumption that the triple correlations of the turbulent fluctuation which vanish at the center of the jet are negligible throughout the jet.

These assumptions result in an expression for the shear which is identical to the form suggested by Karman in 1937:

$$\frac{\tau}{\rho} = \frac{\overline{v^2}\,\lambda^2}{\nu}\,\frac{\partial \bar{U}}{\partial r}$$

In addition, Lin assumes

(4) $\overline{v^2}$ and λ are constant. This final assumption amounts to a constant shear coefficient, and the form of the solution is the same as that for a laminar jet:

$$\frac{\bar{U}}{\bar{U}_m} = \frac{1}{\left(1 + \xi^2/4\right)^2}$$

where $\xi \sim \frac{r}{x}$.

2. Temperature

With the usual boundary layer approximations, the equation for the temperature, $\bar{\Theta}$, is

$$\bar{U}\frac{\partial \bar{\Theta}}{\partial x} + \bar{V}\frac{\partial \bar{\Theta}}{\partial r} = \frac{1}{r}\frac{\partial}{\partial r}\left(\overline{l v}\; r \frac{\partial \bar{\Theta}}{\partial r}\right)$$

The same general boundary conditions apply to the temperature as were applied to velocity.

(a) Momentum Transfer Theory

Since the above equation in $\bar{\Theta}$ is the same as the equation of motion (in $\bar{U}$), corresponding to the Momentum Transfer Theory, it follows that the temperature distribution

is the same as the velocity distribution.

(b) Modified Vorticity Transfer Theory

The previously obtained solutions for $\bar{U}$ and $\bar{V}$ are put into the temperature equation, along with the assumption that $\overline{lv} = - c \chi^2 \frac{\partial \bar{U}}{\partial r}$ as before.

This leads to a solution for $\frac{\bar{\theta}}{\bar{\theta}_m}$ as an exponential function which converges much more rapidly than the velocity.

(c) In solving for the temperature distribution, Lin uses a constant coefficient of thermal diffusion, analogous to the use of a constant shear coefficient. This leads to a power law relationship between the velocity and temperature distribution which he writes

$$\frac{\bar{\theta}}{\bar{\theta}_m} = \left(\frac{\bar{U}}{\bar{U}_m}\right)^{1/\epsilon_a}$$

where ϵ_a is not given by the theory but must be determined experimentally.

H. DISCUSSION

1. Isothermal Jet (Jet #1)

(a) The Nature of the Flow:

The series of oscillograms in Fig. 15 as well as the disappearance of $\overline{uv}$ -correlation toward the edge of the jet may be considered as proof that the "turbulent" jet is completely turbulent only from the axis out to approximately $r = r_o$. For $r > r_o$, there exists first an annular transition region, in which the flow at a point alternates between the turbulent and laminar regimes. Of course, the fraction of the total time during which the turbulent state prevails decreases as the radial distance is increased. Near the edge of the jet, and extending to zero velocity, is what might be termed the "laminar collar". A principal difference between this laminar region and the laminar sublayer in, say, turbulent pipe flow, is that here there exists an appreciable radial mean velocity component. In this way, the situation probably more closely resembles the laminar sublayer along a porous wall with fluid addition. The other essential difference between this "laminar collar" and a solid-wall sublayer is that here the shear stress goes to zero.

It will be noted that the general location of the transition region in the jet is about the same as the location of the $\frac{u'}{\overline{U}}$ maximum (Fig. 13). This may mean that a part of

the "turbulence" is not due to the usual turbulent velocity fluctuations, but to actual differences in local mean velocity at a point, as the flow oscillates between the laminar and turbulent states. This explanation was first given by Liepmann [45] to account for the high apparent turbulence level in the transition region (i.e., from a laminar boundary layer to a turbulent one) along a wall. It should be noted, however, that no predominantly one-sided bursts were seen here.

The other matter of interest on the general nature of the flow is the location of the fully developed region of the jet. As mentioned previously, apparent similarity of velocity and temperature profiles is reached just before $\frac{x}{d} = 10$. A more sensitive indication of complete mechanical similarity should be given by the turbulent motion. Fig. 14 shows very clearly, by the disappearance of the central minimum in the $\frac{u'}{U_o}$ distributions, that in Jet #1 the fully developed region may be considered to start between $\frac{x}{d} = 15$ and 20. That this value is not universal for round turbulent jets can be seen from the readings of Kuethe [25], whose $\frac{u'}{U_o}$ has lost the central minimum before $\frac{x}{d} = 10$. The existence of such a minimum on the axis is, of course, a remnant of the potential cone.

Another possible indicator of the condition of the jet is the kinetic energy crossing planes normal to the axis. In the fully developed region it may be expected that the rate of flow of turbulent kinetic energy will be a fixed fraction of the total kinetic energy flow. Fig. 21 roughly confirms our previous conclusion. The drop off at 40 diameters is probably experimental

scatter; the extremely low mean speeds at this station reduced the measurement accuracy.

(b) Mean Velocity and Temperature; Comparison with Theories:

On Fig. 22 there is plotted the results of the three theories briefly discussed in Section G, and the experimentally observed points. For purposes of comparison, the theories and experiment have all been matched at $r = r_o$. This seems to be an especially suitable abcissa in view of the fact that this radius is approximately the boundary of the completely turbulent jet core.

Since the three theoretical analyses assume a turbulent state across the full width of the jet, the degree of agreement between theory and experiment in the region for $r > r_o$ is evidently of secondary importance. Inspection of the region of $r < r_o$ indicates a fairly good check between the observed points and the curve based upon a constant exchange coefficient. However, a computation of the exchange coefficient distribution from the measured turbulent shear (Fig. 23) shows that ε is not actually constant. This is another excellent illustration of the relative insensitivity of the mean velocity profile for showing the detailed mechanical state of the flow.

The "mixing length" distribution has also been computed from the shear, and plotted on the same figure. The momentum and vorticity transport theories both assume l constant across a section. The mixing length theories also assume l increasing linearly with axial distance: $l = cx$. A calculation of c

at 20 diameters, based on momentum transport, leads to $c = 0.0166$ Tollmien [39] gives an experimental value of 0.0158.

Since Lin's analysis does not explicitly give the temperature profile as a function of the velocity profile, but leaves one constant to be determined by experiment, only the results of the other two theories have been plotted in Fig. 24.

In spite of the considerable scatter, it is evident that theoretical and experimental temperature distributions do not agree if the velocity distributions are matched at $r = r_o$ If, on the other hand, the temperatures had been fitted at the radius where $\bar{\Theta} = \frac{1}{2} \bar{\Theta}_m$, then the experimental and theoretical velocity profiles would show wide divergence, while the temperatures would check moderately well.

Thus it is evident that none of the existing theories gives a satisfactory quantitative relationship between the spread of heat and of momentum in a round turbulent heated jet.

(c) Turbulence:

The velocity fluctuations have been discussed at the beginning of this section. However, a few more specific remarks may be made. It is interesting to note that the local maxima in the turbulent velocity distributions (Fig. 14), for $\frac{x}{d} < 20$ remain at about the same radius, and that this is roughly the radius of the nozzle mouth. Of course, the rather arbitrary curve fairing determines the exact location of the peaks. However, this matter is related to the development of a fully turbulent flow, a problem which still awaits an adequate basic investigation.

In the computation of the rates of flow of kinetic energy (Fig. 21), two assumptions have been made: first, that the ratio of v'-energy to u'-energy is the same at all sections as it is at $\frac{x}{d} = 20$, the only section at which v' was measured; second, that the w'-energy at each section is equal to the v'-energy. The figure shows $\frac{E_T}{E_{T_o}}$, the ratio of the total rate of flow of kinetic energy past a section to the initial rate of flow of energy out of the orifice. It also shows $\frac{E_M}{E_{T_o}}$, the ratio of mean flow energy to the initial mean flow energy, which is also E_{T_o}, since the turbulent kinetic energy is initially negligible. $\frac{E'}{E_T}$, the fraction of the total kinetic energy that is contained in the turbulence, is also given.

One other result, shown clearly by Kuethe [25], but perhaps not emphasized sufficiently in its practical implications, is the rapid increase of turbulence within the potential cone. The sharp rise in $\frac{u'}{U_o}$ after $\frac{x}{d} = 1$ shows that the disturbance propagates from the initial annular mixing region inward at an angle of nearly 30^o. The significance of this result as a description of the flow in the working sections of open jet wind tunnels is obvious.

(d) Shear:

The turbulent shear stress is, of course, proportional to the $\overline{uv}$-correlation, which is plotted in dimensionless form in Fig. 16. The corresponding correlation coefficient, R_{uv}, also plotted in Fig. 16, reaches a maximum value of about 0.42. F. Wattendorf's maximum of 0.33 and H. Reichardt's maximum of 0.24, both computed by von Karman [31] for pipe flow, are

values of $\frac{\overline{uv}}{u'^2}$ instead of $\frac{\overline{uv}}{u'v'}$. The maximum value of $\frac{\overline{uv}}{u'^2}$ at this section of the jet is 0.34, in good agreement with the former. However, it should be mentioned that in a single plane mixing region, Liepmann and Laufer [13] have obtained a maximum $\frac{\overline{uv}}{u'v'}$ of about 0.56, while in a turbulent boundary layer, Schubauer and Klebanoff [24] recorded a maximum on the order of 0.50. In accordance with a remark made in the introduction, it seems reasonable to expect that all fully developed turbulent shear flows will have maximum correlation coefficients of the same order, probably in the fully turbulent region, "far" from the boundaries. There is still not enough known about turbulent shear flow to permit a rationalization of the differences in $(R_{uv})_{max.}$ given above.

The extreme scatter in R_{uv} at large r is due both to the transition nature of the flow and to the fact that one factor in the calculation is a small difference between relatively large quantities, each of which already has the usual amount of experimental scatter. Theis condition is even more accentuated in the hot jet.

C. C. Lin has given the author a method of calculating the shear stress distribution at a section from the velocity profile for the isothermal case. The method, outlined in Appendix II, has also been used by Squire [46] for several flow configurations.

A comparison between the dimensionless shear stress computed in this way, and the directly measured values, is given in Fig. 25. The curves agree well in shape; the reason for the discrepancy in magnitude is not evident. For this calculation the mean velocity profile has been corrected for the effect of turbulence level upon the instrument reading.

(e) Scale:

The correlation function $\frac{\overline{u_1 u_2}}{u'^2}$ between points symmetrical about the jet axis is quite similar to the corresponding function as it has been measured in isotropic turbulence. The scale L, obtained by an integration of the R_u curve, turns out to be approximately $0.23\ r_o$, i.e., about an eighth of the diameter of the fully turbulent core or about a thirtieth of what might be called the total jet width.

The microscale, λ, is determined crudely by fitting a parabola at the vertex of the correlation curve. However, it should be noted that there still exists no analysis giving the proper correction to the shape of this curve for the non-zero hot-wire length, so that the λ value is undoubtedly much too high. Since λ is a function of the smallest eddies, it is to be expected that the λ length correction will be appreciably greater than the L length correction given by Skramstad [15].

In the single plane mixing region, Liepmann and Laufer [13] found λ effectively constant across a section. If we assume this to be roughly true for the round jet, and use Taylor's approximation [1] for the rate of dissipation of turbulent energy into heat for isotropic turbulence,

$$\text{dissipation} = 15\,\nu\,\frac{\overline{u^2}}{\lambda^2}$$

it is possible to make a rough estimate of the energy balance across the jet. Computation of the dissipation terms (in the turbulent energy equation) involving derivatives of the turbulent energy shows them to be negligible here. The rate of production of

turbulent energy from mean flow kinetic energy is computed directly from the measured shear and mean velocity

$$\text{production} = \overline{uv}\,\frac{\partial \bar{U}}{\partial r}$$

Then, the turbulent energy equation requires that at each point

diffusion = production - dissipation.

The sign of the diffusion is chosen so that a positive term means a net addition of turbulent energy to the region by diffusion.

The result, plotted in Fig. 26, is to be taken more as qualitative than quantitative. A comparison between this and the corresponding figure for the half-jet[13] shows the essential difference clearly: in the full jet, the maximum rate of dissipation occurs in the maximum velocity region, where the production goes to zero; in the half-jet, maximum dissipation and production occur at about the same point. Therefore, in the full jet there is an appreciable central region with large positive diffusion, while the half-jet has no such region. As seems reasonable, in both examples the rate of production is a maximum in the vicinity of the inflection point of the velocity profile.

2. Hot Jet (Jet #2)

As remarked previously, the addition of appreciable heat, with the resulting change of relative density between jet and receiving medium does not seem to have changed the fundamental nature of the flow.

(a) Fluctuations:

Although, as far as can be judged with the existing experimental scatter, the turbulence distributions, $\frac{u'}{\bar{U}_m}$ and $\frac{v'}{\bar{U}_m}$

in the hot jet at $\frac{x}{d} = 15$ indicate a fully developed jet, still the temperature fluctuation shows an appreciable central minimum. Measurements at larger axial distances will be necessary to find out whether this distribution is characteristic of the fully developed region.

It may be noted that, just as in the case of the isothermal jet, v' is a bit higher than u' near the axis, but considerably lower elsewhere.

Although the curve fairing here, and particularly in the correlation distributions, may not follow all of the points, it should be remarked that considerations of jet symmetry (and in some cases, correlation anti-symmetry) were included in the curve drawing.

Since the mean temperature distribution is appreciably wider than the mean velocity distribution, it is not at all surprising to find concurrently that $\frac{\vartheta'}{\bar{\Theta}_m} > \frac{u'}{\bar{U}_m}$ in the outer portions of the jet. However, the most direct indication of the difference between turbulent heat transfer and momentum transfer is given by the correlations, to be discussed shortly.

(b) Double Correlations:

As was anticipated, the correlation between temperature fluctuation and axial velocity fluctuation maintains the same sign across the jet. The numerical values of $\frac{\overline{\vartheta u}}{\bar{\Theta}_m \bar{U}_m}$ and of $R_{\vartheta u}$, as given in Fig. 19 show this correlation to be appreciably lower than the lateral transport correlations.

It is extremely interesting to note that, consistent with previous results, the maximum $\frac{\overline{uv}}{u'v'}$ reached in the

hot jet is about 0.4. On the other hand, the maximum $\frac{\overline{\vartheta v}}{\vartheta' v'}$ appears to be on the order of 0.56.

The experimental scatter, which is extremely difficult to avoid in measurements in turbulent flow with appreciable heating, shows up best in these correlation values.

The extremely tedious computation has several steps which involve small differences of relatively large quantities, each of which has a reasonable amount of experimental scatter already. A brief outline of the procedure is given in Appendix III.

Due to the appreciable density fluctuations in the flow, the turbulent shear stress and lateral heat transfer rate cannot be expressed simply as $\tau = -\rho\overline{uv}$ and $Q = -c_p\rho\overline{\vartheta v}$ respectively. Instead, as discussed in Appendix V of Part I, inclusion of the density fluctuations leads to the approximate expressions,

$$\frac{\tau}{\bar{\rho}_m \bar{U}_m^2} = -\frac{\bar{T}_{am}}{\bar{T}_a}\left\{\left(\frac{\overline{uv}}{\bar{U}_m^2}\right) - \frac{\bar{U}}{\bar{U}_m}\cdot\frac{\bar{\theta}_m}{\bar{T}_a}\left(\frac{\overline{\vartheta v}}{\bar{\theta}_m \bar{U}_m}\right)\right\}$$

$$\frac{Q}{c_p \bar{\rho}_m \bar{\theta}_m \bar{U}_m} = -\frac{\bar{T}_{am}}{\bar{T}_a}\left[1 - \frac{\bar{\theta}}{\bar{T}_a}\right]\left(\frac{\overline{\vartheta v}}{\bar{\theta}_m \bar{U}_m}\right)$$

The results of the application of these equations, given in Fig. 27, show that inclusion of the density fluctuations has not altered the nature of the curves from what would have been obtained by using the constant density form.

The generalization of the method of Appendix II to the variable density case is essentially more complicated, and has

not been carried out.

3. Sources of Error

In general, the sources of error in the present investigation are the same as in all hot-wire measurements (see, for example, discussions in references 47 and 48), and need not be discussed here.

The principal additional source of error inherent in the hot jet measurements was the extreme difficulty of determining $\bar{R}_a$ with sufficient accuracy with the present equipment. Since the ϑ'-sensitivity of a hot-wire is proportional to $(\bar{R}_a - R_r)$, it can be seen that at the outer edges of the jet, where the transition nature of the flow already causes inaccuracies, the values are extremely uncertain. These difficulties, plus the necessity for taking relatively small differences, has led to occasional wild points at the outer edge of the correlation coefficient curves, which fall well outside of the plotted coordinate range.

Due to the relatively large experimental scatter of these measurements in a turbulent jet, as compared, for example with isotropic turbulence, it was felt that hot-wire length corrections were not appropriate. This was also true because of the uncertainty of the absolute value such high turbulence levels measured by the standard hot-wire equations, which assume small disturbances, and are valid to perhaps $\frac{u'}{\bar{U}} \approx 0.15$.

However, as indicated in Appendix I, the error in

turbulence reading due to large levels is not necessarily large, and the investigation can, in any case, be considered to give a good picture of the turbulent flow field.

It is hoped that in the future a more detailed comparison of temperature and velocity fluctuations in a turbulent shear flow with heat transfer can be carried out. The particular new measurements that would seem to be of significance are: a) $\frac{\overline{\vartheta_1 \vartheta_2}}{\vartheta'^2}$ correlation curve, for comparison with the $\frac{\overline{u_1 u_2}}{u'^2}$ curve. This would also permit computation of a "thermal scale" and a "thermal microscale"; b) the spectrum of the temperature fluctuations, as well as that of longitudinal and radial velocity fluctuations.

APPENDIX I: EFFECT OF TURBULENCE ON INSTRUMENT READINGS

Although no corrections have been made for the effect of turbulence, except in the case of the shear distribution computed from the mean velocity profile, it is well to point out the nature of these corrections.

(a) Total-Head Tube:

If we neglect static pressure fluctuations, and neglect the effect of lateral velocity fluctuations, the total dynamic pressure at the tube mouth is

$$\bar{P} = \frac{\rho}{2} \overline{(\bar{U} + u)^2} \tag{1}$$

Therefore, since $\overline{\bar{U} u} = 0$,

$$\bar{P} = \frac{\rho}{2} \left(\bar{U}^2 + \overline{u^2} \right)$$

and the dynamic pressure corresponding to mean velocity is

$$\frac{\rho}{2} \bar{U}^2 = \frac{\bar{P}}{1 + \frac{\overline{u^2}}{\bar{U}^2}} \tag{2}$$

The justification for neglecting v' in the first approximation is that the secondary increase in P due to a v' or w' fluctuation is at least partially balanced out by the directional sensitivity of the instrument.

(b) Hot-Wire: Mean Velocity:

A similar approach to the reading of a hot-wire anemometer goes as follows: If the total velocity to which

the hot-wire responds is q , then

$$q = \sqrt{(\bar{U}+u)^2 + v^2} \tag{3}$$

where w , the component along the length of the wire is neglected in the first approximation by reasoning similar to the above.

It is desired to learn $\bar{U}$, but the hot-wire actually measures $\bar{q}$. The relationship between them may be obtained by writing

$$\bar{q} = \bar{U}\,\overline{\sqrt{1 + 2\frac{u}{\bar{U}} + \frac{u^2}{\bar{U}^2} + \frac{v^2}{\bar{U}^2}}} \tag{4}$$

or, assuming $v^2 \approx u^2$ for this calculation,

$$\bar{q} = \bar{U}\,\overline{\sqrt{1 + 2\frac{u}{\bar{U}} + 2\frac{u^2}{\bar{U}^2}}} \tag{4a}$$

Expanding the radical out only to terms in $\frac{u^2}{\bar{U}^2}$, on the rough assumption that $\frac{u}{\bar{U}} << 1$, it turns out that

$$\bar{q} = \bar{U}\left[1 + \frac{1}{2}\frac{\overline{u^2}}{\bar{U}^2}\right]$$

where the average value of the linear term is z ero.

Therefore, as an indication of order of magnitude,

$$\bar{U} = \frac{\bar{q}}{1 + \frac{1}{2}\frac{\overline{u^2}}{\bar{U}^2}} \tag{5}$$

(c) Hot-Wire: Turbulence:

Up to the present time there exists no solution of the

hot-wire response equation valid for general large fluctuations [49]. A graphical solution has been given by Martinelli and Randall [50] for periodic fluctuations, but the application of this technique to a study of random turbulence does not appear to be feasible. Thus, it appears that at the present time an experimental approach to this problem as well as to the one discussed in (b) would be more fruitful.

Up to the present time no measurements have been made at the GALCIT to determine the effect of turbulence upon mean speed readings, but some preliminary measurements have been carried out on the effect of turbulence upon hot-wire readings of the turbulence.

The procedure was to vibrate a hot-wire sinusoidally in the flow direction of a relatively low-turbulence air stream. The vibrating device was the GALCIT Vibrator, constructed by F. Knoblock and C. Thiele in 1937 [51] for the purpose of determining hot-wire time-constants to permit proper compensation for thermal lag. The hot-wire circuit was properly compensated and the true turbulence level determined by measurement of the amplitude and frequency of the oscillation and the speed of the air stream.

A comparison between the true and measured turbulence levels is given in Fig. 28 for the same hot-wire at three different speeds. It is surprising to notice that the curve is concave upward for a range before the main drop-off begins. The appreciable deviation of the points at the highest speed

indicates that the curve may be dependent upon the sensitivity or temperature of the hot-wire; and, of course, the applied compensation for thermal lag was correct only for relatively low turbulence levels.

It is hoped that tests may be made in the near future to determine the effects of high turbulence upon the readings of both mean velocity and turbulence level with the hot-wire anemometer.

APPENDIX II: CALCULATION OF SHEAR DISTRIBUTION FROM VELOCITY PROFILE

Consider the "boundary-layer form" of the Navier-Stokes equation in cylindrical coordinates:

$$\bar{U}\frac{\partial \bar{U}}{\partial x} + \bar{V}\frac{\partial \bar{U}}{\partial r} = \frac{1}{\rho r}\frac{\partial}{\partial r}(r\tau) \tag{1}$$

We transform the equation in the conventional fashion, by assuming similarity, changing to an independent variable $\eta = \frac{r}{x}$ and taking a stream function in the form $\Psi = A x F(\eta)$, where A is a constant. The velocity components are then

$$\left.\begin{aligned} \bar{U} &= \frac{1}{r}\frac{\partial \Psi}{\partial r} = \frac{AF'}{x\eta} \\ \bar{V} &= -\frac{1}{r}\frac{\partial \Psi}{\partial x} = \frac{A}{x}\left[F' - \frac{F}{\eta}\right] \end{aligned}\right\} \tag{2}$$

Next, we assume an expression for the shear:

$$\tau = B\rho x^{n-1} f(\eta) \tag{3}$$

Substituting Eqs. (2) and (3) into Eq. (1) and simplifying the resulting equation,

$$\frac{A^2}{x^3}\left\{-\frac{F'^2}{\eta} - F\frac{d}{d\eta}\left(\frac{F'}{\eta}\right)\right\} = B x^{n-2}\frac{d}{d\eta}(\eta f) \tag{4}$$

and we now choose $n = -1$ so that x disappears from the equation and the similarity requirement is satisfied. Combining the two terms on the left side, and multiplying through the equation by η :

$$A^2\frac{d}{d\eta}\left(\frac{FF'}{\eta}\right) = -B\frac{d}{d\eta}(\eta f)$$

which immediately integrates as

$$f = \frac{A^2}{B} \cdot \frac{FF'}{\eta^2} \tag{5}$$

where the constant of integration is zero.

This gives the shear in simplest form:

$$\tau = \rho \frac{A^2}{r^2} FF' \tag{6}$$

although for calculation purposes, a more convenient form is

$$\frac{\tau}{\rho} = \frac{A^2}{x^2} \frac{FF'}{\eta^2}$$

APPENDIX III: PROCEDURE FOR DOUBLE CORRELATION MEASUREMENT IN HOT JET

The general technique followed in the measurement of $\overline{uv}$ and $\overline{\vartheta v}$ correlations is that described in Section G of Part I. The outline given there assumes a perfectly symmetrical X-meter. Unfortunately, the measurements in a flow with both velocity and temperature fluctuations are even more sensitive to meter unsymmetry than the $\overline{uv}$ measurements in an isothermal flow.

Due to the difficulty of obtaining an instrument symmetrical with sufficient accuracy, it was necessary to compute $\overline{uv}$ and $\overline{\vartheta v}$ in the hot jet with no assumptions of symmetry. Thus, the mean squares of the fluctuating voltages of the two wires are

$$\overline{e_1^2} = \beta_1^2\overline{\left(\frac{\vartheta}{\bar{\Theta}}\right)^2} + \delta_1^2\overline{\left(\frac{u}{\bar{U}}\right)^2} + \varepsilon_1^2\overline{\left(\frac{v}{\bar{U}}\right)^2} + 2\beta_1\delta_1\frac{\overline{\vartheta u}}{\bar{\Theta}\bar{U}} + 2\beta_1\varepsilon_1\frac{\overline{\vartheta v}}{\bar{\Theta}\bar{U}} + 2\delta_1\varepsilon_1\frac{\overline{uv}}{\bar{U}^2}$$

$$\overline{e_2^2} = \beta_2^2\overline{\left(\frac{\vartheta}{\bar{\Theta}}\right)^2} + \delta_2^2\overline{\left(\frac{u}{\bar{U}}\right)^2} + \varepsilon_2^2\overline{\left(\frac{v}{\bar{U}}\right)^2} + 2\beta_2\delta_2\frac{\overline{\vartheta u}}{\bar{\Theta}\bar{U}} - 2\beta_2\varepsilon_2\frac{\overline{\vartheta v}}{\bar{\Theta}\bar{U}} - 2\delta_2\varepsilon_2\frac{\overline{uv}}{\bar{U}^2}$$

Since there are two unknowns, readings must be taken at two different hot-wire sensitivities. Then the two pairs of differences give

$$\overline{e_1^2} - \overline{e_2^2} = (\beta_1^2 - \beta_2^2)\overline{\left(\frac{\vartheta}{\bar{\theta}}\right)^2} + (\delta_1^2 - \delta_2^2)\overline{\left(\frac{u}{\bar{U}}\right)^2} + (\varepsilon_1^2 - \varepsilon_2^2)\overline{\left(\frac{v}{\bar{U}}\right)^2}$$
$$+ 2(\beta_1\delta_1 - \beta_2\delta_2)\frac{\overline{\vartheta u}}{\bar{\theta}\bar{U}} + 2(\beta_1\varepsilon_1 + \beta_2\varepsilon_2)\frac{\overline{\vartheta v}}{\bar{\theta}\bar{U}} + 2(\delta_1\varepsilon_1 + \delta_2\varepsilon_2)\frac{\overline{uv}}{\bar{U}^2}$$

$$\overline{e_1'^2} - \overline{e_2'^2} = (\beta_1'^2 - \beta_2'^2)\overline{\left(\frac{\vartheta}{\bar{\theta}}\right)^2} + (\delta_1'^2 - \delta_2'^2)\overline{\left(\frac{u}{\bar{U}}\right)^2} + (\varepsilon_1'^2 - \varepsilon_2'^2)\overline{\left(\frac{v}{\bar{U}}\right)^2}$$
$$+ 2(\beta_1'\delta_1' - \beta_2'\delta_2')\frac{\overline{\vartheta u}}{\bar{\theta}\bar{U}} + 2(\beta_1'\varepsilon_1' + \beta_2'\varepsilon_2')\frac{\overline{\vartheta v}}{\bar{\theta}\bar{U}} + 2(\delta_1'\varepsilon_1' + \delta_2'\varepsilon_2')\frac{\overline{uv}}{\bar{U}^2}$$

Thus, the u'- , v'- and ϑ'- sensitivity of each wire must be determined separately. $\overline{\left(\frac{\vartheta}{\bar{\theta}}\right)^2}$, $\overline{\left(\frac{u}{\bar{U}}\right)^2}$ and $\overline{\left(\frac{v}{\bar{U}}\right)^2}$ are known from previous measurements, and the above pair of linear equations can be solved simultaneously for $\frac{\overline{uv}}{\bar{U}^2}$ and $\frac{\overline{\vartheta v}}{\bar{\theta}\bar{U}}$.

REFERENCES

1. G. I. Taylor, Proc. Roy. Soc., A 151 (1935);
2. G. I. Taylor, Jour. Aero. Sci., 4 (1936-37);
3. G. I. Taylor, Proc. Roy. Soc., A 164 (1938);
4. Th. v. Kármán, Jour. Aero. Sci., 4 (1937);
5. Th. v. Kármán and L. Howarth, Proc. Roy. Soc., A. 164 (1938);
6. A. N. Kolmogoroff, C. R. (Doklady), 30, No. 4 (1941);
7. A. N. Kolmogoroff, C. R. (Doklady), 32, No. 1 (1941);
8. A. Obukhoff, C. R. (Doklady), 32, No. 1 (1941);
9. L. Onsager, (Abstract) Phys. Rev., 62 (1945);
10. C. F. v. Weizsäcker, unpublished, (1946);
11. W. Heisenberg, unpublished, (1946);
12. G. K. Batchelor, Proc. Roy. Soc., A 186 (1946);
13. H. W. Liepmann and J. Laufer, T. N. (in press), N.A.C.A. (1947);
14. L. F. G. Simmons and C. Salter, Proc. Roy. Soc., A 165 (1938);
15. H. L. Dryden, G. B. Schubauer, W. C. Mock, Jr. and H. K. Skramstad, T.R. No. 581, N.A.C.A. (1937);
16. G. I. Taylor, Proc. 5th Int. Cong. Appl. Mech. (1938);
17. H. L. Dryden, Proc. 5th Int. Cong. Appl. Mech. (1938);
18. S. Atsumi, Guggenheim Aero. Lab., C.I.T., (unpublished, 1939);
19. S. Corrsin, A.E. Thesis, C.I.T. (1942);
20. D. C. MacPhail, Jour. Aero. Sci., 8 (1940);
21. G. K. Batchelor and A. A. Townsend, F. M. 991, Aero. Res. Council (1946);
22. C. Thiele, Rept. for Contract NAw-640 (unpublished), N.A.C.A. (1940);

23. D. C. MacPhail, T.N. No. Aero. 1374, R.A.E. (1944);

24. G. B. Schubauer and P. Klebanoff, A.C.R. No. 5K27, N.A.C.A. (1946);

25. A. M. Kuethe, Jour. Appl. Mech., Sept., (1935);

26. S. Corrsin, A.C.R. No. 3L23, N.A.C.A. (1943);

27. L. Prandtl, Aerodynamic Theory, Vol. III, ed. by W. F. Durand, J. Springer, (1935);

28. G. I. Taylor, Phil. Trans. Roy. Soc., A 215 (1915); Proc. Roy. Soc., A 135 (1932);

29. Th. v. Kármán, Gott. Nachr. Math. Phys. Klasse (1930);

30. Modern Developments in Fluid Dynamics, ed. by S. Goldstein, Oxford Press (1938);

31. Th. v. Kármán, Proc. 4th Int. Congr. Appl. Mech. (1934);

32. P. Y. Chou, Chinese Jour. Phys., 4, Jan. (1940);

33. P. Y. Chou, Quart. Appl. Math., 3,No. 1 (1945);

34. P. Y. Chou, Quart. Appl. Math., 3,No. 3 (1945);

35. H. Reichardt, Naturwissenschaften, 26 (1938);

36. F. L. Wattendorf, Jour. Aero. Sci., 3, No. 8 (1936);

37. P. Ruden, Naturwissenschaften, 21,No. 21/23 (1933);

38. W. Tollmien, Z.A.M.M., 6, Dec. (1926);

39. S. Tomotika, Proc. Roy. Soc., A 165 (1938);

40. L. Howarth, Proc. Camb. Phil. Soc., 34 (1938);

41. C. C. Lin, (unpublished, 1940);

42. L. Prandtl, Z.A.M.M., 22, Oct. (1942);

43. H. Görtler, Z.A.M.M., 22, Oct. (1942);

44. W. H. Bowen, M. S. Thesis, C.I.T. (1938);

45. H. W. Liepmann, A.C.R. No. 3H30, N.A.C.A. (1943);

46. H. B. Squire, Rept. No. Aero.2023, R.A.E. (1945);

47. H. L. Dryden, v. Kármán Anniversary Volume (1941);

48. L. F. G. Simmons, R. & M. 1919, A.R.C. (1939);

49. H. L. Dryden and A. M. Kuethe, T. R. 320, N.A.C.A. (1929);

50. R. C. Martinelli and R. D. Randall, Trans. A. S. M. E., Jan. (1946);

51. F. D. Knoblock, Ph. D. Thesis, C.I.T. (1937).

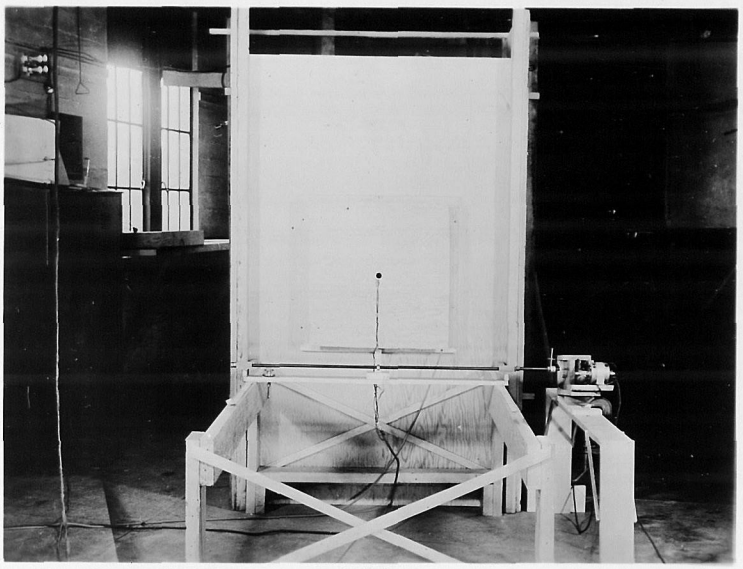

Figure 2a: Jet #1, view along axis into orifice

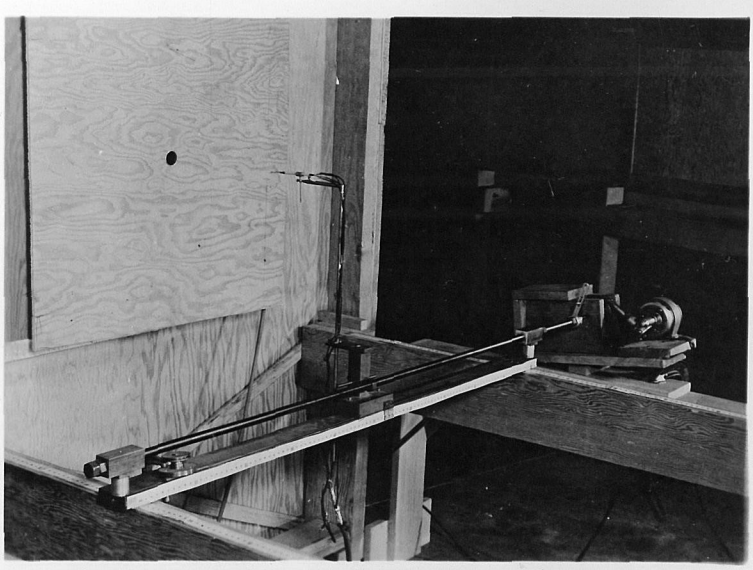

Figure 2b: Jet #1, close-up showing traversing mechanism

ONE INCH HEATED JET #2

(APPROX. $\frac{1}{8}$ FULL SIZE)

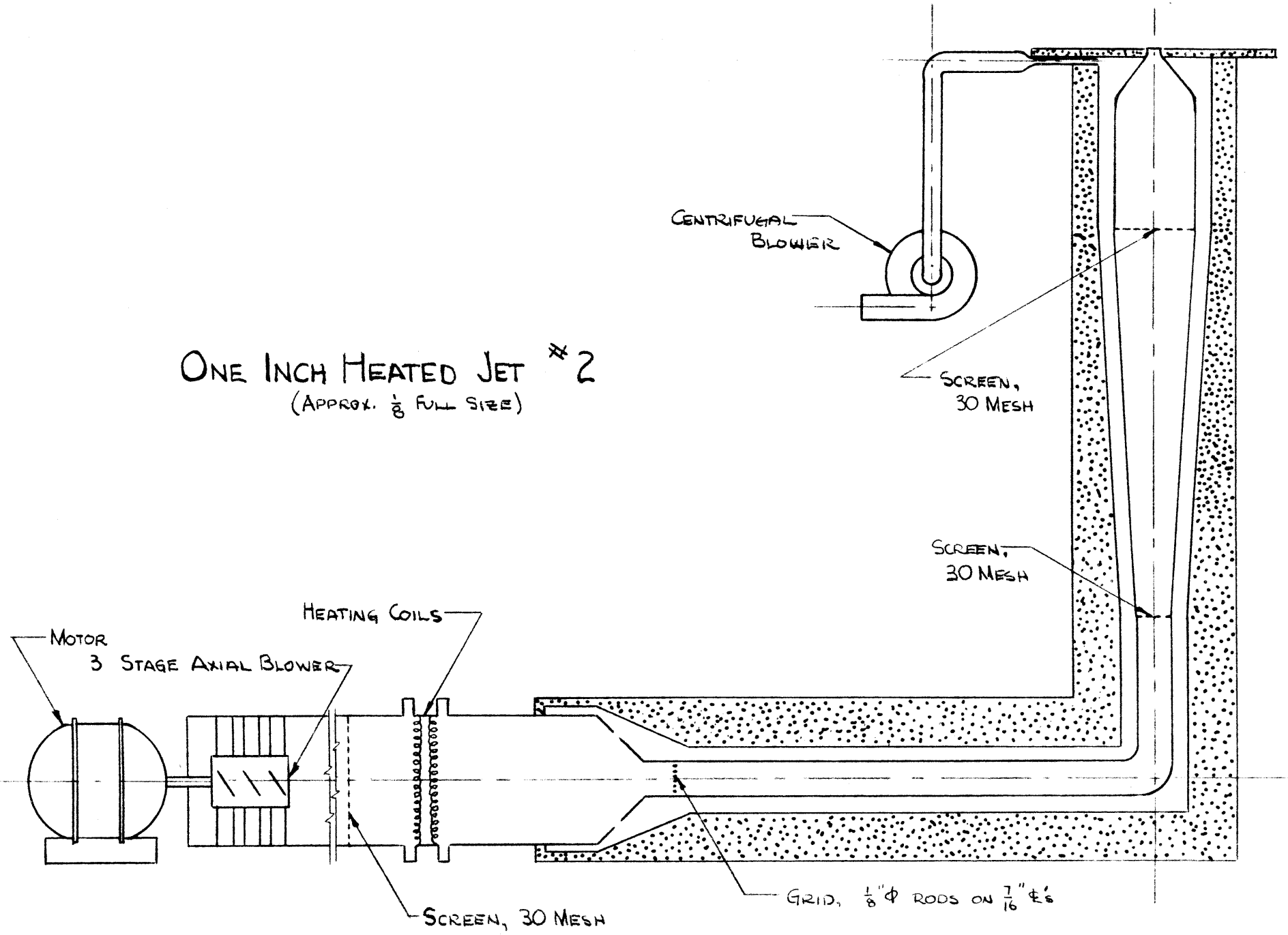

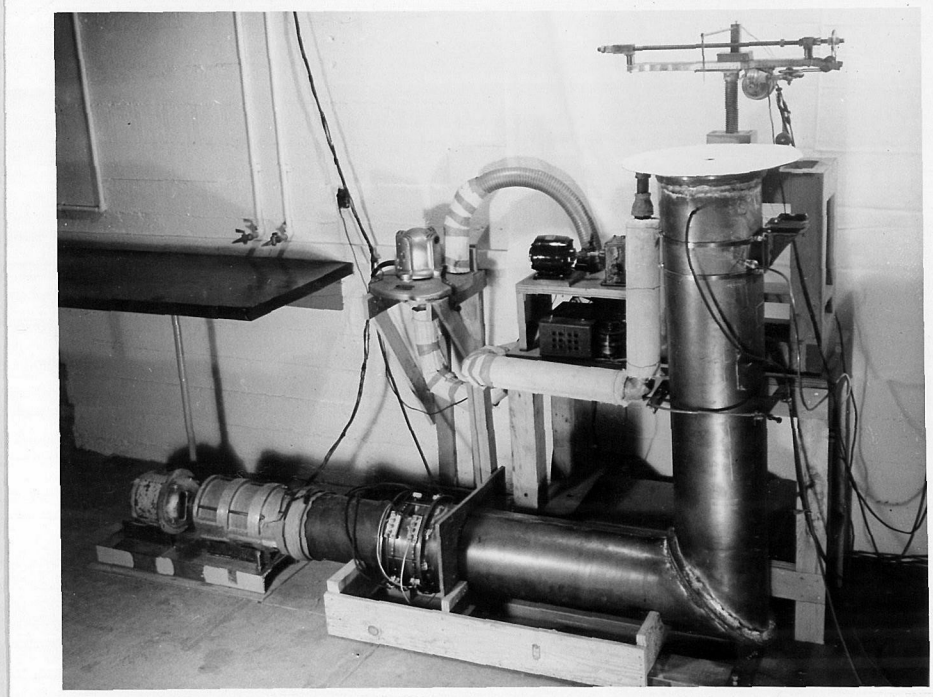

Figure 4a: Jet #2, general view

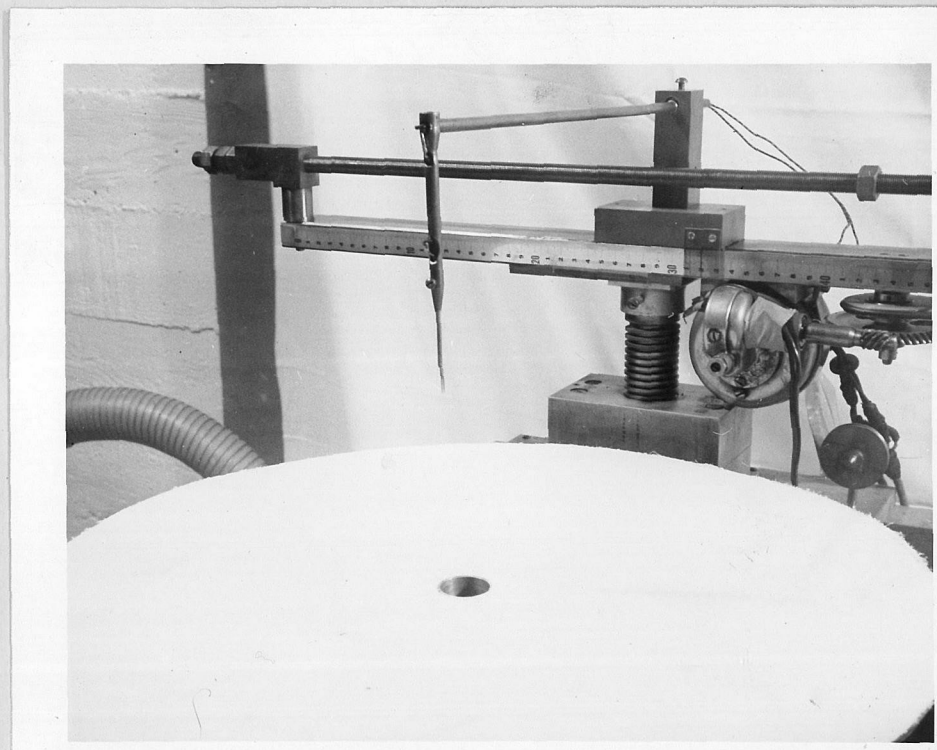

Figure 4b: Jet #2, close-up showing traversing mechanism

TYPICAL FOUR HOT-WIRE CIRCUIT

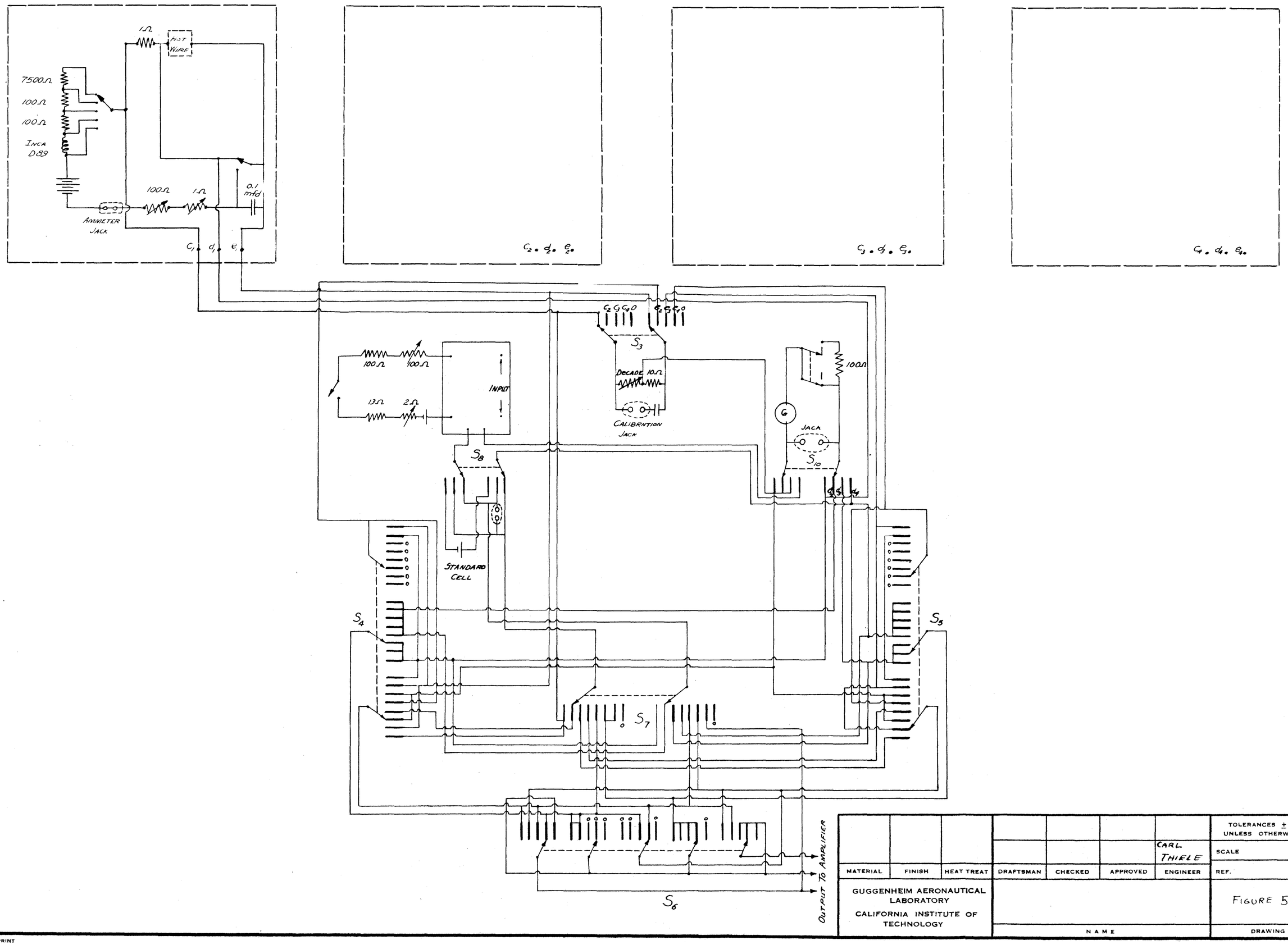

							TOLERANCES ± .010 OR ± 1/64 UNLESS OTHERWISE NOTED
						CARL THIELE	SCALE
MATERIAL	FINISH	HEAT TREAT	DRAFTSMAN	CHECKED	APPROVED	ENGINEER	REF.
GUGGENHEIM AERONAUTICAL LABORATORY CALIFORNIA INSTITUTE OF TECHNOLOGY							FIGURE 5
			NAME				DRAWING NO.

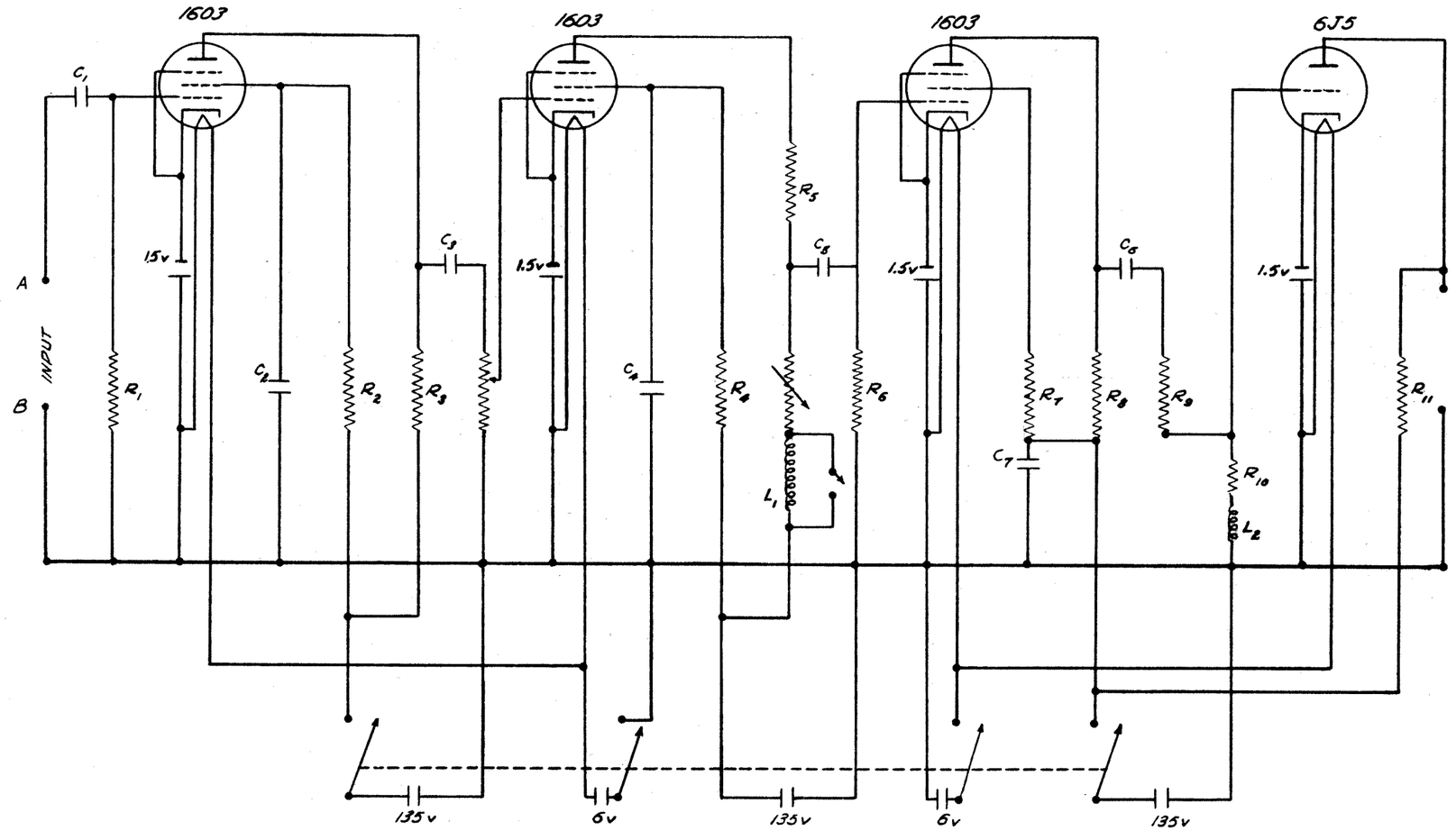

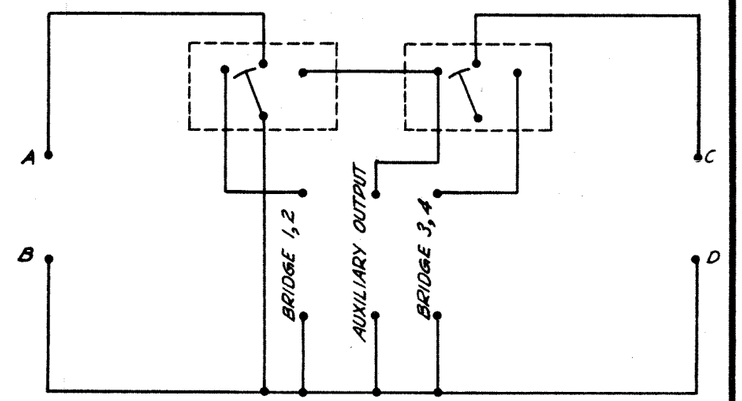

R_1 = 1 meg.
R_2 = 1 meg.
R_3 = 250,000
R_4 = 1 meg.
R_5 = 250,000

R_6 = 1 meg.
R_7 = 1 meg.
R_8 = 250,000
R_9 = 250,000
R_{10} = 250,000
R_{11} = 7000

C_1 = .5 μf
C_2 = 4 μf
C_3 = 1 μf
C_4 = 4 μf
C_5 = .5 μf
C_6 = .5 μf
C_7 = 4 μf

L_1 = 1.92 h
L_2 = 2 h

							TOLERANCES ± .010 OR ± 1/64 UNLESS OTHERWISE NOTED
						CARL THIELE	SCALE
MATERIAL	FINISH	HEAT TREAT	DRAFTSMAN	CHECKED	APPROVED	ENGINEER	REF.
GUGGENHEIM AERONAUTICAL LABORATORY CALIFORNIA INSTITUTE OF TECHNOLOGY							FIGURE 6
			NAME				DRAWING NO.

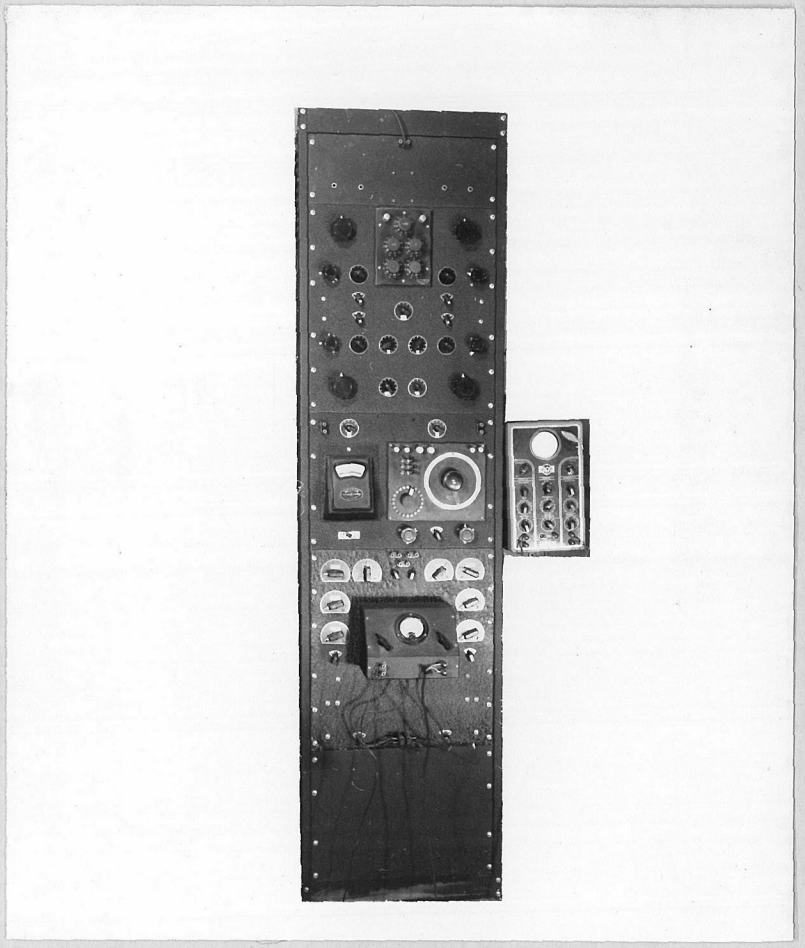

Figure 7: Four-wire, two-amplifier hot-wire set

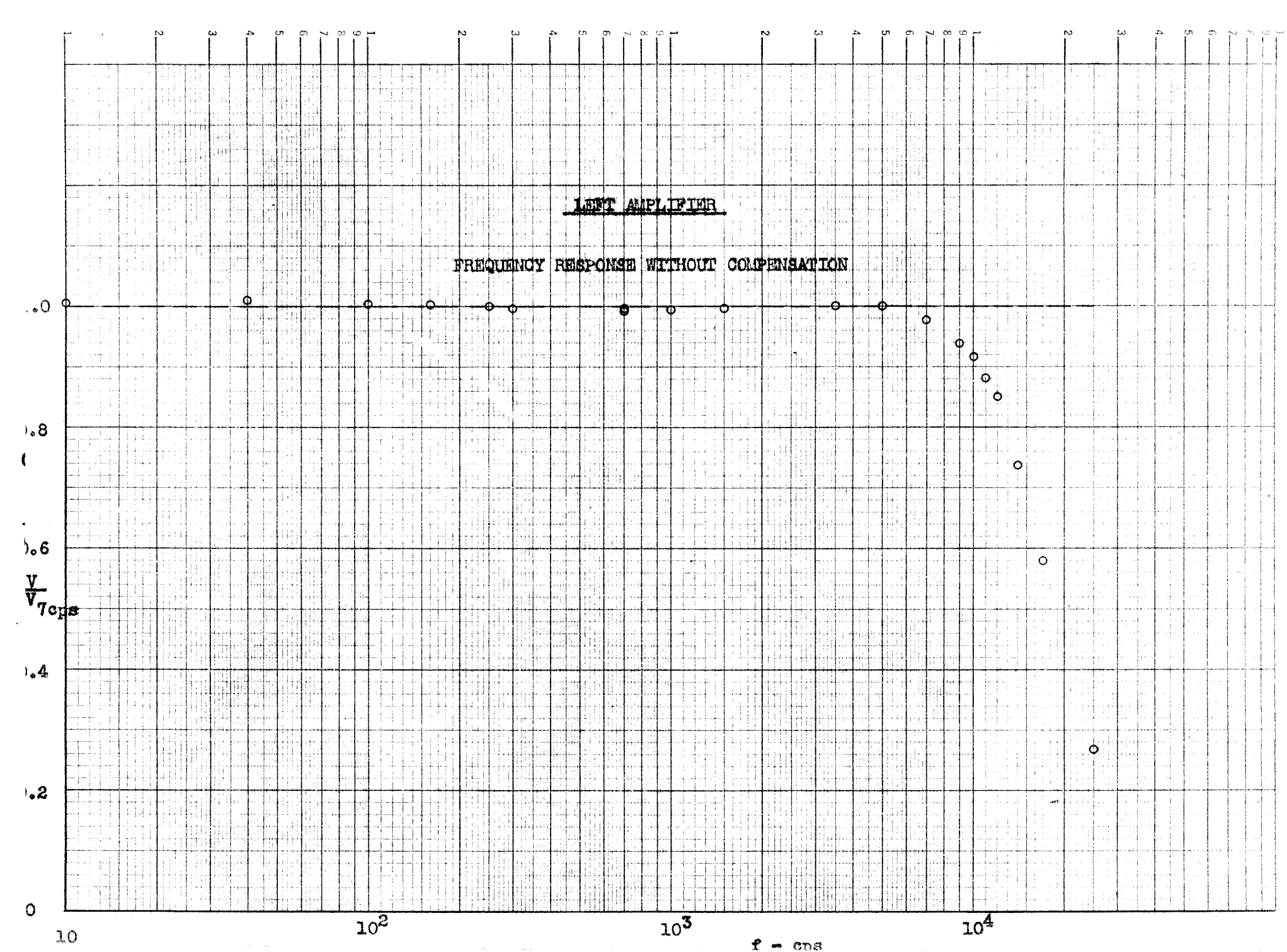
LEFT AMPLIFIER
FREQUENCY RESPONSE WITHOUT COMPENSATION
1.0
0.8
0.6
0.4
0.2
0
V/V7cps
10
10^2
10^3
10^4
f - cps

Fig. 8

LEFT AMPLIFIER

FREQUENCY RESPONSE WITH TYPICAL COMPENSATION SETTING

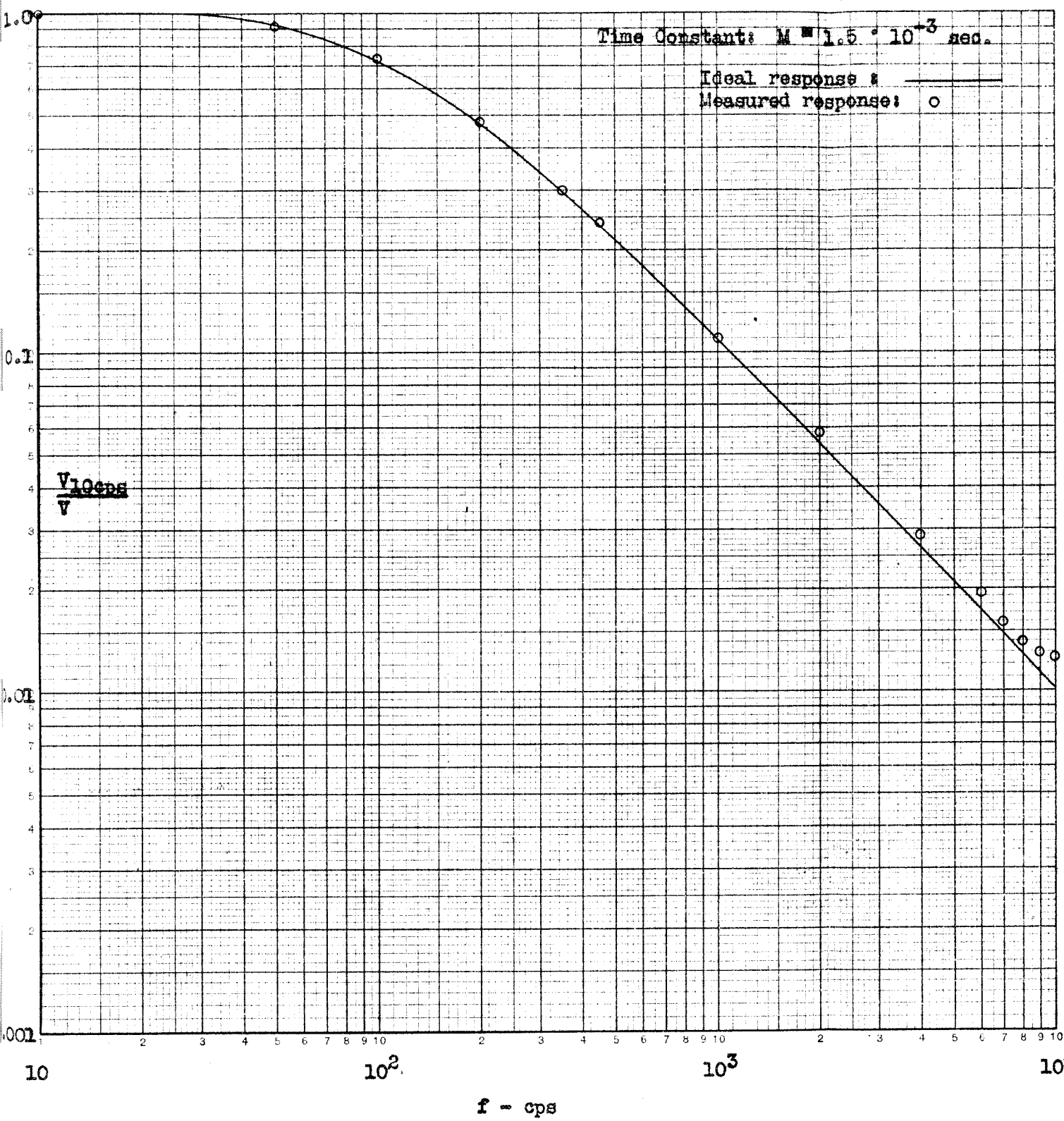

ONE INCH HEATED JET

SAMPLE PHOTOGRAPHIC RECORD

NOTE: THE LATERAL OFFSET OF THE RECORDS IS DUE TO INSTRUMENT SPACING

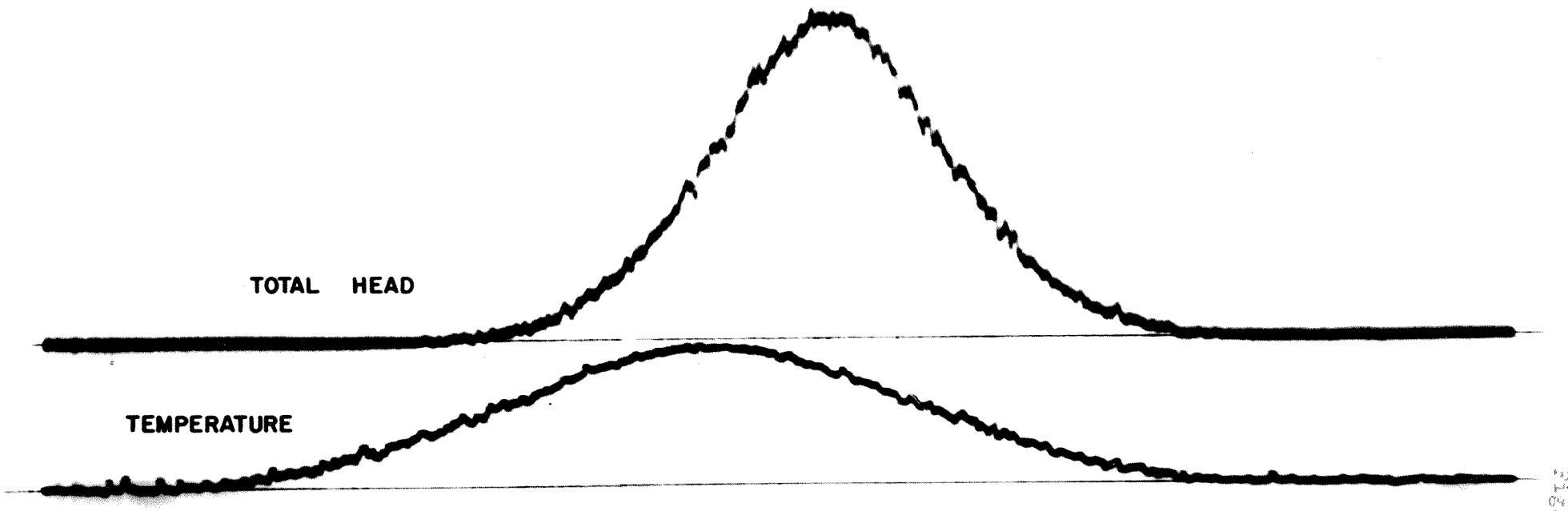

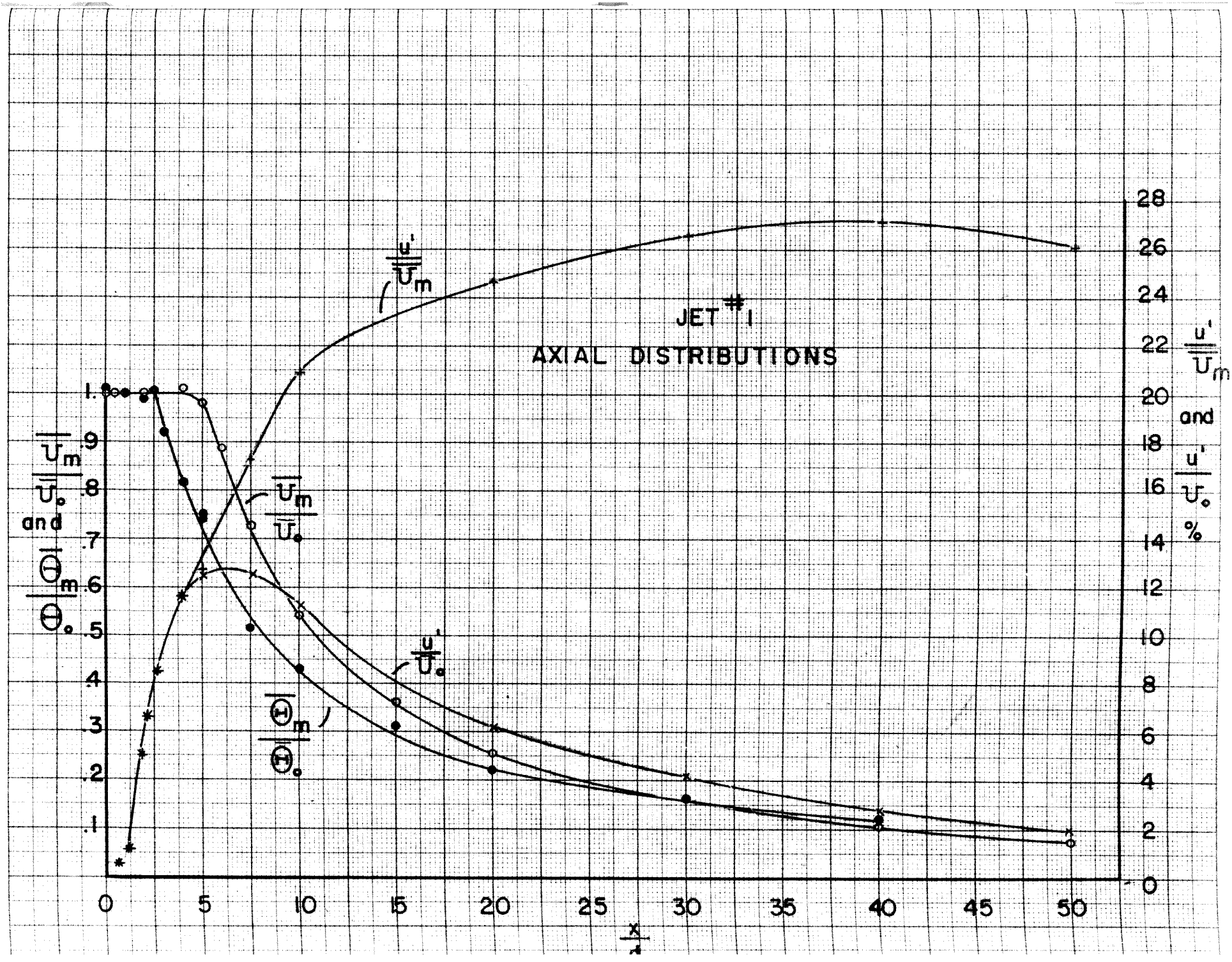
JET #1
AXIAL DISTRIBUTIONS
$\frac{\overline{u'}}{\overline{U}_m}$
$\frac{\overline{U}_m}{\overline{U}_o}$
$\frac{\overline{u'}}{\overline{U}_o}$
$\frac{\overline{\Theta}_m}{\overline{\Theta}_o}$
$\frac{\overline{U}_m}{\overline{U}_o}$ and $\frac{\overline{\Theta}_m}{\overline{\Theta}_o}$
$\frac{\overline{u'}}{\overline{U}_m}$ and $\frac{\overline{u'}}{\overline{U}_o}$ %
$\frac{x}{d}$
0 5 10 15 20 25 30 35 40 45 50
1. .9 .8 .7 .6 .5 .4 .3 .2 .1
28 26 24 22 20 18 16 14 12 10 8 6 4 2 0

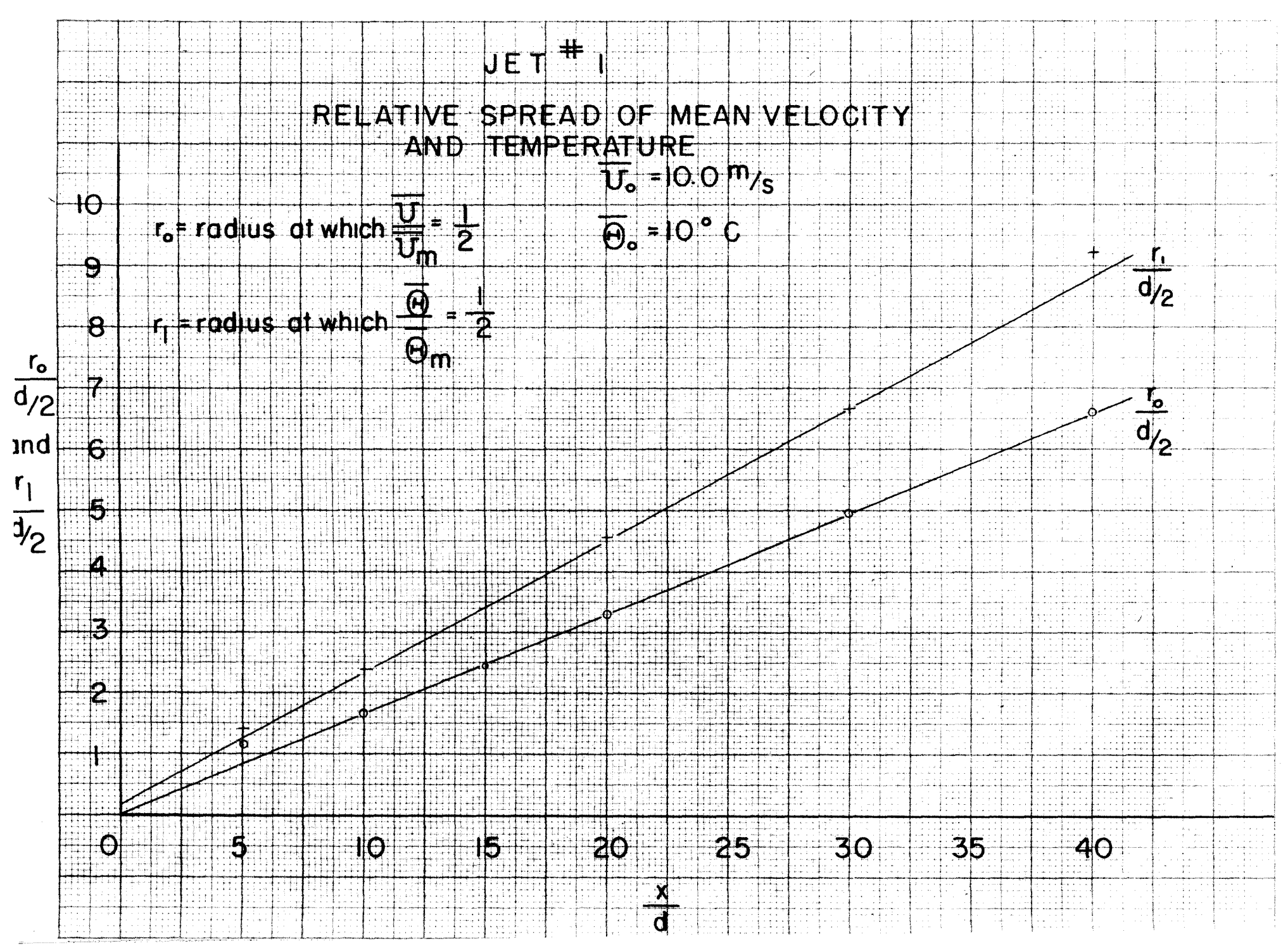
JET # 1
RELATIVE SPREAD OF MEAN VELOCITY AND TEMPERATURE
$\overline{U}_o$ = 10.0 m/s
$\overline{\Theta}_o$ = 10° C
r_o = radius at which $\frac{\overline{U}}{\overline{U}_m} = \frac{1}{2}$
r_1 = radius at which $\frac{\overline{\Theta}}{\overline{\Theta}_m} = \frac{1}{2}$
$\frac{r_1}{d/2}$
$\frac{r_o}{d/2}$
$\frac{r_o}{d/2}$ and $\frac{r_1}{d/2}$
$\frac{x}{d}$
0
5
10
15
20
25
30
35
40
1
2
3
4
5
6
7
8
9
10

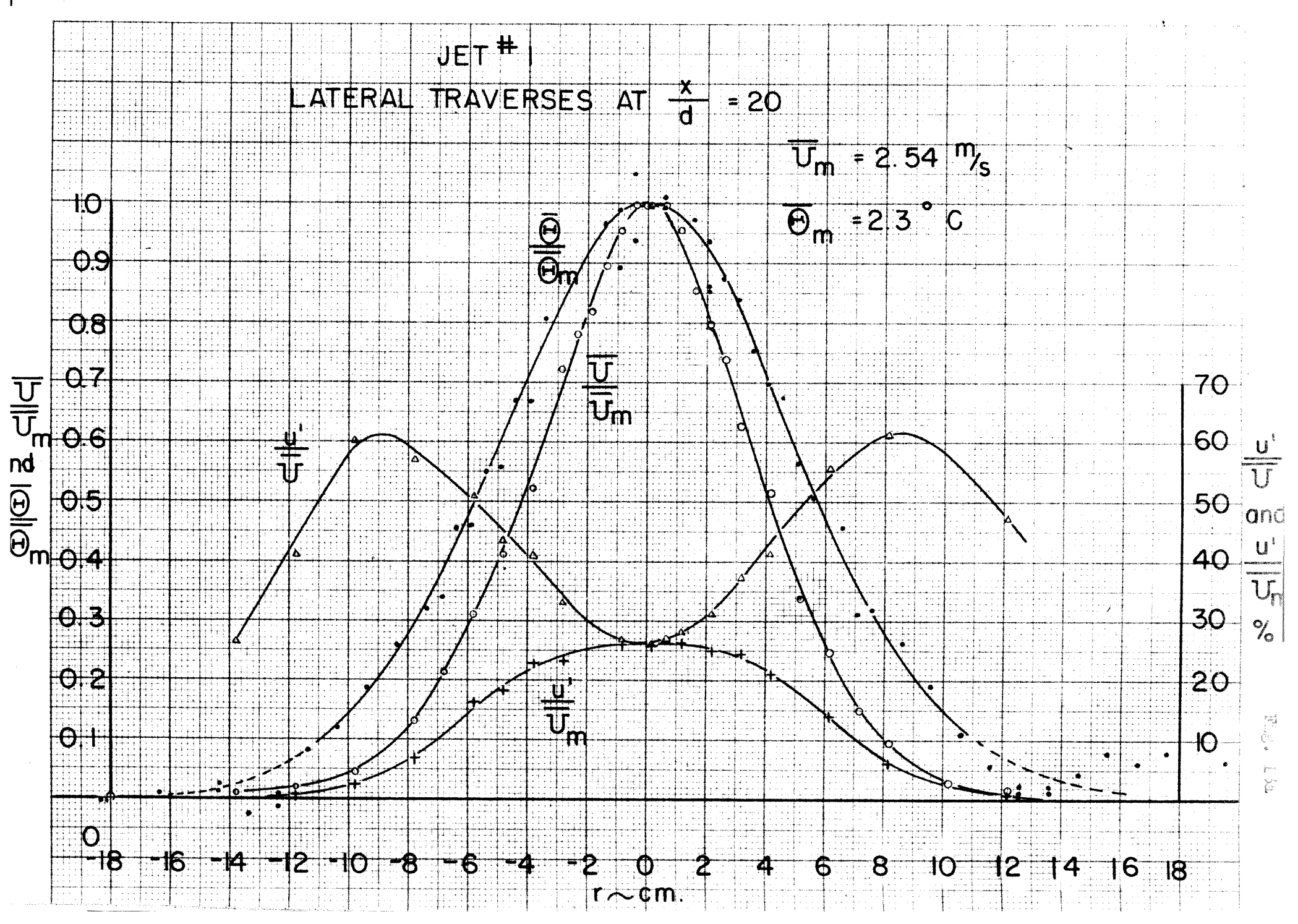
JET # 1
LATERAL TRAVERSES AT x/d = 20
$\overline{U}_m$ = 2.54 m/s
$\overline{\Theta}_m$ = 2.3 °C
$\frac{\overline{\Theta}}{\overline{\Theta}_m}$
$\frac{\overline{U}}{\overline{U}_m}$
$\frac{u'}{\overline{U}}$
$\frac{u'}{\overline{U}_m}$
$\frac{\overline{U}}{\overline{U}_m}$ and $\frac{\overline{\Theta}}{\overline{\Theta}_m}$
$\frac{u'}{\overline{U}}$ and $\frac{u'}{\overline{U}_m}$ %
1.0
0.9
0.8
0.7
0.6
0.5
0.4
0.3
0.2
0.1
0
70
60
50
40
30
20
10
-18 -16 -14 -12 -10 -8 -6 -4 -2 0 2 4 6 8 10 12 14 16 18
r ~ cm.

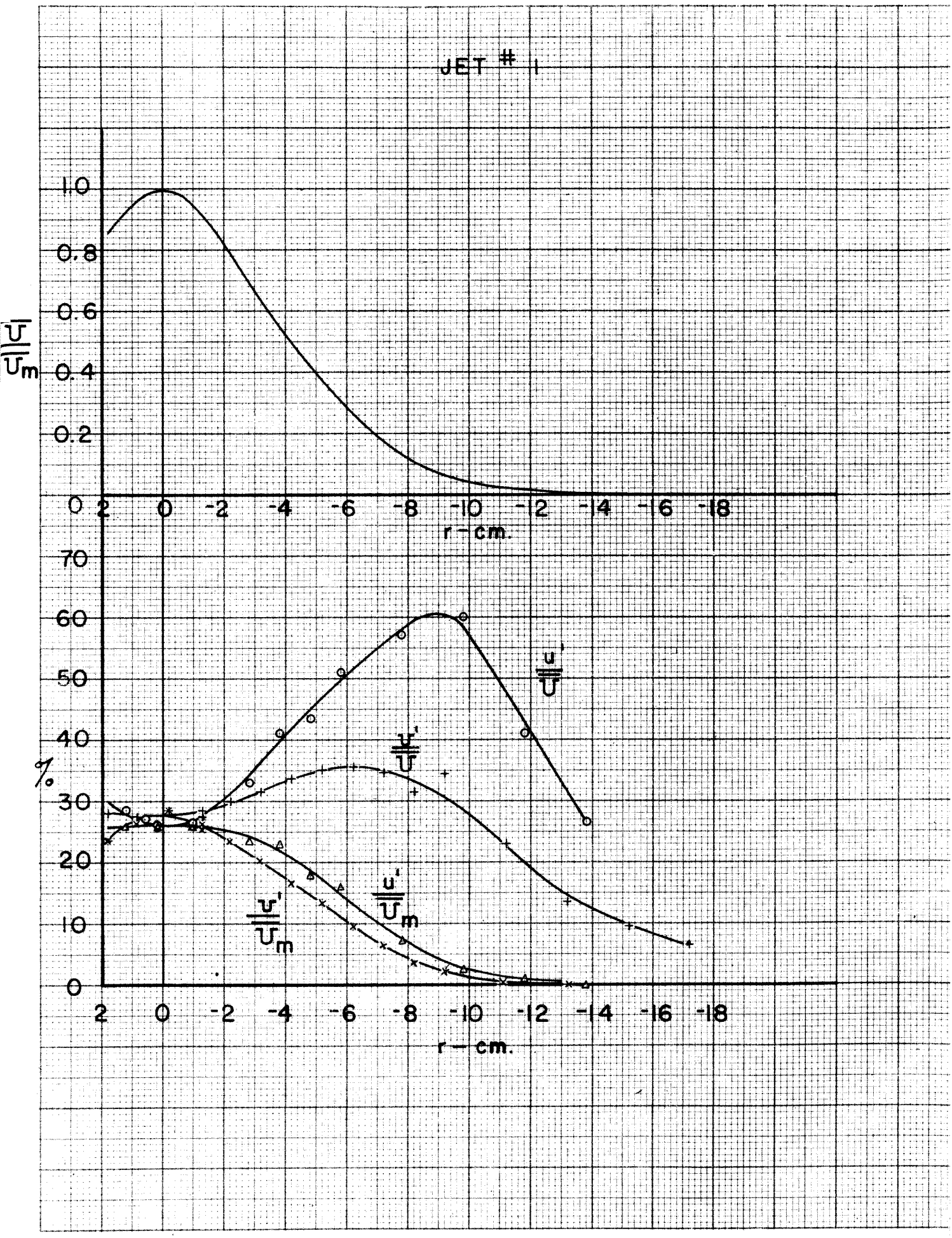
JET # 1
1.0
0.8
0.6
0.4
0.2
0
$\frac{\bar{U}}{U_m}$
2 0 -2 -4 -6 -8 -10 -12 -14 -16 -18
r - cm.
70
60
50
40
30
20
10
0
%
$\frac{u'}{\bar{U}}$
$\frac{v'}{\bar{U}}$
$\frac{u'}{U_m}$
$\frac{v'}{U_m}$
2 0 -2 -4 -6 -8 -10 -12 -14 -16 -18
r — cm.

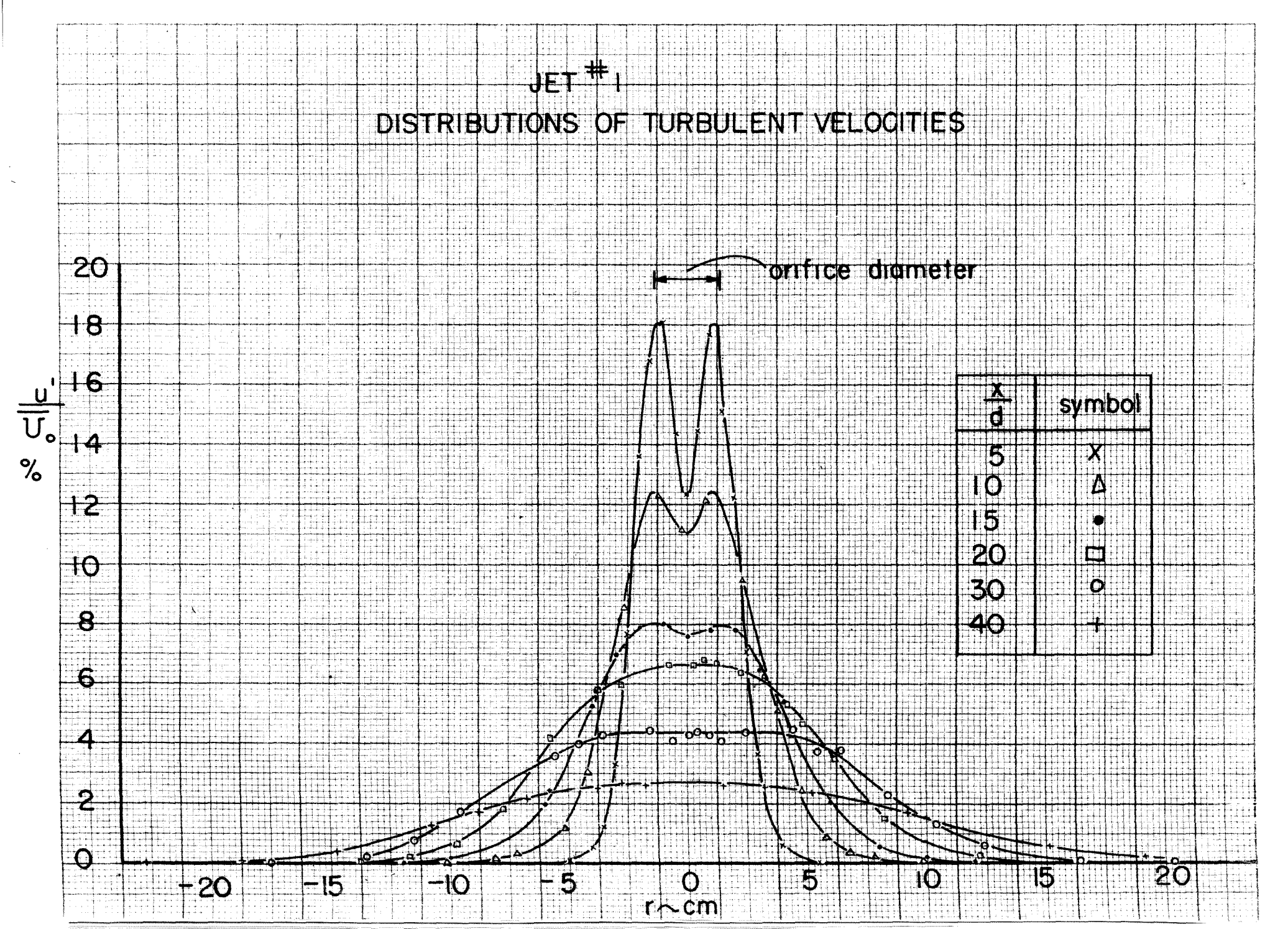
JET # 1
DISTRIBUTIONS OF TURBULENT VELOCITIES
orifice diameter
u'/U₀ %
20
18
16
14
12
10
8
6
4
2
0
-20
-15
-10
-5
0
5
10
15
20
r ~ cm
x/d
symbol
5
10
15
20
30
40

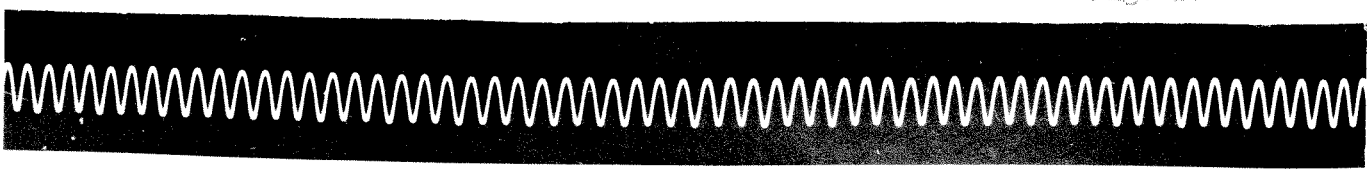

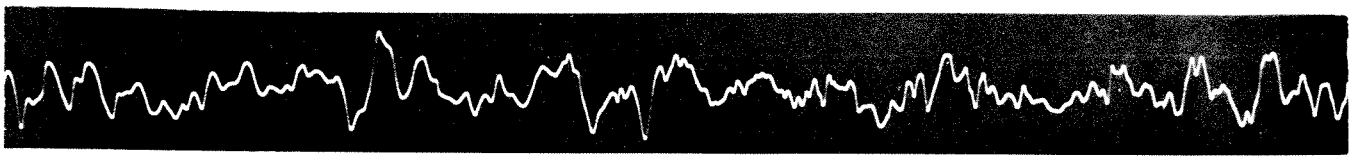

(a) r = 0 (on axis)

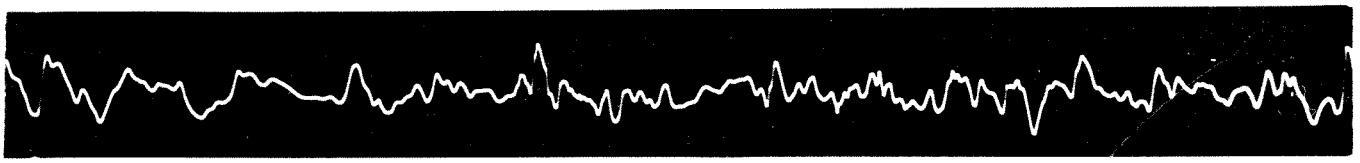

(b) r = 4.5 cm = 1.07 r_o

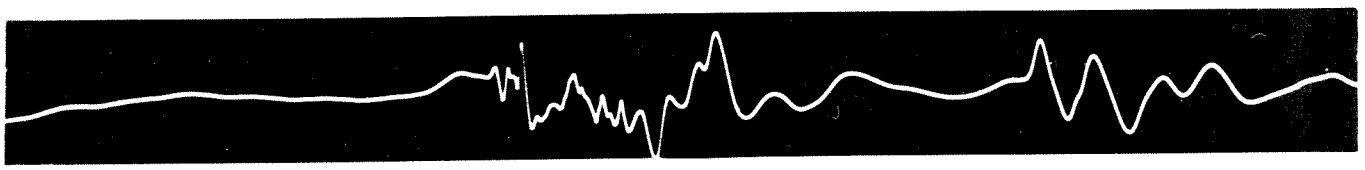

(c) r = 7.5 cm = 1.79 r_o

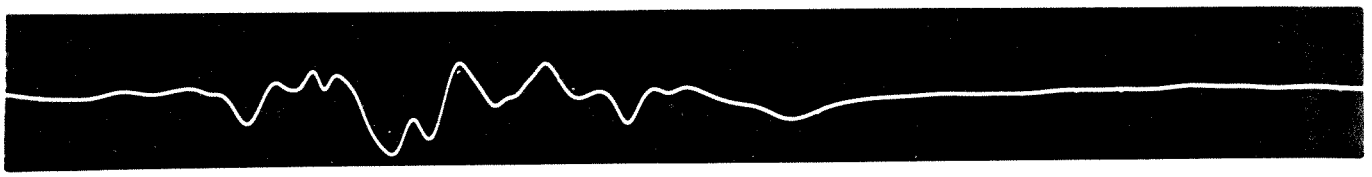

(d) r = 9.5 cm = 2.26 r_o

(e) r = 14.5 cm = 3.45 r_o

One-inch heated jet, x = 20 diameters

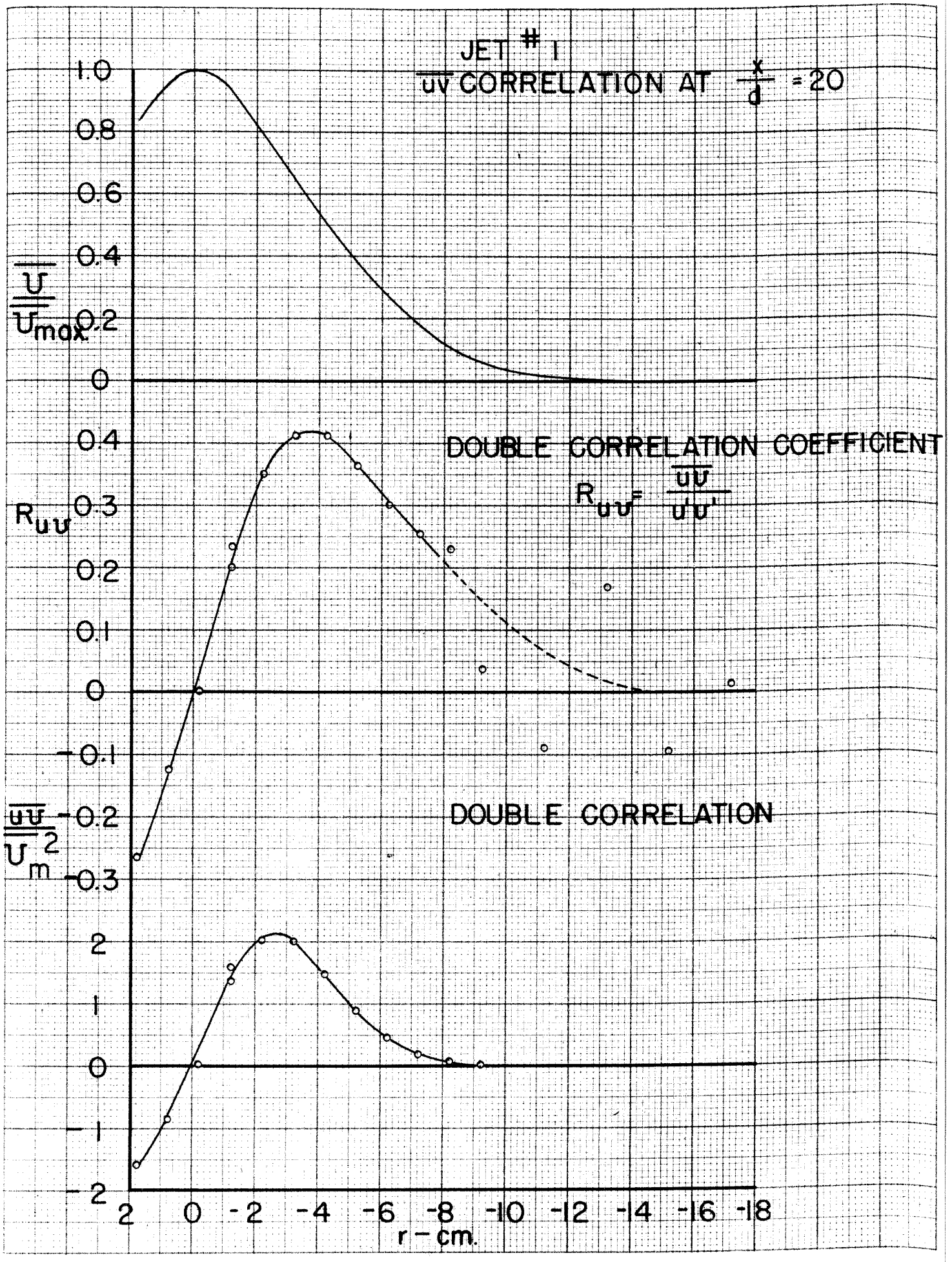
JET # 1
$\overline{uv}$ CORRELATION AT $\frac{x}{d}$ = 20
$\frac{\overline{U}}{U_{max}}$
1.0
0.8
0.6
0.4
0.2
0
DOUBLE CORRELATION COEFFICIENT
$R_{uu'} = \frac{\overline{uu'}}{u'u'}$
$R_{uu'}$
0.4
0.3
0.2
0.1
0
DOUBLE CORRELATION
$\frac{\overline{uu'}}{U_m^2}$
-0.1
-0.2
-0.3
2
1
0
-1
-2
2 0 -2 -4 -6 -8 -10 -12 -14 -16 -18
r - cm.

JET # 1

DOUBLE CORRELATION SYM. ABOUT AXIS (i.e., $= r_1 = -r_2$)

$\frac{x}{d} = 20$

$$R = \frac{\overline{u_1 u_2}}{\overline{u^2}}$$

SCALE: $L = \int_0^\infty R\, d(\Delta r) = 0.95$ cm.

MICRO-SCALE: $\lambda = 0.57$ cm.

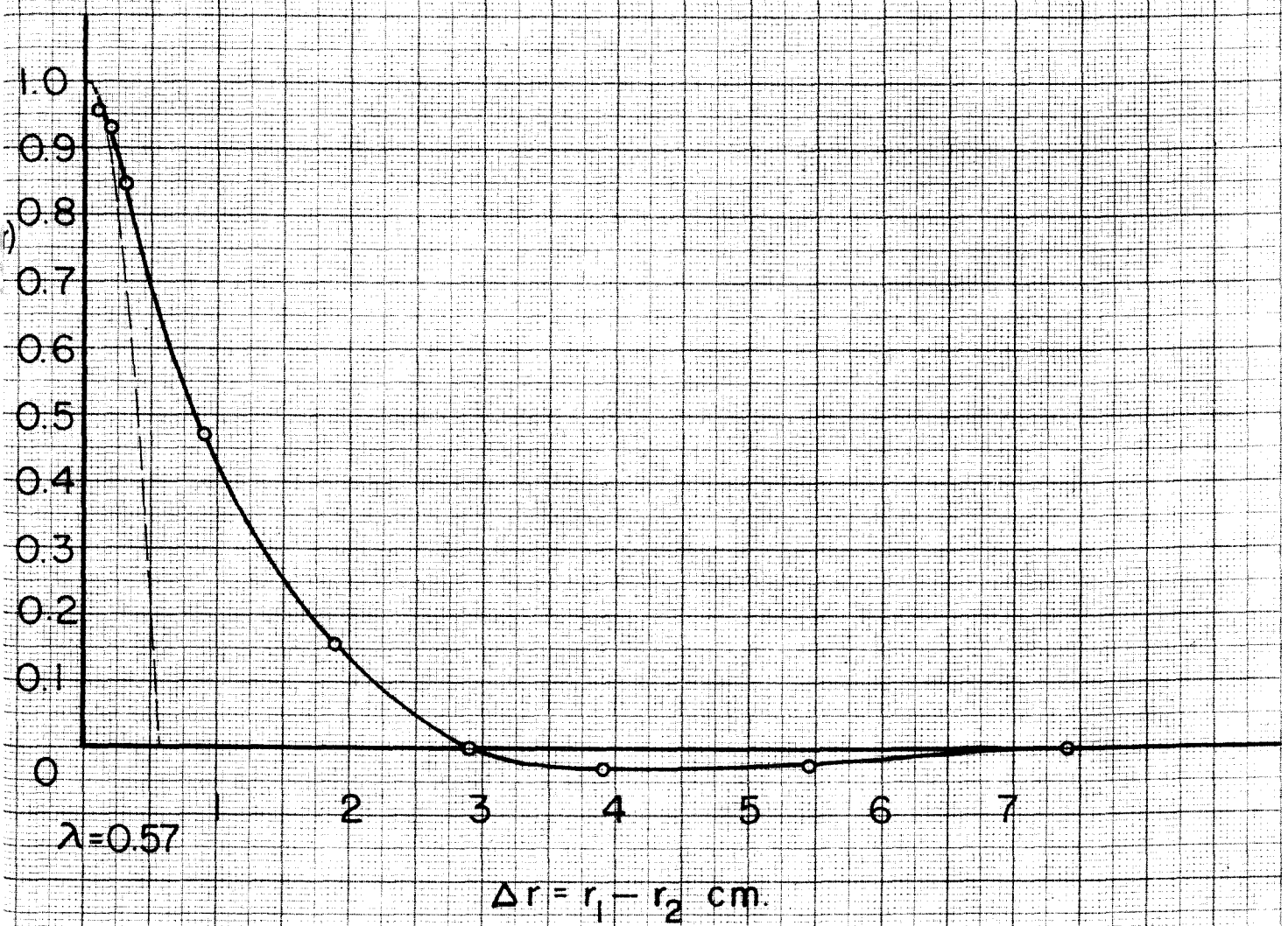

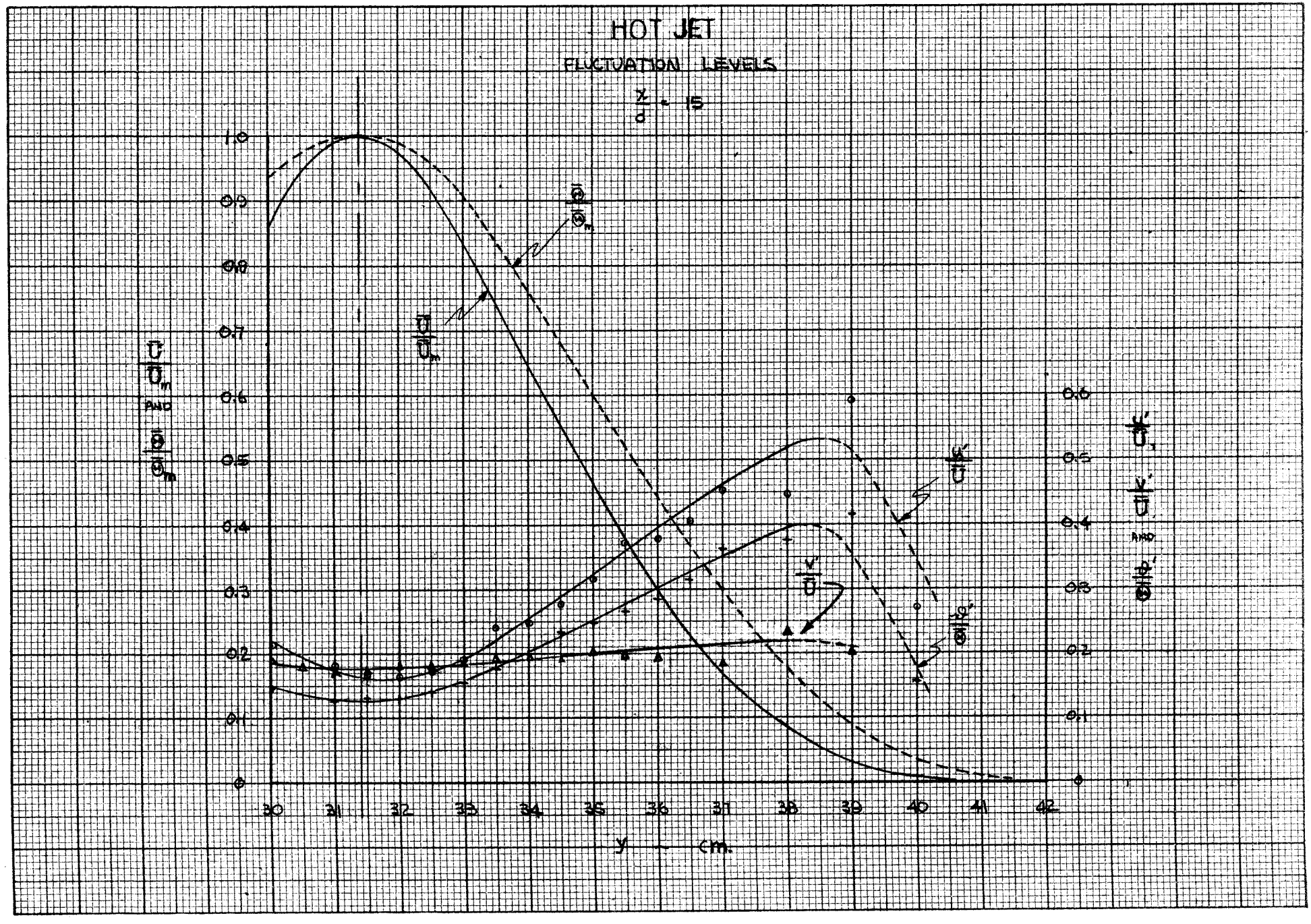
HOT JET
FLUCTUATION LEVELS
x/d = 15
1.0
0.9
0.8
0.7
0.6
0.5
0.4
0.3
0.2
0.1
0
U/U_m AND θ/θ_m
θ'/θ_m
U'/U
V'/U
θ'/θ
0.6
0.5
0.4
0.3
0.2
0.1
30
31
32
33
34
35
36
37
38
39
40
41
42
y — cm.

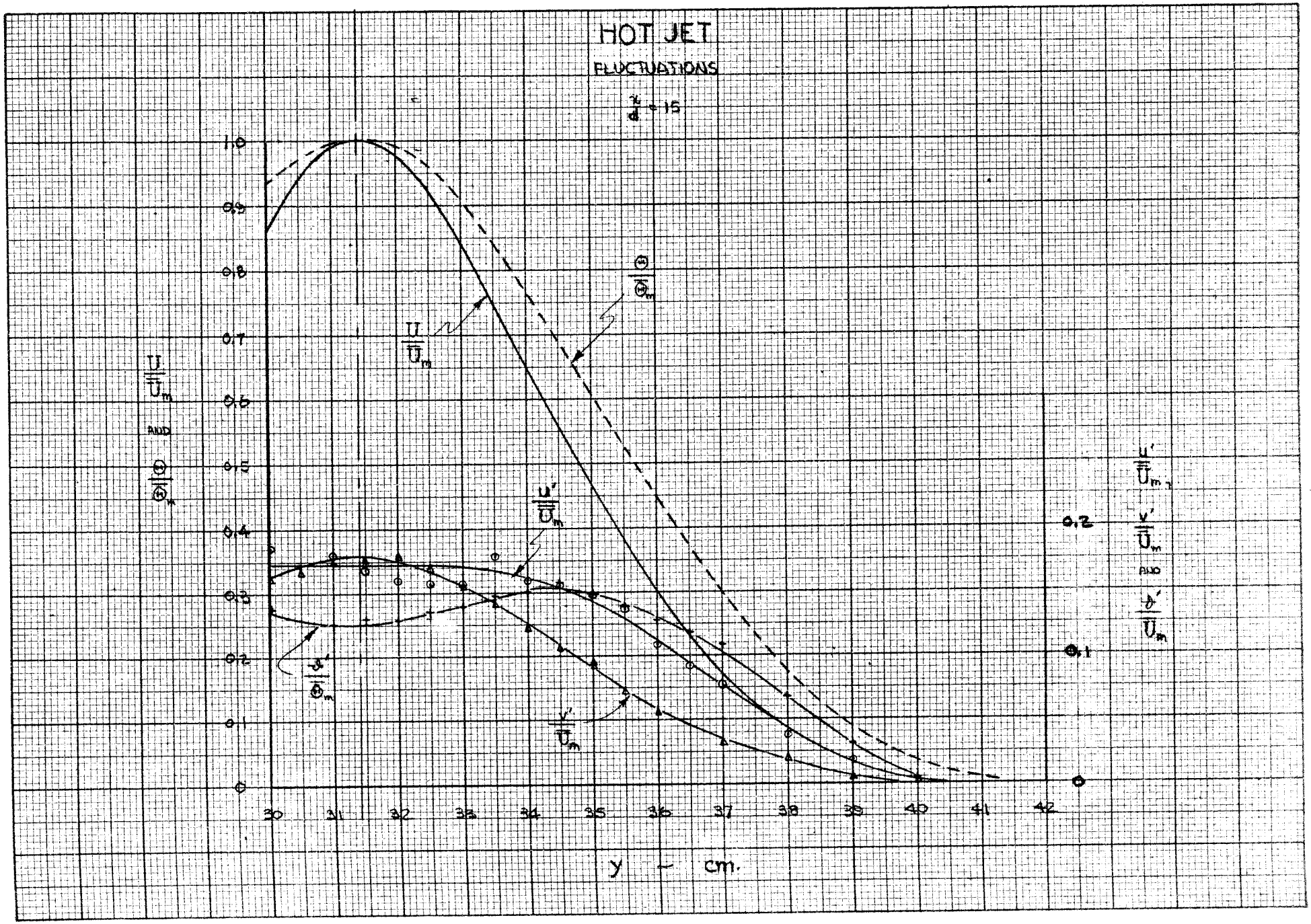
HOT JET
FLUCTUATIONS
x/d = 15
1.0
0.9
0.8
0.7
0.6
0.5
0.4
0.3
0.2
0.1
0
U/Um AND Θ/Θm
U/Um
Θ/Θm
u'/Um
v'/Um
θ'/Θm
30
31
32
33
34
35
36
37
38
39
40
41
42
y — cm.
u'/Um
0.2
v'/Um AND θ'/Um
0.1
0

Fig. 13b

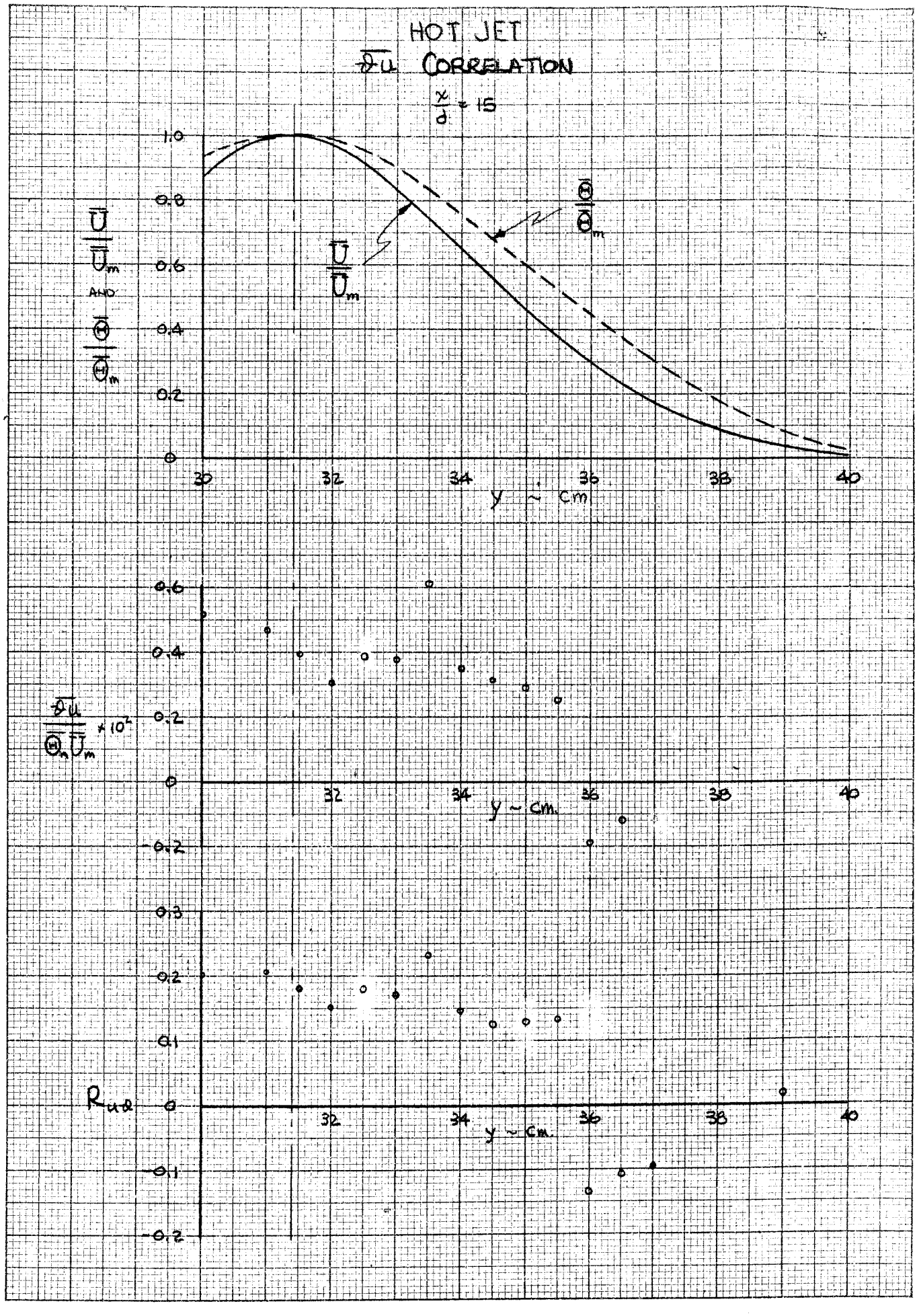
HOT JET
$\overline{\theta u}$ CORRELATION
$\frac{x}{d} = 15$
$\frac{\overline{U}}{\overline{U}_m}$ AND $\frac{\overline{\theta}}{\overline{\theta}_m}$
$\frac{\overline{U}}{\overline{U}_m}$
$\frac{\overline{\theta}}{\overline{\theta}_m}$
1.0
0.8
0.6
0.4
0.2
0
30
32
34
36
38
40
y ~ cm
$\frac{\overline{\theta u}}{\overline{\theta}_m \overline{U}_m} \times 10^2$
0.6
0.4
0.2
0
-0.2
32
34
36
38
40
y ~ cm.
R_{uq}
0.3
0.2
0.1
0
-0.1
-0.2
32
34
36
38
40
y ~ cm.

Fig. 20

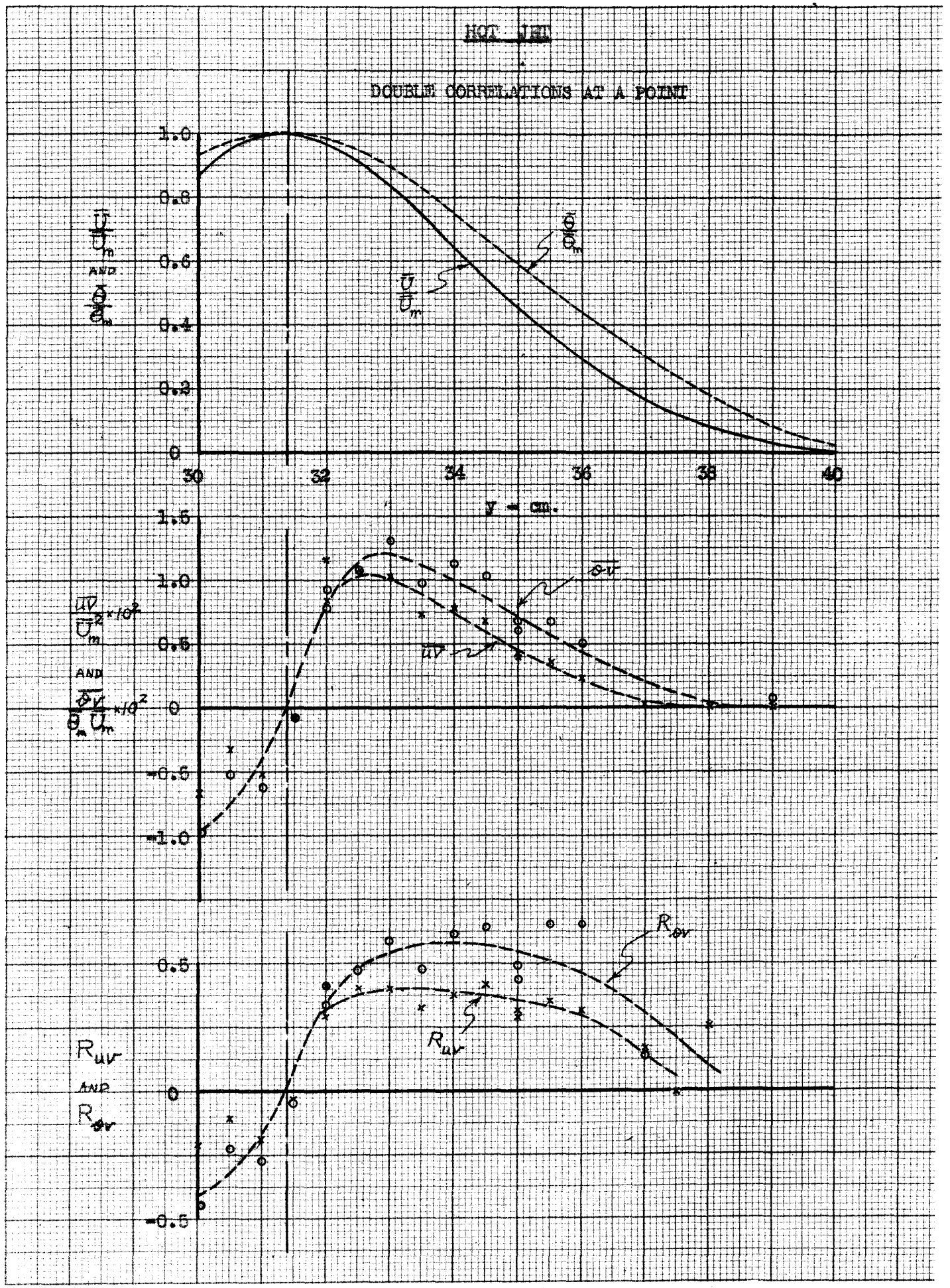
HOT JET
DOUBLE CORRELATIONS AT A POINT
$\frac{\overline{U}}{U_m}$ AND $\frac{\overline{\theta}}{\theta_m}$
$\frac{\overline{\theta v}}{\theta_m U_m}$
$\frac{\overline{U}}{U_m}$
1.0
0.8
0.6
0.4
0.2
0
30
32
34
36
38
40
y - cm.
$\frac{\overline{uv}}{U_m^2} \times 10^2$ AND $\frac{\overline{\theta v}}{\theta_m U_m} \times 10^2$
$\overline{\theta v}$
$\overline{uv}$
1.5
1.0
0.5
0
-0.5
-1.0
R_{uv} AND $R_{\theta v}$
$R_{\theta v}$
R_{uv}
0.5
0
-0.5

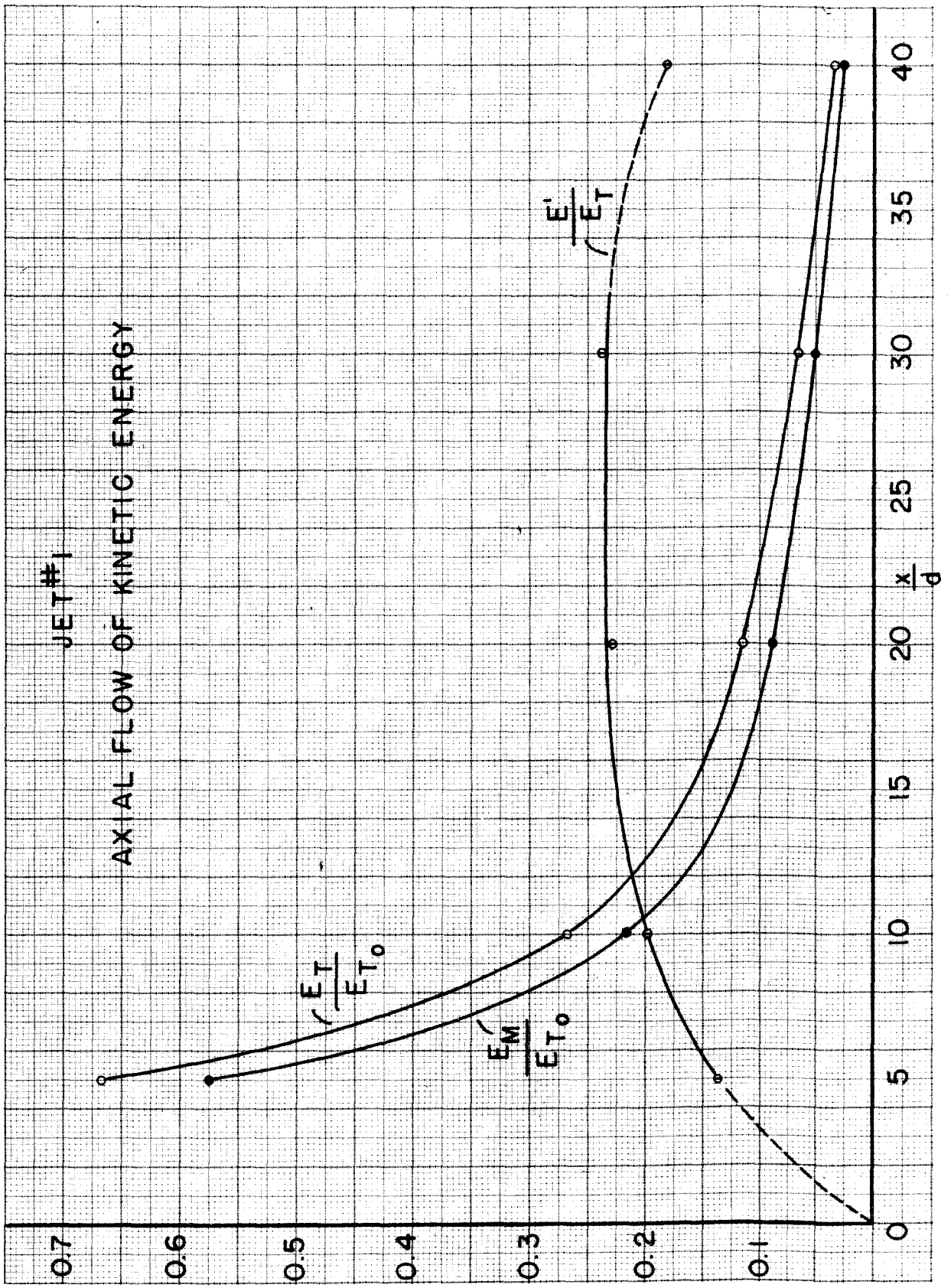
JET #1
AXIAL FLOW OF KINETIC ENERGY
$\frac{E_T}{E_{T_o}}$
$\frac{E_M}{E_{T_o}}$
$\frac{E'}{E_T}$
0.7
0.6
0.5
0.4
0.3
0.2
0.1
0
5
10
15
20
25
30
35
40
$\frac{x}{d}$
$\frac{E_T}{E_{T_o}}$ $\frac{E_M}{E_{T_o}}$ and $\frac{E'}{E_T}$

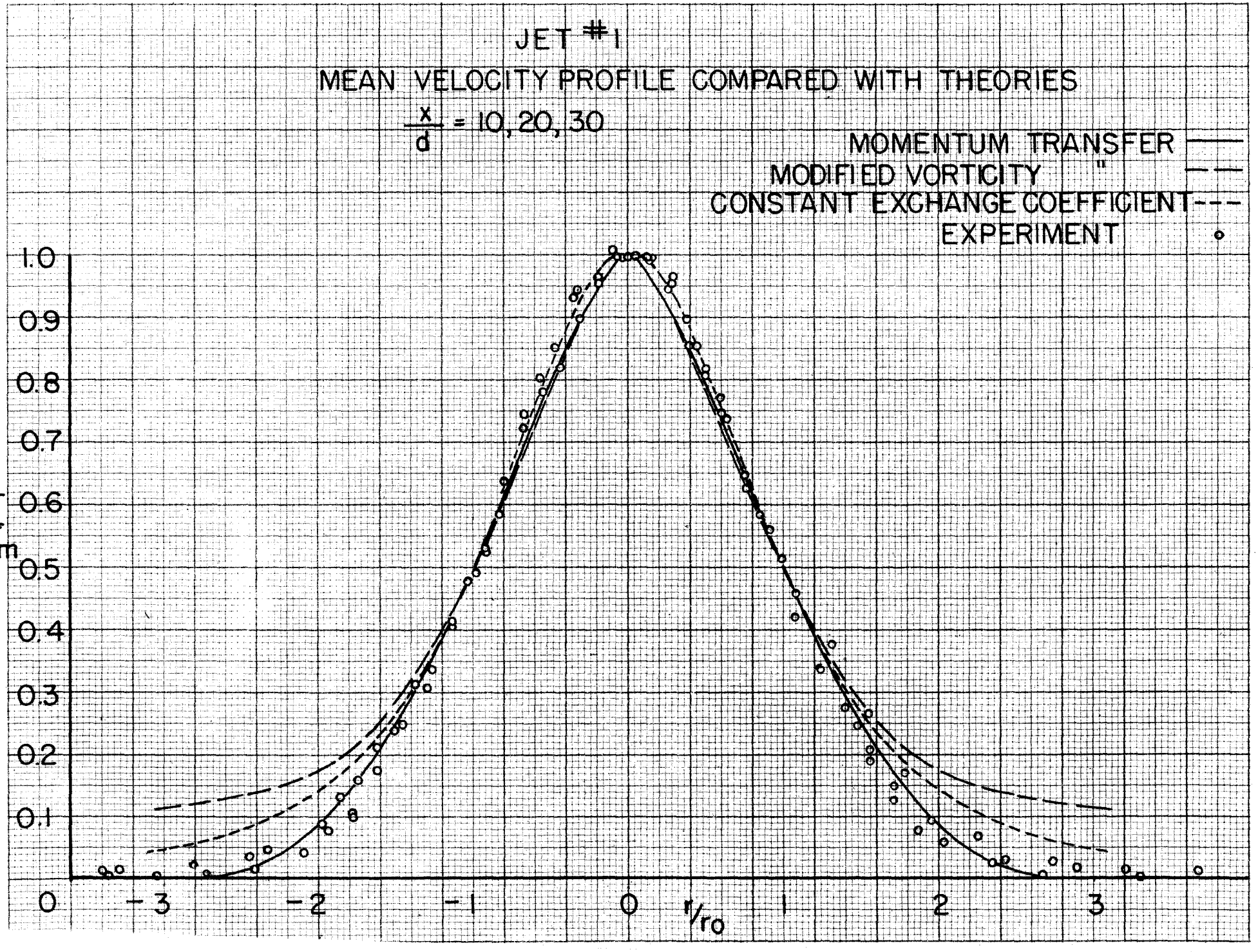
JET #1
MEAN VELOCITY PROFILE COMPARED WITH THEORIES
x/d = 10, 20, 30
MOMENTUM TRANSFER
MODIFIED VORTICITY "
CONSTANT EXCHANGE COEFFICIENT
EXPERIMENT
1.0
0.9
0.8
0.7
0.6
0.5
0.4
0.3
0.2
0.1
0
U/Um
-3
-2
-1
0
r/ro
1
2
3

Fig. 22

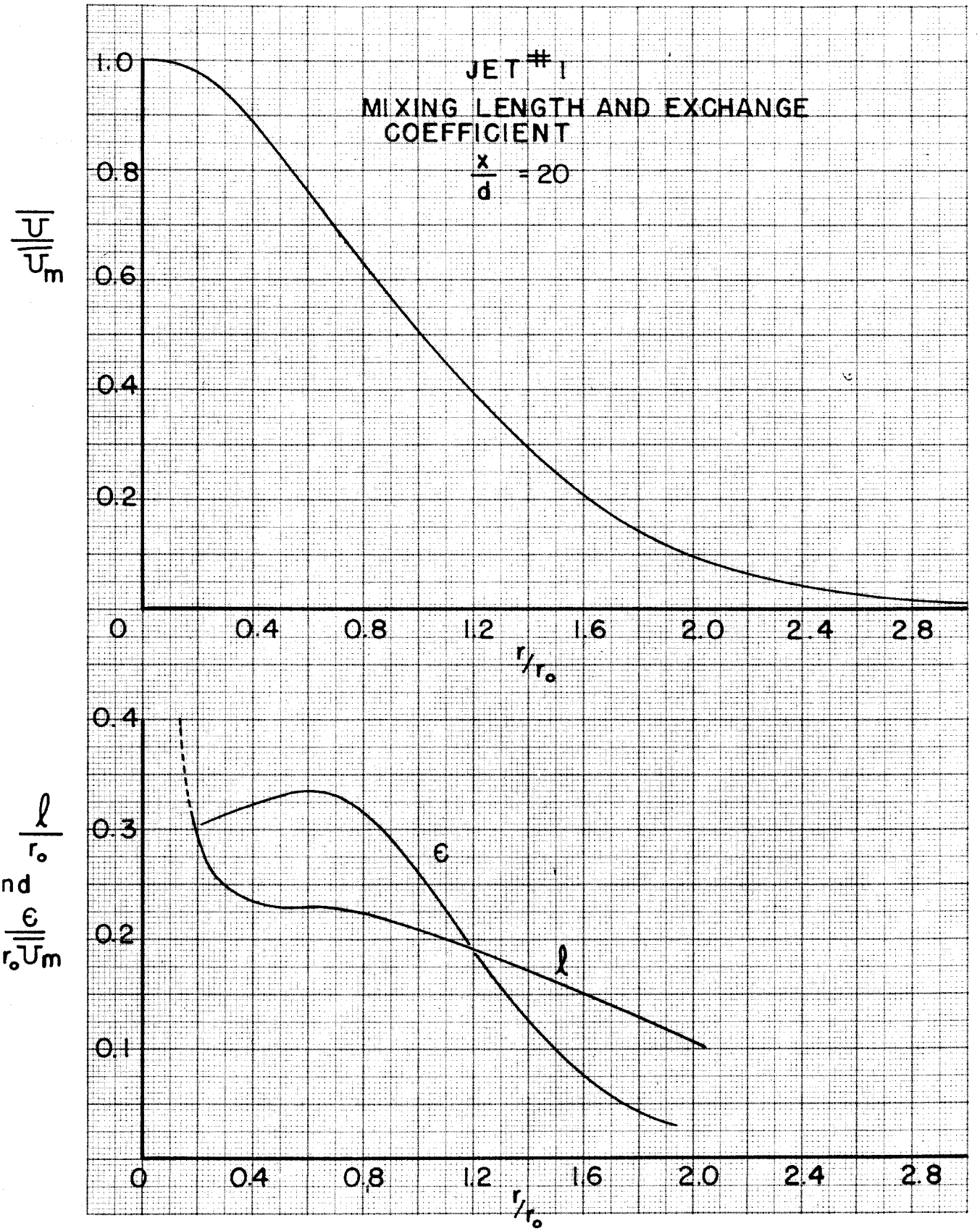
JET # 1
MIXING LENGTH AND EXCHANGE COEFFICIENT
x/d = 20
U/Um
1.0
0.8
0.6
0.4
0.2
0
0.4
0.8
1.2
1.6
2.0
2.4
2.8
r/ro
l/ro and ε/roUm
0.4
0.3
0.2
0.1
ε
l
0
0.4
0.8
1.2
1.6
2.0
2.4
2.8
r/ro

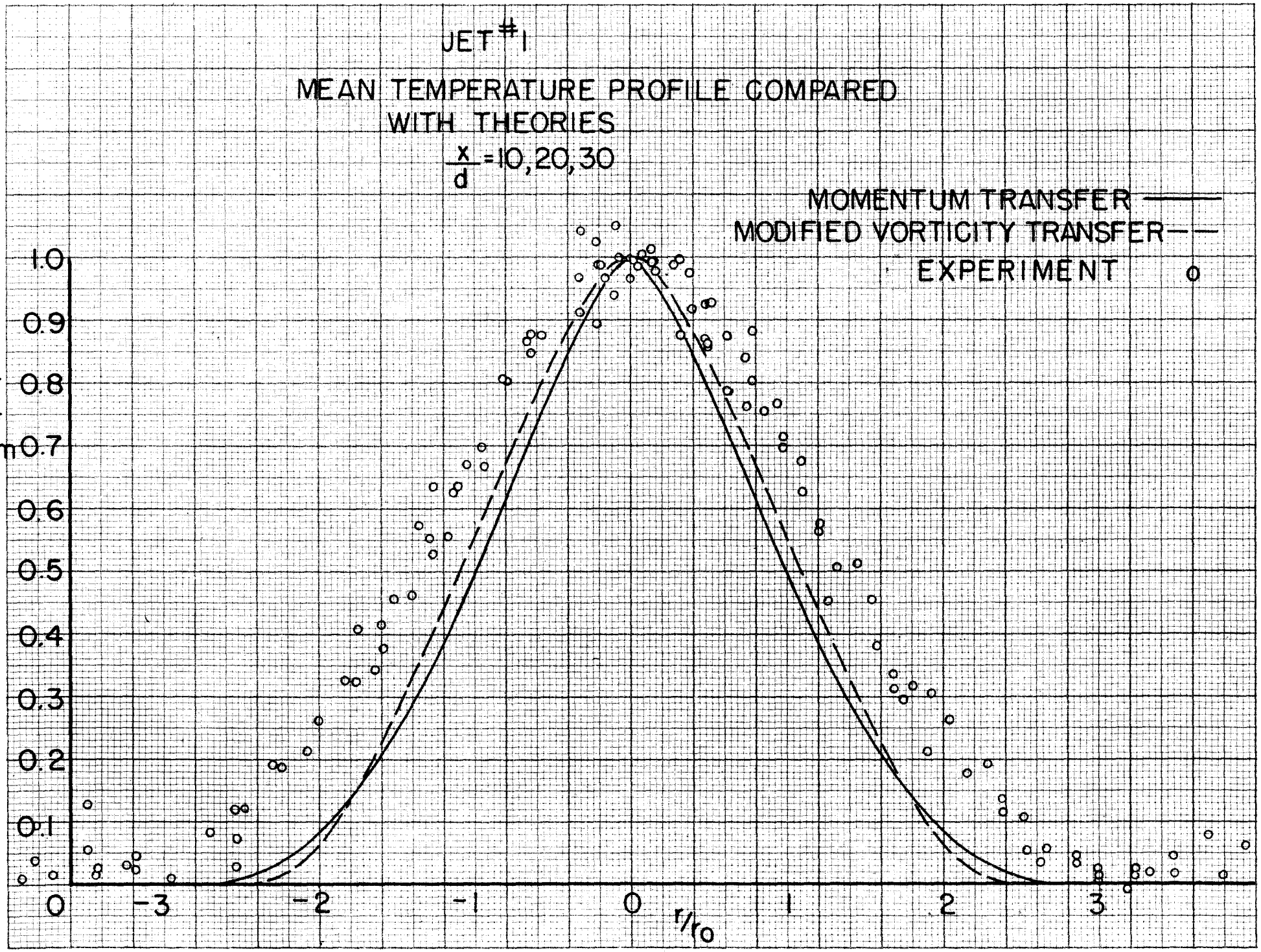
JET #1
MEAN TEMPERATURE PROFILE COMPARED WITH THEORIES
x/d = 10, 20, 30
MOMENTUM TRANSFER ——
MODIFIED VORTICITY TRANSFER - -
EXPERIMENT o
θ/θm
1.0
0.9
0.8
0.7
0.6
0.5
0.4
0.3
0.2
0.1
0
-3
-2
-1
0
1
2
3
r/ro

Fig. 24

JET #1

COMPARISON OF MEASURED SHEAR AND SHEAR COMPUTED FROM VELOCITY PROFILE

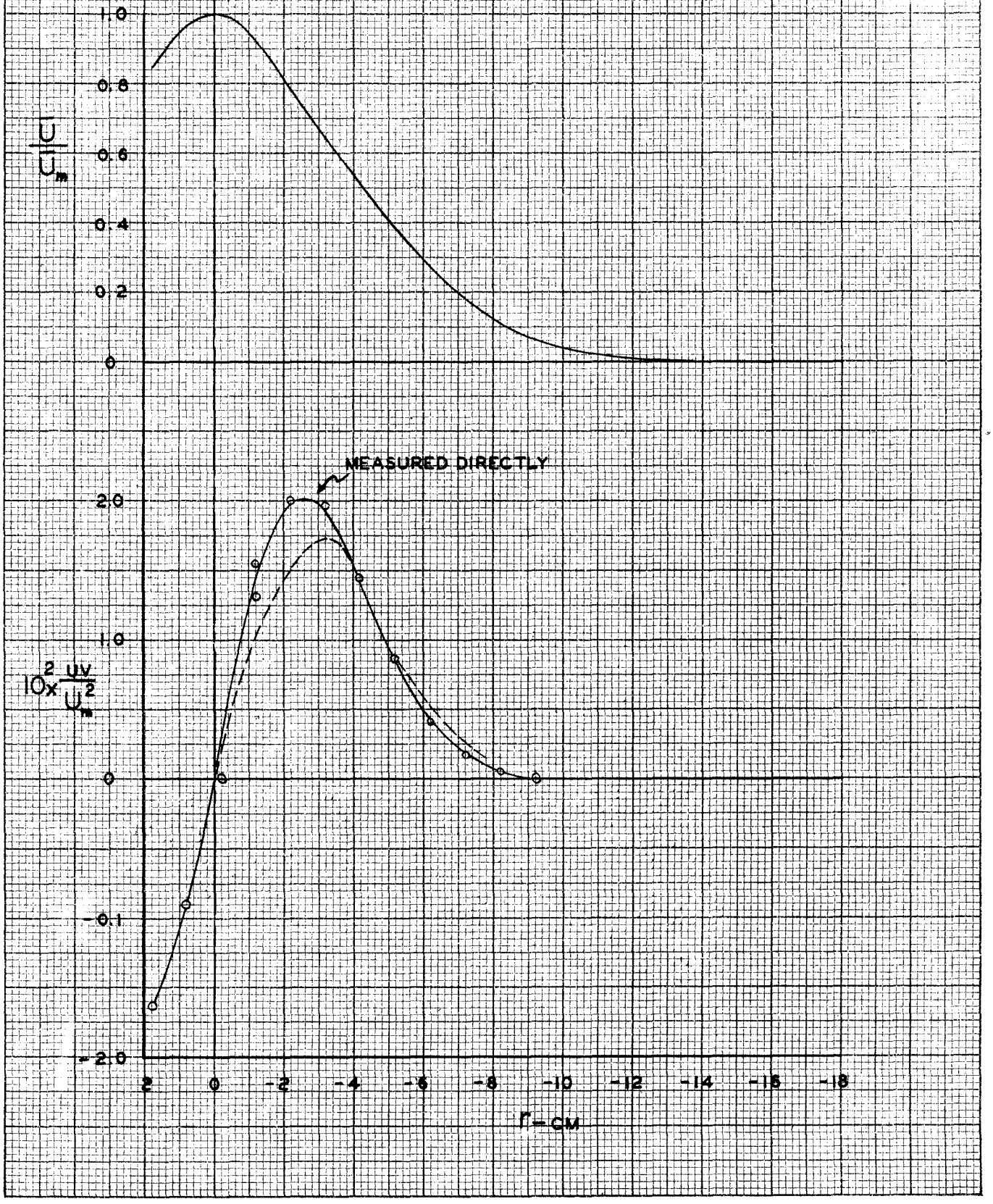

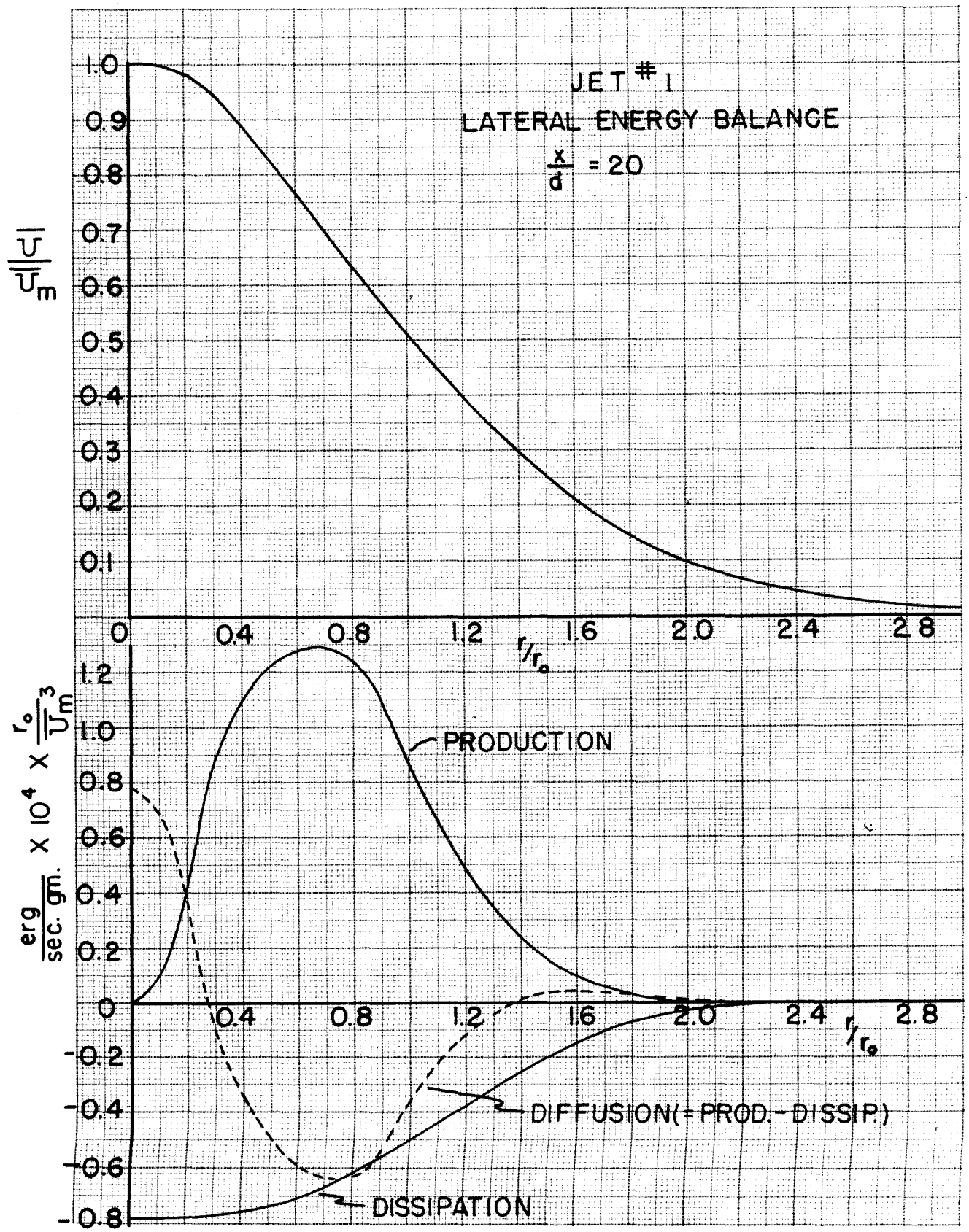
JET # 1
LATERAL ENERGY BALANCE
x/d = 20
U/Um
r/ro
PRODUCTION
DIFFUSION(=PROD.-DISSIP.)
DISSIPATION
erg/sec. gm. X 10^4 X ro/Um^3

Fig. 27

HOT JET

MOMENTUM AND HEAT TRANSFER

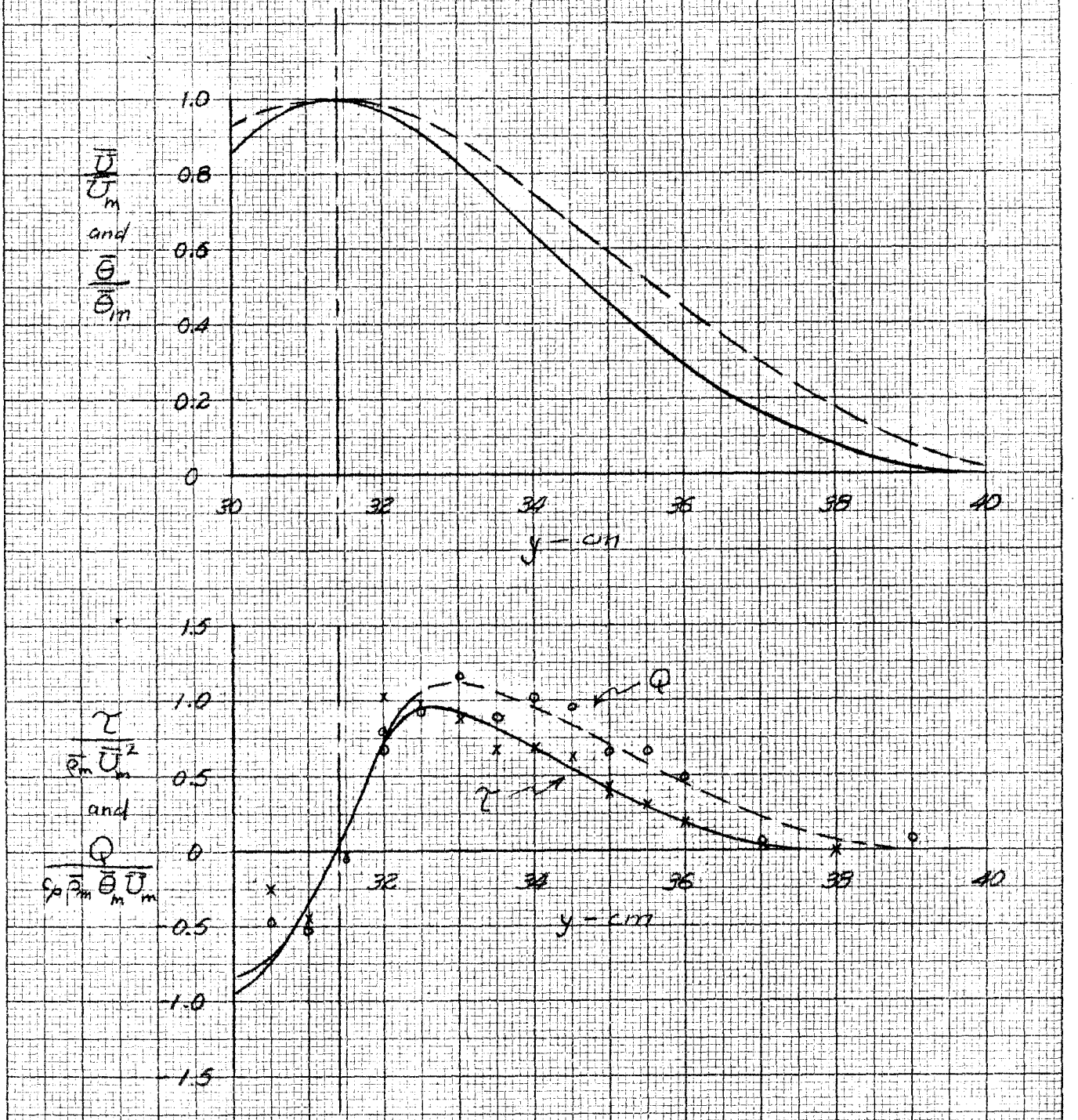

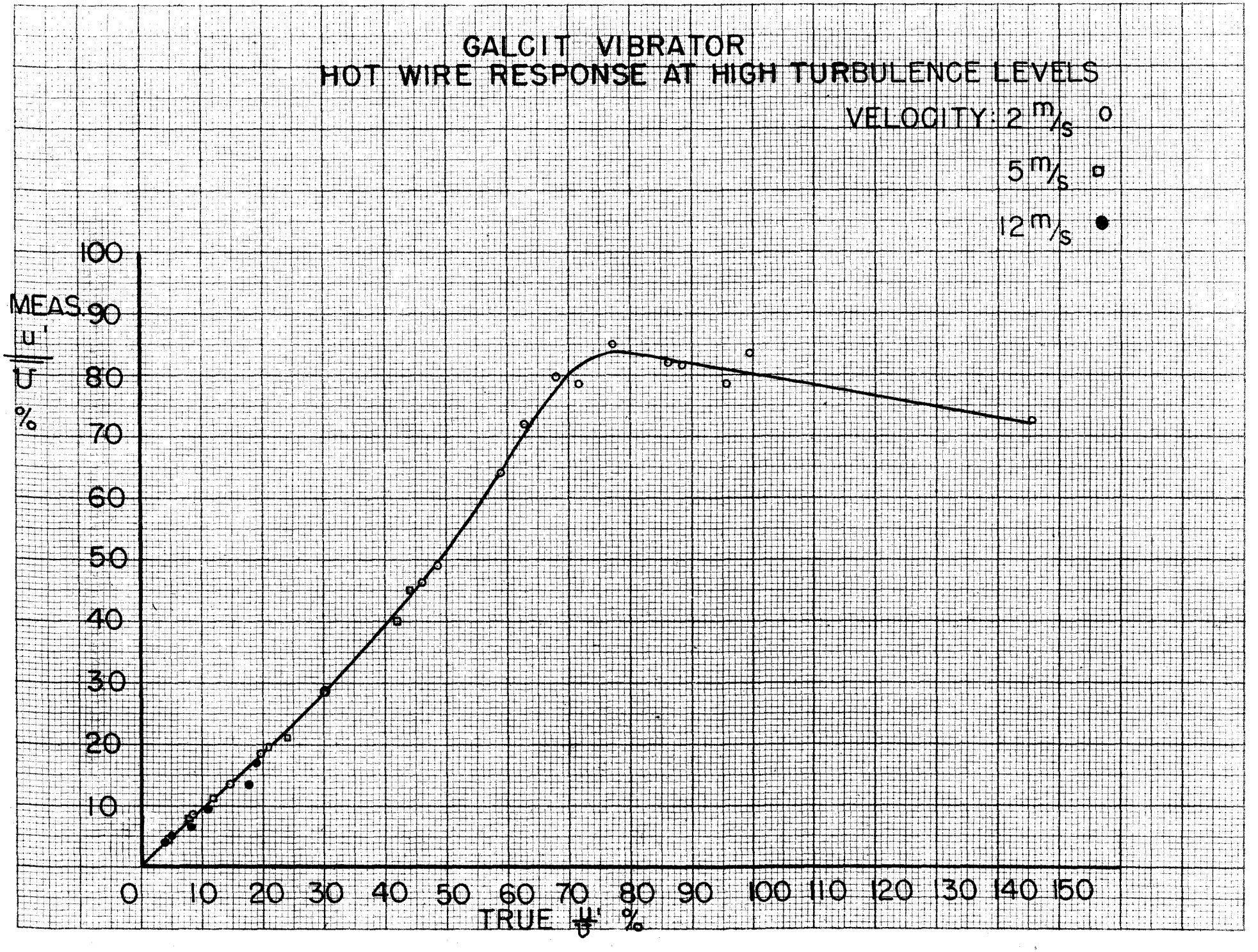
GALCIT VIBRATOR
HOT WIRE RESPONSE AT HIGH TURBULENCE LEVELS
VELOCITY: 2 m/s o
5 m/s □
12 m/s ●
MEAS. u'/U %
100
90
80
70
60
50
40
30
20
10
0 10 20 30 40 50 60 70 80 90 100 110 120 130 140 150
TRUE u'/U %